Distribution Agreement

In presenting this thesis or dissertation as a partial fulfillment of the requirements for an advanced degree from Emory University, I hereby grant to Emory University and its agents the non-exclusive license to archive, make accessible, and display my thesis or dissertation in whole or in part in all forms of media, now or hereafter known, including display on the world wide web. I understand that I may select some access restrictions as part of the online submission of this thesis or dissertation. I retain all ownership rights to the copyright of the thesis or dissertation. I also retain the right to use in future works (such as articles or books) all or part of this thesis or dissertation.

Signature:

_____ _____

Jasmine Yoojoo Lee Date

The development and functional testing of cellular therapies against protein tyrosine kinase 7 (PTK7) to treat high-risk neuroblastoma

By

Jasmine Yoojoo Lee
Doctor of Philosophy

Graduate Division of Biological and Biomedical Sciences
Cancer Biology

_____

H. Trent Spencer, Ph.D.
Advisor

_____

Christopher Doering, Ph.D.
Committee Member

_____

Kelly C. Goldsmith, MD
Committee Member

_____

Haydn T. Kissick, Ph.D.
Committee Member

_____

Sarwish Rafiq, Ph.D.
Committee Member

Accepted**:**

_____

Kimberly J. Arriola, MPH, Ph.D.
Dean of the James T. Laney School of Graduate Studies

_____

Date

The development and functional testing of cellular therapies against protein tyrosine kinase 7 (PTK7) to treat high-risk neuroblastoma

By

Jasmine Yoojoo Lee
B.S., University of Colorado Denver, 2017

Advisor: H. Trent Spencer, Ph.D.

An abstract of
A dissertation submitted to the Faculty of the
James T. Laney School of Graduate Studies of Emory University
in partial fulfillment of the requirements for the degree of
Doctor of Philosophy
in Graduate Division of Biological and Biomedical Sciences,
Cancer Biology
2023

Abstract

The development and functional testing of cellular therapies against protein tyrosine kinase 7 (PTK7) to treat high-risk neuroblastoma

By Jasmine Yoojoo Lee

New therapies for high-risk neuroblastoma (NB) are needed as it's the most common extracranial pediatric solid tumor with an alarming survival rate of <50%. Immunotherapies utilize cells or proteins of the immune system to treat diseases such as cancer. A form of immunotherapy that's at the forefront of treating previously difficult to treat cancer is chimeric antigen receptor (CAR) T-cell therapy which has been largely successful for hematological malignancies but has not had the same success in solid tumors. Another variety of immunotherapies are monoclonal antibodies, a form of targeted therapy utilizing lab-engineered antibodies. In recent years, a monoclonal antibody against a disialoganglioside, GD2, has significantly improved survival for high-risk NB patients. However, toxicities can occur and not all patients respond, underpinning the need to identify additional targets. Protein tyrosine kinase 7 (PTK7) has been identified as a promising NB target in a model that represents the post-chemotherapy refractory/recurrent NB patient population. The primary aim of the research presented in this dissertation was to determine the feasibility of targeting PTK7 through cellular-based immunotherapies. We engineered anti-PTK7 CARs and found PTK7 CAR T cells specifically target and kill PTK7-expressing NB cell lines. *In vivo*, PTK7 CAR T cells regress an aggressive NB metastatic model and improve survival. The primary T cells utilized in these studies were of an alpha-beta ($\alpha\beta$) subtype, the subtype choice for the CAR T-cell therapies currently tested in humans, largely due to the abundance and ease of cell isolation and expansion. Unlike $\alpha\beta$ T cells, gamma-delta ($\gamma\delta$) T cells lie on a bridge between both innate and adaptive immunity and therefore have an intrinsic ability of inducing potent cytotoxicity against cancer cells without priming. Our lab has previously shown that non-modified *ex vivo* expanded $\gamma\delta$ T cells are cytotoxic against NB cells. To further enhance the effectiveness of this cell-based immunotherapy, we modified $\gamma\delta$ T cells to express PTK7 CAR and show early evidence of preclinical utility *in vitro* and *in vivo*. This work supports ongoing studies to further optimize these cellular therapies against PTK7 to treat NB and other cancers.

The development and functional testing of cellular therapies against protein tyrosine kinase 7 (PTK7) to treat high-risk neuroblastoma

By

Jasmine Yoojoo Lee
B.S., University of Colorado Denver, 2017

Advisor: H. Trent Spencer, Ph.D.

A dissertation submitted to the Faculty of the
James T. Laney School of Graduate Studies of Emory University
in partial fulfillment of the requirements for the degree of
Doctor of Philosophy
In Graduate Division of Biological and Biomedical Sciences,
Cancer Biology
2023

Acknowledgements

I would like to first and foremost thank my PhD Advisor, Dr. Trent Spencer. Your mentorship over the past four years is what I consider the perfect amount of both guidance and trust in my ability to drive my dissertation research forward. You have been nothing short of encouraging, and always remembered to challenge me as a scientist. You were not only supportive in the lab, but also in my career aspirations and decision to pursue an industry internship during my studies. I hope to make as big of an impact as a mentor to someone else, like you have for me.

To Dr. Kelly Goldsmith, thank you for taking a chance and taking me in as a fresh-out-of-college graduate. I learned so much from you during my two years before graduate school, then continued to learn from you during our collaboration on this project. Your support has been instrumental in a lot of the opportunities I've been fortunate enough to have during my time here at Emory.

To the mentor that first sparked my interest in cancer research, Dr. Patricia Ernst, thank you for your patience, passion for research, endless opportunities you provided me with as an undergrad, and lastly, the best skiing/snowboarding lab outings in Breckenridge.

Dr. Chris Doering, thank you for your expertise and most thoughtful guidance and questions to consider that were critical to this project. I'd like to thank my committee members, Dr. Sarwish Rafiq and Dr. Haydn Kissick. I always looked forward to your feedback and conversations during my committee meetings; you have pushed me to be a better scientist.

To the current and former members of the Spencer/Doering Gene and Cell Therapy Lab, I will miss our open and fun discussions of research questions and experimental strategies; I learned a lot from each of you. Thank you for also being a great support system, and good group of people I can talk to about anything.

To all the friends I met both inside and outside of Emory, your support has been critical. I'd like to acknowledge a few in particular, Jenny Shim, Leon McSwain, Hunter Jonus, Sherri Smart, Jane Park, Brian Mott, Maple Mott, Lillian Na, Gianna Branella, Rae Hunter, Kiran Parwani, Austre Schiaffino, Ash Thapa, Victor Maximov, Carlyn Harris, Passang, and Kevin Chen. You made Atlanta feel like home, and I could not imagine my experience here both in and out of graduate school without your support.

Lastly, I'd like to acknowledge my family. To my grandparents who live in Korea, thank you for your words of encouragement during my graduate studies. To my sister, thank you for taking on the difficult role of being the oldest immigrant child; your sacrifices and actions that helped pave the way for me in some areas don't go unnoticed. To my mom and dad, thank you for the remarkable sacrifices you made to move us to the US, and continued support throughout my life.

Table of Contents

List of Figures and Tables

A subset of figures were created with BioRender.com

Chapter 1: Introduction

1.1 Neuroblastoma

NB background, diagnosis, risk factors, and molecular features

Neuroblastoma (NB) is an aggressive heterogeneous disease that mostly affects patients <10 years old, with a median diagnosis age of 18 months [1,2]. It's a solid tumor derived from the neural crest of the sympathetic nervous system and most commonly arises in or around the adrenal glands (**Figure 1.1.1A**). NB is diagnosed through several radiographic imaging and histopathological features. Tumor imaging is typically obtained by contrast MRI and extent of metastatic disease measured by metaiodobenzylguanidine (MIBG) scan [3]. This imaging method is specific to NB given almost 90% of NBs express a noradrenaline transporter that allows MIBG uptake to tumor cells [4].

Familial NB only account for 1-2% of cases and are associated with high genetic predisposition through anaplastic lymphoma kinase (ALK) and paired mesoderm homeobox protein 2B (PHOX2B) germline mutations. Two common molecular features of high-risk NB are ALK mutation and MYCN amplification (**Figure 1.1.2A-B**). Somatic mutations of ALK are present in 14% of high-risk NB [5] and MYCN amplification occurs in 20% of primary tumors and is the most commonly associated with poor outcome [6,7].

NB staging, risk-stratification, and standard of care

NB tumors are categorized by two different systems. The International Neuroblastoma Staging System (INSS) and newer International Neuroblastoma Risk Group (INRG). INSS is utilized to assess the extent of resection when staging, however this may vary drastically between institutions [8]. To better determine a uniform staging system, the INRG was developed where the disease is determined by primary and metastatic tumor imaging prior to any treatment. Importantly, patients are also classified under risk stratification from low-risk, intermediate-risk, and high-risk that's mainly determined by MYCN amplification status and histopathology. Low-risk patients will undergo only observation or resection while intermediate-risk patients may receive

surgery and 4-8 cycles of chemotherapy. However, high-risk NB patients (~50% patients) undergo intensive multimodal therapy starting from induction chemotherapy, surgery, consolidation therapy, hematopoietic stem cell transplantation (AHSCT), and lastly maintenance immunotherapy (**Figure 1.1.3A**). Maintenance therapy initially only included a differentiating agent isotretinoin; however, three immunotherapies were added to the regimen based on the following. A monoclonal antibody against a disialoganglioside (GD2), granulocyte-macrophage colony-stimulating factor (GM-CSF), and interleukin 2 (IL-2) significantly improved patient survival compared to standard therapy [9]. These results were the first evidence that immunotherapies can be effective against NB and led to further preclinical and clinical therapies against GD2 and others (described further in Chapter 1.2.g).

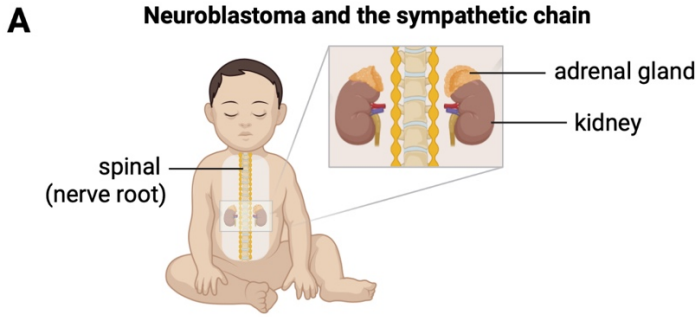

Figure 1.1. 1. Neuroblastoma background, diagnosis, and risk factors

(A) Graphical depiction of a neuroblastoma patient and the sympathetic chain, including the adrenal glands, where tumors most commonly arise.

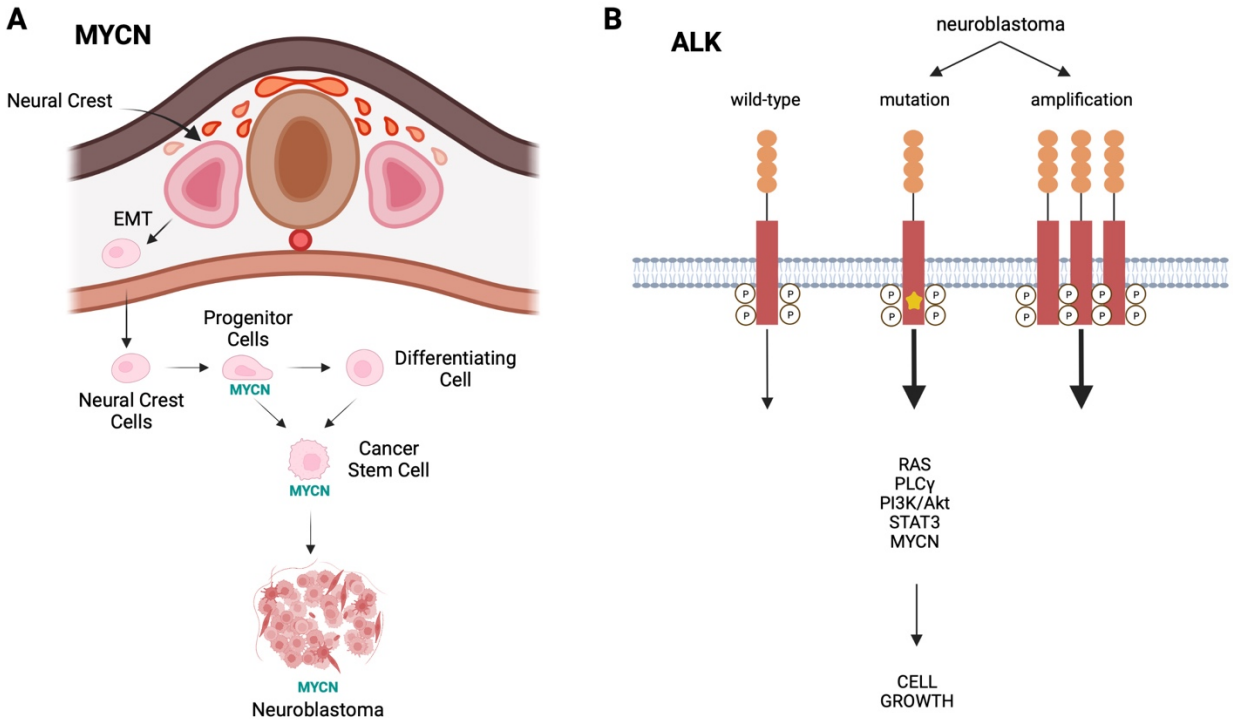

Figure 1.1. 2. Common molecular features of neuroblastoma

(A) Graphical depiction of MYCN in NB. Multipotent progenitor cells from the neural crest undergo epithelial-to-mesenchymal-transition (EMT). MYCN is highly expressed in the multipotent cells of the neural crest and downregulated during differentiation. Aberrant MYCN expression induces a cancer stem cell-like phenotype of apoptotic resistance [10]. **(B)** Various aberrant activation of ALK in cancer. Aberrant activation of ALK in neuroblastoma can occur by gene amplification or somatic mutations [11].

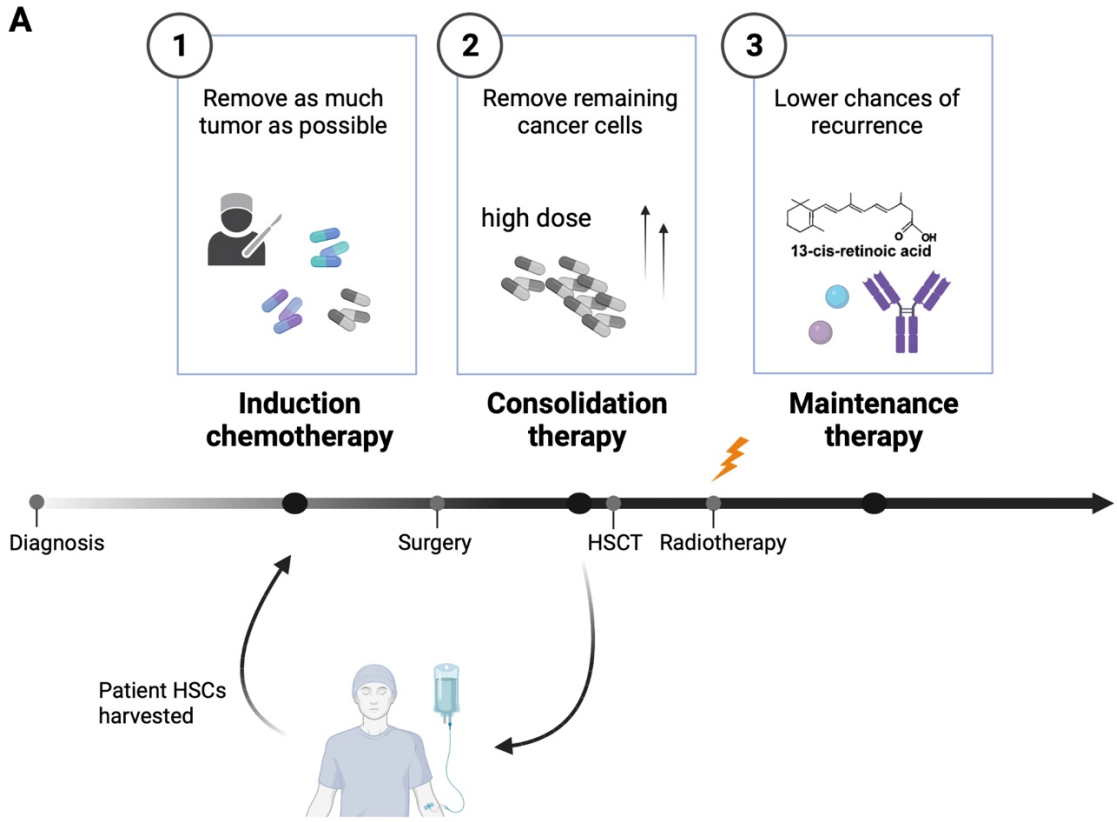

Figure 1.1. 3. Multimodal therapy for high-risk neuroblastoma

(A) Induction chemotherapy typically involves four-six different agents, most commonly carboplatin, cisplatin, cyclophosphamide, doxorubicin, vincristine, and topotecan. Patient hematopoietic stem cells (HSC) are collected prior to consolidation therapy. Myeloablative consolidation therapy is given to eliminate remaining cancer cells and followed by hematopoietic stem cell transplantation (AHSCT) for recovery. Finally, radiation therapy and maintenance immunotherapy (anti-GD2 antibody, cytokines, and isotretinoin) are administered to lower the chance of recurrence.

1.2 Cancer Immunotherapies

1.2.a. History

Cancer immunotherapies, although perceived as a more recent type of therapy, was first eluded to in Germany by physicians Friedrich Fehleisn and Wilhelm Busch in 1866, when they found

significant tumor regression in cancer patients inoculated with erysipelas, a streptococcal skin infection [12,13]. The next, more well-known advancement came in 1891, when William Coley noticed bone cancer patients who developed erysipelas underwent spontaneous remission and pieced his observations together with previous literature from other oncologists [14-16]. He subsequently injected sarcoma patients with live and inactivated *Streptococcus pyogenes* and *Serratia marcescens* into patients' tumors and observed tumor regression. This was the first documented immune-based treatment for cancer, earning Coley the nickname of the Father of Immunotherapy. Since his initial treatment of sarcoma patients, he went on to treat several other malignancies including lymphoma and testicular carcinoma with a reported total 1,000+ patient response (regression or complete cure) [17]. However, due to lack of understanding the mechanism of action behind these treatments, Coley's advancements were forgotten and sometimes denied until after 1945, when interferon was discovered [18] and the first cancer vaccine was developed [19].

It wasn't until 1977 when Lloyd Old, the pioneer of immuno-oncology, described cancer cells as unique, in their differing recognition by the immune system. Old predicted immunotherapies will join surgery, chemotherapy, and radiation therapy as one of the pillars of cancer therapies [20]. However, it wouldn't be until several decades later, that immunotherapy would be widely accepted as such. The theory of cancer immunosurveillance was first proposed in 1957 [17], then later confirmed T cells provide anti-tumor surveillance and play a role in anti-tumor responses [21]. Relevant to the work presented in this dissertation, T cells and their critical role in immunity was discovered in 1967 [22] and the first human tumor antigen recognized by T cells in 1991 [23].

1.2.b. Monoclonal antibodies and immune checkpoint inhibitors

Antibodies were discovered and established in 1890's by Paul Ehrlich, Emil Behring, and Kitasato Shibasaburo [24,25]. Antibodies bind a specific antigen to induce cell death in various ways, including

direct cell-killing, indirect killing, and immune-cell mediated killing (**Figure 1.2.1A-C**) and in 1997, rituximab, became the first monoclonal antibody approved by the Food and Drug Administration (FDA) for treatment of non-Hodgkin's lymphoma [26].

A specific class of monoclonal antibodies that have shown the most promise in treating cancer are checkpoint inhibitors and due to their success, are currently approved by the FDA for treatment of over nine different cancer types [17]. Immune checkpoint molecules are ligand-receptor pairs that are capable of inducing inhibition or stimulatory immune responses (**Figure 1.2.2A**). The first immune checkpoint molecule, cytotoxic T-cell lymphocyte antigen number 4 (CTLA-4), was discovered in 1987 and its function and potential as a target for anti-cancer therapy was proposed by James Allison *et al.* in 1995 [27,28]. Ipilimumab, a monoclonal antibody against CTLA-4 was the first checkpoint inhibitor that gained FDA approval in 2011 and over 20% of the patients treated prior to its approval still show no evidence of disease today [17]. Currently, there are several FDA approved checkpoint inhibitors against another well-known checkpoint molecule, programmed cell death-1 (PD-1) and its ligand PD-L1, that has shown critical breakthroughs in cancer therapy (**Figure 1.2.2B**).

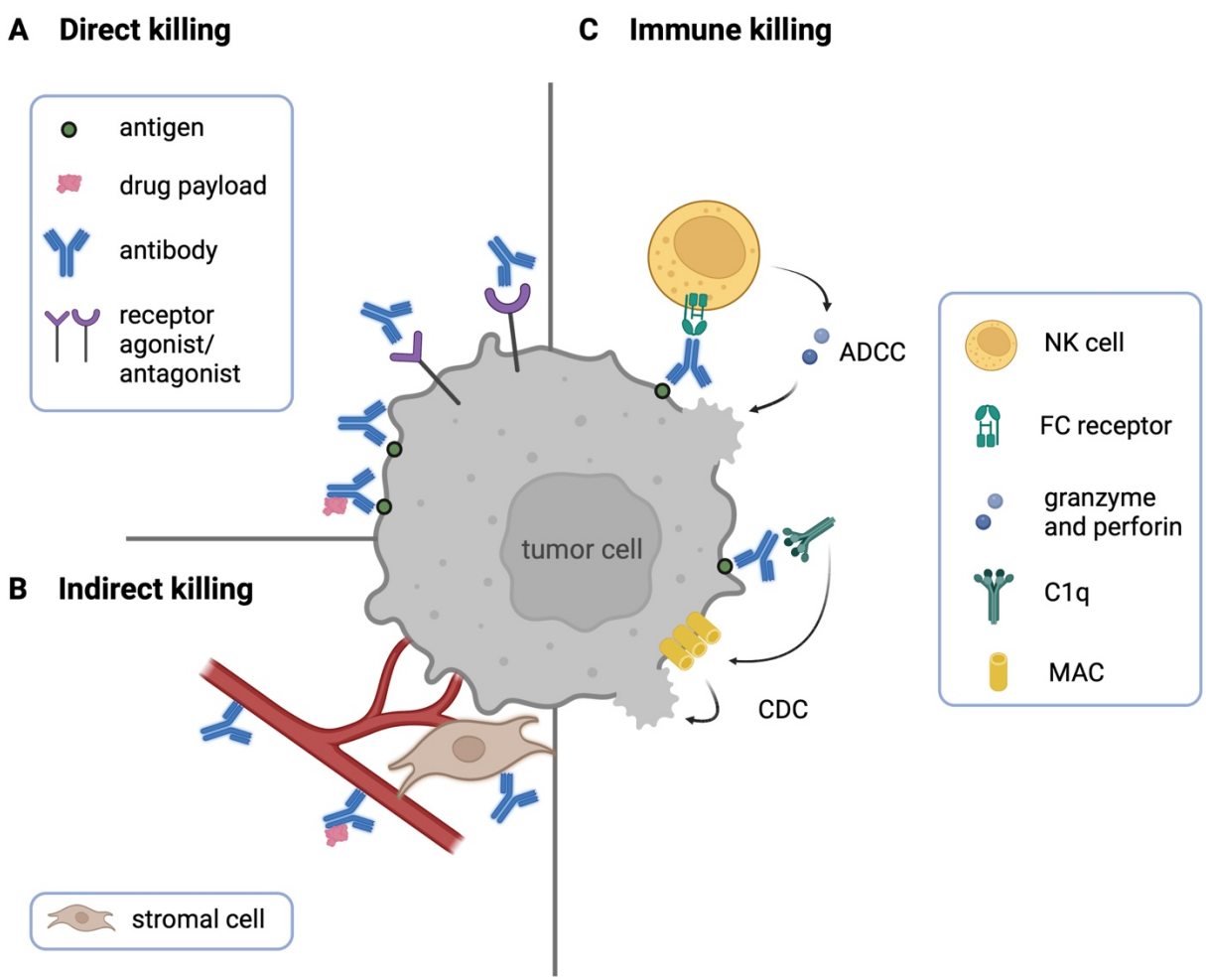

Figure 1.2. 1. Antibody-induced killing of tumor cells

(A) Direct tumor cell killing can be induced by receptor agonists and receptor antagonist (blocking of dimerization, kinase activity, and downstream signaling), all leading to apoptosis. Antibodies may also be conjugated to a toxic payload to induce cell death. **(B)** Vasculature and stromal cells that help form the tumor structure can also be directly targeted. **(C)** Immune-cell mediated killing can be activated by NK cell antibody-dependent cellular cytotoxicity (ADCC) or complement-dependent cytotoxicity (CDC).

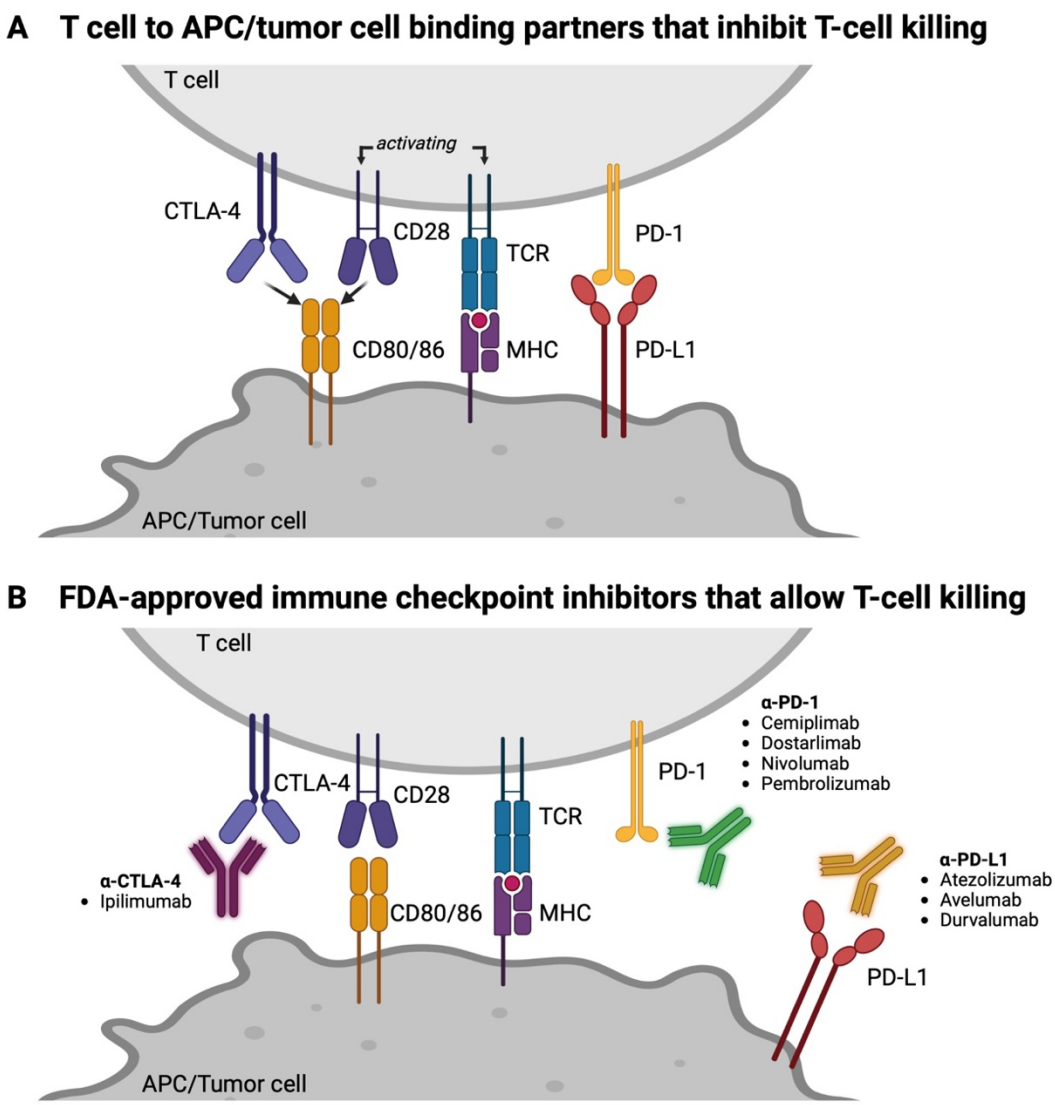

Figure 1.2. 2. Immune checkpoint inhibitors for cancer

(A) T-cell activation requires T-cell receptor (TCR) binding to both an antigen and the molecule that presents the antigen, major histocompatibility complex (MHC). A second signal induced by co-stimulation through binding of CD80/86 to CD28 is required. CTLA-4 competes with the CD28 molecule to inhibit T-cell activation. PD-1 on T cells bind to PD-L1 on antigen presenting cells (APC) or tumor cells as a regulatory mechanism of preventing autoimmunity in normal conditions. **(B)** Tumor cells take advantage of the PD-1/PD-L1 and CDLA-4/CD80/86 inhibitory systems to "escape" the immune-cell regulation and killing of tumor cells. Listed are the current

FDA-approved immune checkpoint inhibitors in which their purposes are to allow T-cell recognition and killing of tumor cells.

1.2.c. Cytokine therapies

Cytokines are proteins released by both immune and non-immune cells as a method of communication during standard migration, response to inflammation, and tumorigenesis [29]. Unlike other immunotherapies, they are not a targeted therapy, and most FDA-approved cytokines include black box warnings of severe systemic toxicities [30]. However, cytokines such as interleukin 2 (IL-2), interferon-alpha (IFN-α), and granulocyte-macrophage colony-stimulation factor (GM-CSF), have shown some clinical benefits. For example, large doses of IL-2, a T-cell stimulating/growth factor, regressed metastatic cancer in patients [31,32] and IFN-α, an anti-viral and anti-tumor type I interferon, showed clinical benefit in chronic myeloid leukemia (CML) and melanoma [33,34]. GM-CSF modulates the function of innate cells in response to infections and tumorigenesis and have shown positive responses in both prostate and melanoma patients [35,36]. Pertinent to NB, IL-2 and GM-CSF are given in combination with dinutuximab in NB patients following adjuvant therapy, and the triple combination has shown significant success in improving patient survival. However, direct effects of GM-CSF and IL-2 cannot be concluded based on these studies as single agent dinutuximab was not introduced as a study arm [9].

1.2.d. Cancer vaccines

Cancer vaccines fall into two categories based on the timing and purpose of administration. Prophylactic vaccines are designed to prevent the onset of disease, and therapeutic vaccines are administered for treatment of an existing disease. Vaccines against hepatitis B and human papillomavirus are examples of prophylactic vaccines that prevent an infection by oncogenic

viruses and have been pivotal in reducing incidences of hepatocellular carcinoma and cervical cancer [37]. Therapeutic vaccines were initially proposed and tested with the discovery of tumor associated antigens (TAA), while newer approaches in developing personalized recombinant vaccines are thought to be more effective [38]. This involves sequencing of a patient's healthy tissue and tumor tissue in which gene variants specific to the tumor are identified, then prediction algorithms used to screen for these neoantigens most likely to bind to the patients' specific major histocompatibility complex (MHC) molecules. Further research is required to better determine both the effectiveness and mechanisms of action of these vaccines.

1.2.e. Adoptive cell therapies

Adoptive cell therapies (ACT) are allogenic or autologous lymphocytes infused into cancer patients (**Figure 1.2.3A-B**). This variety of therapy first showed promise in 1966, when co-transplantation of patient-derived leukocytes and autologous tumor cells demonstrated tumor regression of advanced cancers [39]. Tumor-infiltrating lymphocytes (TILs) isolated from patient tumor and expanded *ex vivo* have been first utilized as therapy in the 1980, with a promising objective response (OR) of 34%, however this response was not sustained long term [40]. It wasn't until following studies that included lymphodepletion prior to ATC, that complete tumor regression with sustained response was seen [41]. Strides in high-throughput technology development have made it possible to enrich for neoantigen-specific TILs; however, not all cancers have effector T cells with anti-tumor activity, making TIL-based therapies ineffective, and as a result, created a need for engineered T cells to target a greater range of cancer types.

T-cell receptor (TCR)-engineered therapy was designed to overcome such issues but is limited due to their dependence on tumor antigen presentation by MHC. One way to overcome this limitation, is by engineering a complex to mimic the same effector T-cell signaling domains while eliminating the need for MHC presentation for antigen recognition. The first generation of

these chimeric antigen receptor (CAR) T cells included an antigen binding region made up of the single chain variable fragments of monoclonal antibodies against the antigen of interest, a hinge domain for flexibility of the binding domain, and importantly, the CD3ζ domain that simulates the start of TCR signaling. First-generation CARs showed promise pre-clinically, however did not live up to the hype in clinical trials, due to failed T-cell proliferation and cytokine production [42,43]. Improved versions have been made since, including second-generation and third-generation CARs that add single or dual co-stimulatory domains such as CD28 or 4-1BB that aids in cytokine production, or most decorated, fourth-generation CARs that include further modifications to improve antitumor efficacy of T cells.

CAR T-cell therapies against an antigen, CD19, has shown remarkable success in hematological cancers, and trials against CD22 and B-cell maturation antigen (BCMA)-target shows early promise in the same cancer types. Early clinical trials have not shown the same success of CAR T-cell therapy for solid tumors, mainly attributed to lack of trafficking, tumor immunosuppressive microenvironment, and persistence. In NB, clinical efficacy of CAR T cells against GD2 has been shown to be safe and feasible, but significant barriers in efficacy remained, until very recently in April 2023, when a clinical trial for relapsed or refractory high-risk NB treated with third-generation CAR T cells resulted in an overall response rate of 63% (17/27) [44].

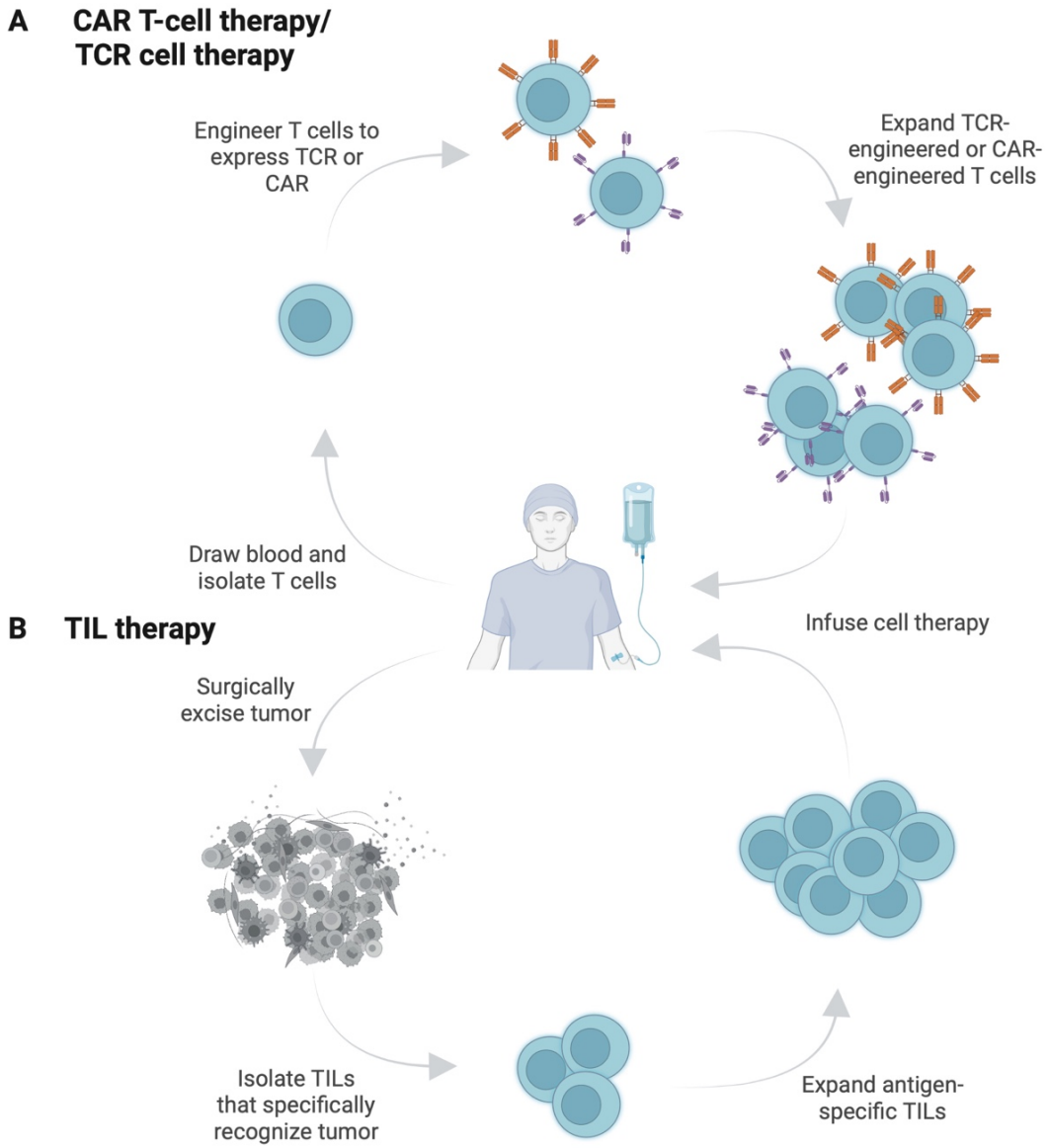

Figure 1.2. 3. Adoptive cell therapies for cancer

(A) Chimeric antigen receptor (CAR) T-cell and TCR cell therapies are manufactured in a similar process where patient or donor T cells are engineered to express CAR or endogenous TCR, then activated and expanded to infuse back into the patient for treatment. **(B)** Tumor infiltrating lymphocyte (TIL) therapy starts with the excision of bulk tumor from a patient followed by isolation and expansion of TILs that specifically recognize the tumor, prior to reinfusion.

1.2.f. $\gamma\delta$ T-cell therapies

The identification of the third TCR chain, γ chain, led to the discovery of $\gamma\delta$ T cells in 1984 [45-47]. Like $\alpha\beta$ T cells, a subset of $\gamma\delta$ T cells may clonally expand during infections and act upon secondary challenges in a similar method [48]. In addition, like NK cells, $\gamma\delta$ T cells react to infected or neoplastic cells through receptor-ligand interactions without prior exposure [49,50]. Jointly, these functions have set $\gamma\delta$ T cells on a bridge between both innate and adaptive immunity. There are eight Vδ TCR subtypes, of which, Vδ1, Vδ2, and Vδ3 are the most used segments, therefore utilized to classify $\gamma\delta$ subtypes [51-53] and defined as follows. Both Vδ1 and Vδ2 cells have been tested as therapies for cancer [54]. Vδ1+ cells, while may be present in very small numbers in circulating blood, typically lie in mucosal tissues [55] and are important direct responders to viral infections [56,57], while Vδ2+ cells are most present in circulating blood and lymphoid organs. Vδ2's are almost exclusively paired with the Vγ9 chain. Vγ9Vδ2 T cells make up 60-95% of $\gamma\delta$ T cells in adult peripheral blood presenting a TCR repertoire that can effectively respond to phosphoantigens that develop in infected or malignant cells [58,59]. Phosphoantigen stimulation of $\gamma\delta$ T cells and IL-2 can result in selective expansion of Vγ9Vδ2 T cells *ex vivo* [60,61] and utilized to induce antitumor activity. In leu of phosphoantigen stimulation, derivatives such as zoledronate acid are commonly used and tested clinically [62].

Unlike classical $\alpha\beta$ T cells, $\gamma\delta$ T cells are not MHC-restricted which expands the donor pool, making them an ideal candidate for off-the-shelf cellular therapies [49] (**Figure 1.2.4A**). Furthermore, Vγ9Vδ2 T cells express NK cell receptors (NKRs) that promote the innate cytotoxicity against tumor cells, such as C-type lectin-like receptor natural killer group 2 member D (NKG2D), multiple UL16-binding proteins (ULBPs) , Fas ligand (FasL), and of note, CD16, the low-affinity IgG Fc region receptor III (FCγRIII) [54,63-65] (**Figure 1.2.4B**). Vγ9Vδ2 T cells have been shown to be cytotoxic against several solid tumors and leukemia/lymphoma cells [66,67]. In

addition, our lab has previously shown *ex vivo* expanded, non-modified $\gamma\delta$ T cells, in combination with temozolomide and dinutuximab, have anti-tumor effects on NB metastatic tumor model [68].

Historical studies of $\gamma\delta$ T cell-based therapies in patients with blood or solid tumor malignancies revealed a safe profile, however showed limited to no response (e.g. NCT03183232, NCT03183219) [69-71]. Thus, human studies to enhance $\gamma\delta$ T cells with antibody engagers, CARs, or TCRs, are underway with the idea to increase the potency of these cells. A first-in-human trial of a monoclonal antibody-targeting butyltrophin BTN3A to enhance the anti-tumor efficacy of endogenous $\gamma\delta$ T cells, is being tested in patients with advanced-stage relapsed or refractory cancers (NCT04243499), where preliminary results show promotion of immune cell infiltration [72]. Clinical studies with bispecific engagers made up of a T-cell targeting domain and tumor-cell targeting domains are also underway (e.g. NCT04887259), and awaiting interim analysis. Pre-clinical evidence shows bispecific engagers lead to specific tumor cell lysis, selective activity, and/or recruitment of Vγ9Vδ2+ cells at low effector to target ratios in blood and solid tumors [73-77]. Promisingly, in 2020, allogeneic Vγ9Vδ2+ cells prolonged the survival of patients with late-stage lung or liver cancer [78]. Feasibility of utilizing CAR-transduced $\gamma\delta$ T cells was first reported in 2004 with GD2 or CD19 CAR-expressing cells [79]. Current ongoing clinical trials include NKG2D ligand-directed Vγ9Vδ2 CAR T cells in colon and ovarian cancer (NCT04107142) and CD20-directed Vγ1 CAR T cells in B cell lymphoma (NCT04735471). Finally, several clinical studies that test the feasibility of engineering $\alpha\beta$ T cells with $\gamma\delta$ TCR are underway (NCT04688853, NCT03415399, NCT04502082, NCT04634357).

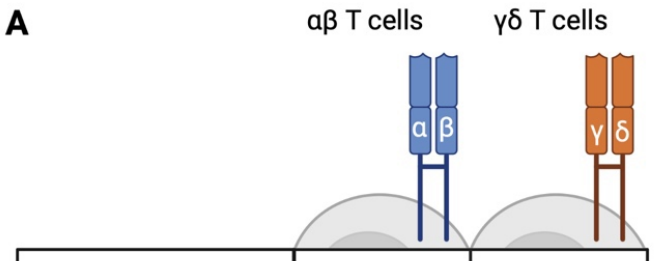

	αβ T cells	γδ T cells
MHC restriction	yes	no
Donor option	+	+++
Intrinsic anti-tumor effector function	+	++
Persistence	++	+

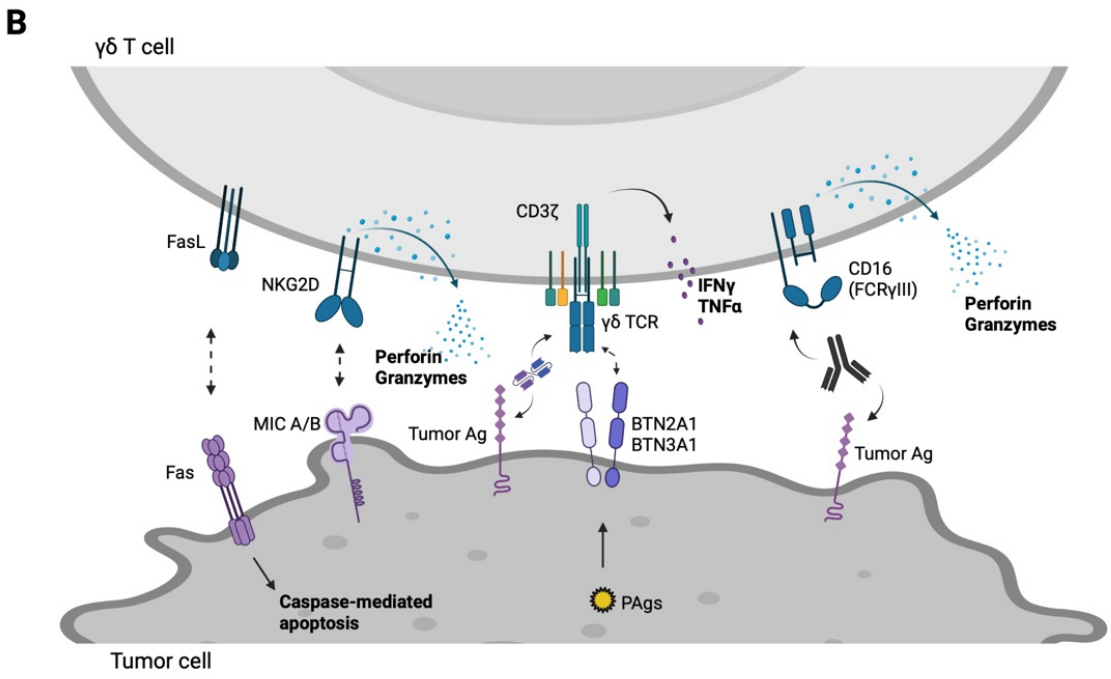

Figure 1.2. 4. *γδ* T cells for cellular therapy

(A) Unlike ***α***β T cells, ***γδ*** T cells are not major histocompatibility complex (MHC) restricted, expanding the cell therapy donor pool beyond the patients' own or a matched pair. ***γδ*** T cells have an intrinsic NK cell-like anti-tumor effector function against tumor cells. Their lack of persistence as compared to ***α***β T cells is a safety advantage or sustained therapy disadvantage of T cells. **(B)** ***γδ*** T cells have multiple mechanisms of inducing tumor-cell death which include Fas/FasL-

mediated apoptosis, NKG2D binding to stress ligands MIC A/B, $\gamma\delta$ T-cell receptor (TCR)-mediated activity and cell death, and finally, through CD16 (FCRγIII) recognition of tumor antigens.

1.2.g. Immunotherapies for neuroblastoma

Currently, disialoganglioside, GD2, is the only antigen targeted with an immunotherapy as standard treatment for high-risk NB. GD2 is an acidic glycolipid that lies on the outer cellular membrane on peripheral neurons, central nervous system, and skin melanocytes [80]. GD2 was found to be highly expressed in primary NB tumor cells in 1986 [81] and subsequently been exploited as an immunotherapeutic target for NB since. Monoclonal antibodies have been developed and tested against NB and in 2015, dinutuximab, a human-murine chimeric antibody, was approved by the FDA and European Medicines Agency (EMA), in combination with GM-CSF, IL-2, and cis-retinoic acid for treatment of high-risk NB patients [82] (**Figure 1.2.5A**).

The success of cancer immunotherapies have been highlighted by the success of checkpoint inhibitors in skin cancers [83] and adult lung carcinomas [84], and CAR T cells in hematological malignancies [85,86]. Unlike adult cancers, pediatric cancers, including NB, lack high tumor mutational burden and downregulate MHC-1 [87], classifying NB to be immunologically "cold". Therefore, investigators focus efforts on targeting NB with synthetic engineering of immunotherapeutic agents. For example, on top of dinutuximab therapy, targeting NB through CAR T cells and antibody-drug conjugates (ADC) has demonstrated early clinical efficacy [88].

In addition to GD2, other molecules have been identified as promising target antigens for NB (**Figure 1.2.5A**) including CD171 (L1CAM) and a checkpoint molecule, B7H3. Early phase immunotherapy clinical trials are underway for the targeting of GD2 and others in published (**Table 1.1**) or unpublished (**Table 1.2**) trials, with the hope of deploying new successful therapies for treating NB.

A

	FDA-approved for NB
Antibodies	• Dinutuximab (anti-GD2)
Cytokines	• IL-2 • GM-CSF

	Under Clinical Trials
NK cells	• Allogeneic NKs • Autologous NKs
CAR T cells	• Anti-GD2 • Anti-B7H3 • Anti-CD171 (LCAM)
Antibodies	• Anti-GD2 BiTE • Nivolumab (anti-PD-1) • Ipilimumab (anti-CTLA-4) • Racotumomab (anti-idiotype, NGcGM3) • Ivosidenib (anti-IDH1) • Bevacizumab (anti-VEGF) • Lorvotuzumab mertansine (anti-CD56 ADC)
Immune-modulatory agent	• Lenalidomide • IL-7
Cancer Vaccines	• GVAX GM-CSF gene vaccine • Bivalent vaccine (anti-GD2L/GD3L) • Allogenic tumor cell line vaccine secreting IL-2/ Lptn

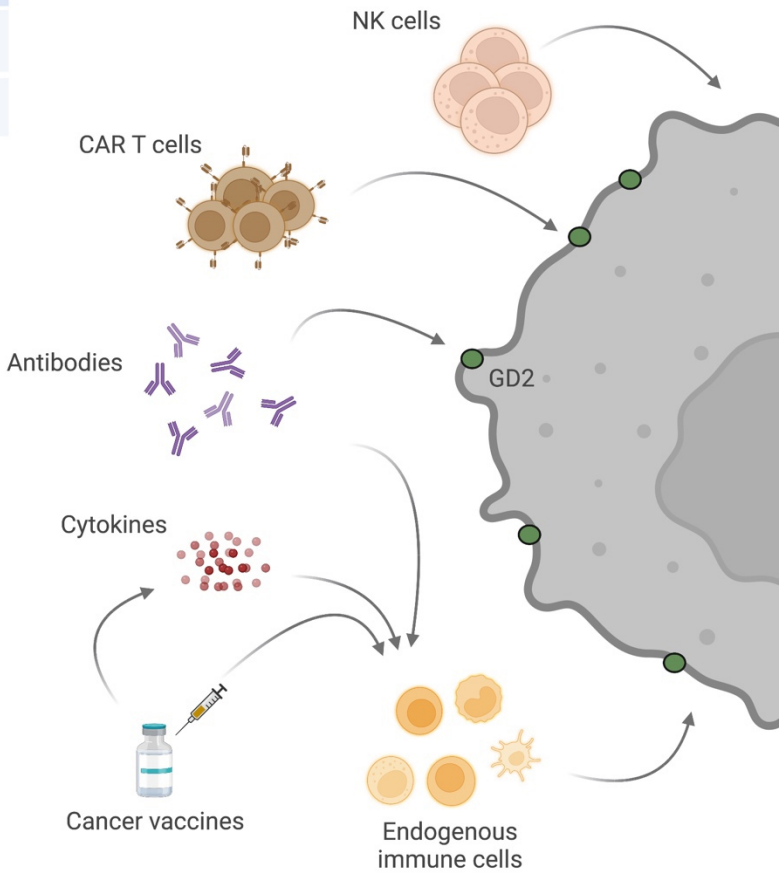

Figure 1.2. 5. Immunotherapies for neuroblastoma

(A) Top: FDA approved immunotherapies and current neuroblastoma maintenance therapy. Bottom: Immunotherapies against associated antigens under clinical trials. Right: Graphical depiction of indicated immunotherapies in (A).

Target	CAR design	Delivery	Disease	Phase	NCT ID	Region	Drug Schedule	Patients/Response	Toxicities	References
GD2 (14.G2a)	CD3ζ	Retroviral	R/R NB	Phase I	NCT00085930	Houston, Texas, US	No lymphodepletion. 1e7-1e8/m2 dose escalation of EBV-specific CAR T cells and CTL CAR T cells.	19 NB 21% (4) OR	No DLT	Louis et al., Blood, 2011
GD2 (14.G2a)	CD28.OX40.CD3ζ + iC9 safety	Retroviral	R/R NB	Phase I	NCT01822652	Houston, Texas, US	Dose escalation of CAR T alone, CAR T with fludarabine-cyclophosphamide, or CAR T with fludarabine-cyclophosphamide and Pembrolizumab.	11 NB No OR	No DLT	Pule et al., Nat Med, 2008 Heczey et al., Mol Ther, 2017
CD171 (L1CAM)	4-1BB.CD3ζ CD28.4-1BB.CD3ζ 4-1BB.CD3ζ + long spacer	Lentiviral	R/R NB, Ganglioneuroblastoma	Phase I	NCT02311621	Seattle, Washington, US	All patients received lymphodepleting chemotherapy after which cryopreserved CD4 and CD8 CARs were administered at a 1:1 ratio at the prescribed dose level. Dose range is 1x10^6/kg-1x10^8/kg.	22 NB No OR	DLT with hyponatremia in 2 patients, self-limited rash in 5 patients	Pinto et al., ANR abstract, 2018
GD2 (KM8138)	CD28.CD3ζ	Retroviral	R/R NB	Phase I	NCT02761915	London, UK	Dose escalation of cyclophosphamide or fludatabine-cyclophosphamide followed by 1e7-10e8/m2 cell dose escalation of CAR T cells	12 NB No OR	No DLT. CRS observed in patients receiving >1e8/m2 (2 G2/3). Regression of soft tissue and bone marrow disease observed in 3 patients.	Straathof et al., Sci. Transl. Med., 2020
GD2	NKT cells 2nd gen, CD28 co-stimulatory, IL-15	Retroviral	R/R NB	Phase I	NCT03294954	Houston, Texas, US	Fludarabine-cyclophosphamide lymphodepletion following by dose level 1 of 3e6/m2 (in interim analysis) of autologous NKT CAR T cells with IL-15	3 NB (interim) 33% (1) OR	No DLT	interim analysis Heczey et al., Nat Med, 2020
GD2 (hu3F8)	CD28.4-1BB.CD27.CD3ζ + iCasp9 safety	Lentiviral	R/R NB	Phase I	NCT02765243	Guangzhou, Guangdong, China	Patients received fludarabine-cyclophosphamide conditioning. The CAR T infusion dose was at average 1.1x10^6/kg.	10 NB No OR	No DLT. CRS observed in 9 patients (4 G1, 5 G2)	Yu et al., J Cancer Res Clin Oncol, 2022
GD2	OX40.CD28.CD3ζ + iCD9 safety	Retroviral	R/R NB, Osteosarcoma, Sarcoma, Melanoma	Phase I	NCT02107963	Bethesda, Maryland, US	Cyclophosphamide-based lymphodepletion with cell dose escalation of 1e5-1e7/kg cell dose escalation of transduced T cells.	Unknown	Unknown	Kaczanowska et al., SITC2022
GD2 (14.G2a)	CD28.4-1BB.CD3ζ + iCASP9 safety	Retroviral	R/R NB and other GD2-positive solid tumors incl. osteosarcoma, Ewing sarcoma	Phase I/II	NCT03373097	Rome, Italy	Fludarabine-cyclophosphamide lymphodepletion followed by infusion of 3e6, 6e6, or 10e6 CAR-positive T cells/kg. 11 patients received multiple infusions with a range of 2-4.	27 NB 63% (17) OR	No DLT. CRS observed in 20 patients (19 G1/2, 1 G3)	Bufalo et al., NEJ, 2023

Table 1. 1. Published CAR-T cell clinical trials for neuroblastoma

Listed top to bottom in the order of publication year. Published clinical trials of CAR T cells target mostly GD2, with one targeting CD171 (L1CAM) antigen. Some studies have concluded, others are ongoing.

Target	Disease	Phase	NCT ID	Region	CAR design/treatment	Estimated Enrollment	Study Start	Study Completon
GD2	NB, Osteosarcoma	Phase I	NCT01953900	Houston, Texas, US	iC9.VZN.CTLs	26 participants All	October 2014	October 2034
GD2	R/R NB, Osteosarcoma, Ewing sarcoma, rhabdomyosarcoma, uveal melanoma, phyllodes breast tumor	Phase I	NCT03635632	Houston, Texas, US	C7R(IL-7)-GD2.CART	94 participants 1 yo - 74 yo	April 2019	December 2038
GD2	R/R NB, R/R Osteosarcoma	Phase I	NCT03721068	Atlanta, Georgia, US Chapel Hill, North Carolina, US	2nd gen.iC9.GD2.CAR.IL-15	18 participants 18 mo and older	Februrary 2019	June 2039
GD2 (14.G2a)	R/R NB	Phase I	NCT01460901	Kansas City, Missouri, US	Allogenic virus specific T cell CD3ζ Retroviral	5 participants 18 mo - 17 yo	July 2019	July 2019
GD2	R/R NB, R/R Osteosarcoma	Phase I	NCT04539366	Los Angeles, California, US Palo Alto, California, US Bethesda, Maryland, US Philadelphia, Pennsylvania, US Seattle, Washington, US Madison, Wisconsin, US	Retroviral vector Autologous GD2CART	67 participants up to 35 yo	June 2021	August 2024
EGFR	R/R solid tumors including NB	Phase I	NCT03618381	Seattle, Washington, US	Arm 1: 2nd gen, 4-1BBz EGFr806CAR(2G)-EGFRt Arm 2: 2nd gen, 4-1BBz EGFR806-EGFRt and CD19CAR(2G)-T2A-HER2tG	36 participants 1 yo - 30 yo	June 2019	June 2038
CD276 (B7-H3)	R/R solid tumors including NB	Phase I	NCT04483778	Seattle, Washington, US	Arm 1: 2nd gen 4-1BBz B7H3-EGFRt-DHFR Arm 2: 2nd gen, 4-1BBz B7H3-EGFRt-EGFRt-DHFR(selected) and 4-1BBz CD19-Her2tG	68 participants up to 26 yo	July 2020	December 2040
GD2, PSMA, CD276 (B7-H3)	R/R NB	Phase I/II	NCT04637503	Guangzhou, Guangdong, China Shenzhen, Guangdong, China Shenzhen, Guangzhou, China Jinan, Shandong, China	multi-4SCAR-T	100 participants 1 yo - 65 yo	November 2020	December 2023
CD276 (B7-H3)	NB, Osteosarcoma, Gastric cancer, Lung cancer	Phase I	NCT04864821	China	Autologous	24 participants 1 yo - 70 yo	May 2021	May 2023
CD276 (B7-H3)	R/R solid tumors including NB	Phase I	NCT04897321	Memphis, Tennessee, US	Unknown	32 participants up to 21 yo	July 2022	February 2026
CD276 (B7-H3)	R/R NB	Phase I	NCT05562024	Jinan, Shandong, China Tianjin, Tianjin, China	Unknown	24 participants 1 yo and older	December 2022	February 2039
GPC2	R/R NB	Phase I	NCT05650749	US	Unknown CAR design	30 participants 1 yo and older	October 2023	January 2026

Table 1. 2. Unpublished CAR-T cell clinical trials for neuroblastoma

Listed top to bottom in the order of study start date. Target antigens include GD2, EGFR, CD276 (B7-H3), PSMA, and GPC2.

1.3 PTK7 identification, expression, and function in neuroblastoma

Protein tyrosine kinase 7 (PTK7) was identified as a promising NB target in the Goldsmith Lab of Emory University and published together with the work presented in this dissertation on targeting PTK7 through CAR T-cell therapy (Lee J.Y. and Jonus H.C. *et al. Cell Rep Med*. 2023). PTK7 was identified through a discovery platform that identifies N-glycoproteins in a model that represents a post-chemotherapy refractory/recurrent patient population (**Figure 1.2.6A**). Cell surface protein expression was validated by flow cytometry in eight NB cell lines and six NB patient-derived xenograft models or primary patient tumors (**Figure 1.2.6B**). In a survival analysis of advanced stage disease (p=0.039) and MYCN amplified tumors (p=0.028), high PTK7 expression was correlated with poor outcome (**Figure 1.2.6C**). Interestingly, PTK7 was not required for NB cell proliferation or chemotherapy response (**Figure 1.2.6D**). Future investigations will test PTK7 involvement in cell motility, tumor initiation, and metastasis. Finally, important to determining a target candidate, normal tissue expression of PTK7 was evaluated with a pediatric-specific microarray (**Figure 1.2.6E**). Most tissues stained negative for PTK7, with the exception of five tissues that stained weakly positive (IHC = 1). The high NB tumor cell expression of PTK7 and low expression in pediatric normal tissues, support further evaluation of PTK7 as a target.

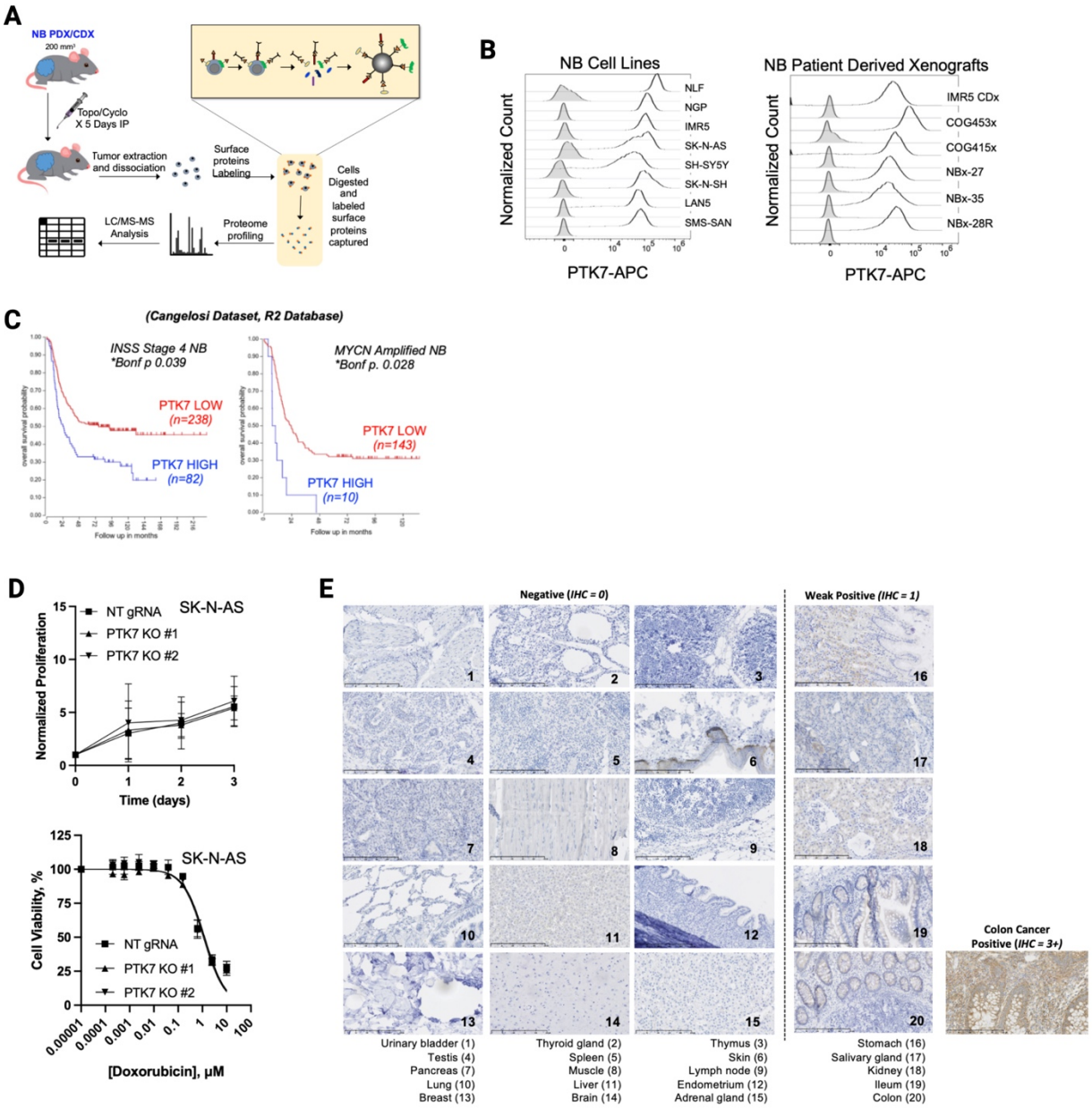

Figure 1.2. 6. Identification of PTK7 as an immunotherapy target in neuroblastoma

(A) Schematic depicting *in vivo* modeling and cell surface capture technique with glycoproteomics used to identify NB cell surface immunotherapy targets. **(B)** Histograms depicting PTK7 expression in an array of NB cell lines (left) and patient-derived xenografts (right). Isotype control is solid grey. **(C)** Survival analysis using the R2 database (Cangelosi Dataset, 10.3390/cancers12092343) depicting the impact of PTK7 expression towards patient prognosis. INSS Stage 4 or MYCN amplification categories were chosen as they most closely represent high

risk disease. **(D)** Top: Normalized proliferation determined by cell-titer glo (CTG) of PTK7 KO cells for NB cell models. n = 3 biological replicates. Bottom: Cell viability of PTK7 KO cells following doxorubicin treatment for 48-hours. IC50 values calculated through non-linear regression. n.s. no significant difference in value in KOs vs NT gRNA control. n = 3 biological replicates. **(E)** PTK7 expression in pediatric normal tissues representative of all major organs. Where possible, duplicate tissues were analyzed and scored representative of both male and female. Figures curtsey of the Goldsmith Lab and published in Lee J.Y. and Jonus H.C. *et al. Cell Rep. Med.*, 2023.

Chapter 2: Engineering and characterization of anti-PTK7 chimeric antigen receptor (CAR)

Jasmine Y. Lee, Gianna M. Branella, Andrew Fedanov, Victor Maximov, Kelly C. Goldsmith, and H. Trent Spencer

Jasmine Y. Lee designed cloning constructs and experiments, conducted all experiments, and wrote this section of the paper.

Gianna M. Branella designed a cloning construct and assisted with preliminary experiments.

Andrew Fedanov produced all lentiviral vectors.

Victor Maximov produced SK-N-AS PTK7 CRISPR/Cas9 knock-out cell lines

Kelly C. Goldsmith and H. Trent Spencer conceived targeting PTK7 with CAR and edited this section of the paper.

Parts of the work in this chapter was published in *Cell Reports Medicine* in 2023. See also Chapter 4 for work published in same paper.

Citation:

Jasmine Y. Lee, Hunter C. Jonus, Arhanti Sadanand, Gianna M. Branella, Victor Maximov, Suttipong Suttapitugsakul, Matthew J. Schniederjan, Jenny Shim, Andrew Ho, Kiran K. Parwani, Andrew Fedanov, Adeiye Pilgrim, Jordan Silva, Robert W. Schnepp, Christopher B. Doering, Ronghu Wu, H. Trent Spencer, and Kelly C. Goldsmith. Identification and targeting of protein tyrosine kinase 7 (PTK7) as an immunotherapy candidate for neuroblastoma cellular therapy. *Cell Rep Med*. 2023.

2.1 Abstract

To determine the feasibility of targeting a candidate marker identified to be highly expressed in neuroblastoma, we designed and developed anti-PTK7 chimeric antigen receptors (CAR). Two variations of the CAR were tested, in which the variable light (VL) and variable heavy (VH) chains of the single-chain variable fragment (scFv) varied. VH-L-VL orientation resulted in higher transduction efficiency and CAR expression/binding to PTK7. Additionally, PTK7 CAR T cells became specifically activated in the presence of several NB cell lines. Similar activation was not observed when CAR T cells were co-cultured with PTK7-negative cell line or NB cell lines with CRISPR/Cas9 knockout of PTK7, showing specific activation of PTK7 CAR to antigen-positive cells. Lastly, different promoters were tested for optimal transgene expression and translation to cell surface CAR expression and showed EF1α-based promoter was the superior promoter to express PTK7 CAR. Together, these data support the use of EF1α-based PTK7 VH-L-VL CAR construct for downstream functional analysis.

2.2 Introduction

The first FDA-approved chimeric antigen receptor (CAR) T-cell therapy, tisagenlecleucel, is a 2nd generation CD19 CAR with CD137 (4-1BB) co-stimulatory and CD3ζ signaling domains [85]. Since its approval, various CAR designs have been tested both preclinically and clinically [89-91]. Traditional CAR components in the order of extracellular to intracellular include the scFv that binds the target, a hinge to increase flexibility of the scFv, transmembrane domain for cell membrane anchoring, co-stimulatory domain to enhance T-cell activity, and lastly a CD3ζ domain that starts the T-cell activation cascade. While exploration of different CAR components is critical for optimization of T-cell persistence and cytotoxic potential, current research in CAR optimization utilize well established targets, most notably, CD19 [91]. Given the recent identification of PTK7 being highly expressed on the cell surface of neuroblastoma (NB) cells (see Chapter 1.3),

our main objective here was to design a sufficient CAR against PTK7 to determine the feasibility of targeting PTK7 in NB.

2.3 Results

Anti-PTK7 scFv sourcing and other CAR components

We first generated two lentiviral-based second-generation PTK7 CAR transgenes. Both versions of the CAR contain a single-chain variable fragment (scFv) that binds PTK7, followed by a CD8 hinge, CD28 co-stimulatory and transmembrane domain, and a CD3ζ signaling domain (**Figure 2.1A**). The variable light (VL) and variable heavy (VH) sequences of the scFv were taken from United States Patent 9102738 on human monoclonal antibodies to PTK7. We chose to utilize the VL and VH regions of clone 12C6 as they show it moderately bound both cell-free and cell-bound PTK7. The two versions of the CAR were made with differences in the orientation of the VL and VH regions of the scFv (VL-linker-VH and VH-linker-VL). Upstream of the CAR transgene, eGFP and P2A ribosomal skipping sequences were used to determine transduction efficiencies. A third lentiviral-based PTK7 CAR was later generated to optimize CAR expression **(Figure 2.1B**). This transgene will be described further in Figure 2.5.

As with other CARs, the components of our PTK7 CAR mimic the endogenous T-cell receptor (TCR) signaling pathway (**Figure 2.2A**). After the scFv on the engineered T cell binds a PTK7 antigen, a downstream signaling cascade is expected to release perforin and granzyme B that induce targeted tumor cell death through apoptosis (**Figure 2.2B**).

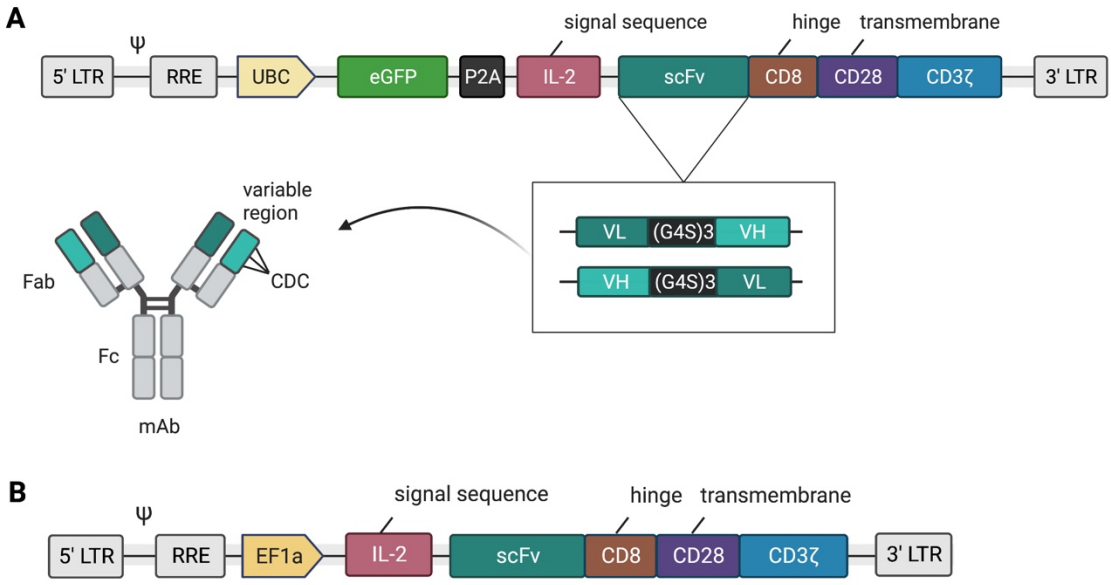

Figure 2. 1. Design of anti-PTK7 CAR DNA constructs

(A) Lentiviral vector-based UBC eGFP PTK7 CAR construct with VL-L-VH or VH-L-VL scFv orientation. **(B)** Lentiviral vector-based EF1a PTK7 CAR construct with VH-L-VL scFv orientation.

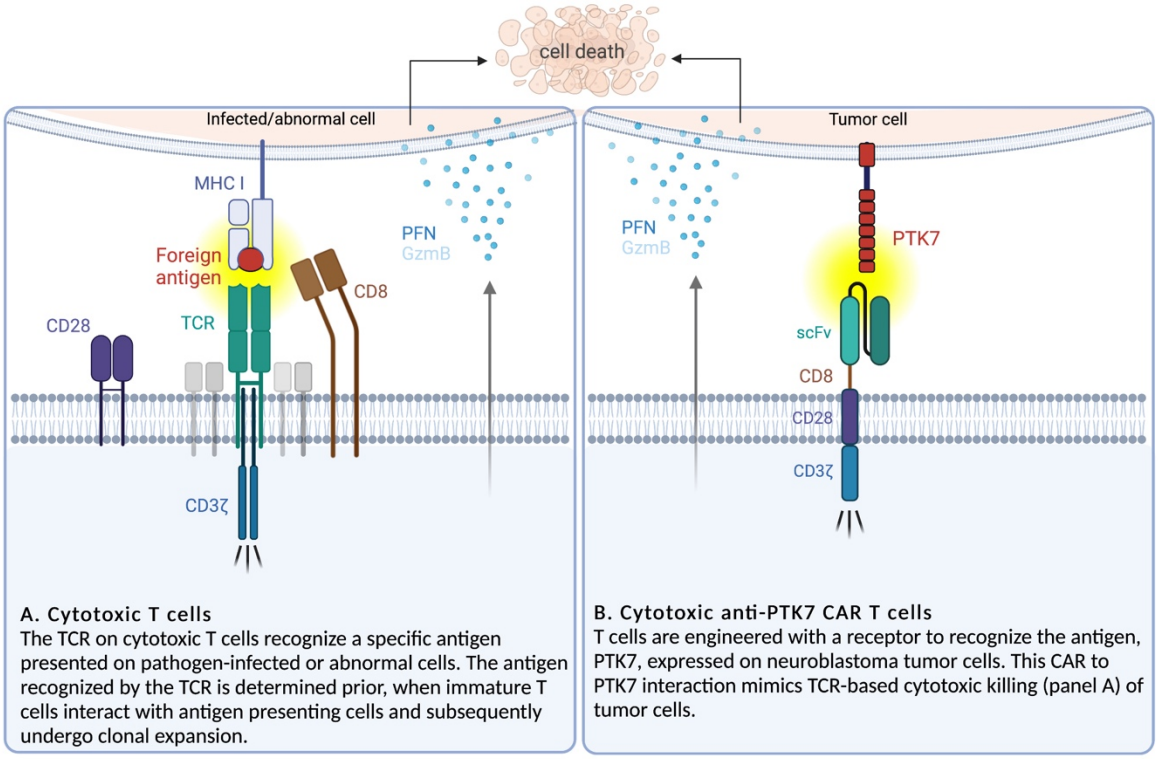

Figure 2. 2. Endogenous T cell-mediated cytotoxicity v. PTK7 CAR T cell-mediated cytotoxicity

(A) Cytotoxic mechanism by endogenous T cells. Binding of TCR on T cells to antigen/MHC complex on antigen presenting cells start a signaling cascade that begins at the CD3ζ domain then through complex sequential signaling not shown, with the eventual release of perforin (PFN) and granzyme B (GzmB) that target the infected or abnormal target cell. CD28, a co-stimulatory domain, is typically required as a second signal to the TCR/CD3ζ signal to induce a potent response. CD8 acts as a co-receptor during T-cell antigen binding. **(B)** Proposed cytotoxic mechanism of anti-PTK7 CAR T cells. MHC-unrestricted tumor cell killing modeled with components of endogenous TCR signaling molecules.

VH-L-VL scFv orientation is superior to VL-L-VH

Jurkat T cells were utilized to confirm CAR protein expression, ability to bind to PTK7, and test antigen-specific CAR activation as follows. Cells transduced with PTK7 CAR lentiviral vectors at multiplicity of infection (MOI) of 2.5, 5, and 10 yielded 22% ± 1, 39% ± 1, and 47% ± 5 GFP+ cells respectively for PTK7 VL-L-VH CAR and 38% ±6, 60% ± 5, and 80% ± 2 GFP+ cells for VH-L-VL CAR (**Figure 2.3A**). Within the transduced (GFP+) population, percent cell surface CAR expression and binding was measured by use of human PTK7-Fc. PTK7 VL-L-VH CAR was expressed in 71% ± 10 of the transduced population, and 89% ± 4 in VH-L-VL CAR (**Figure 2.3B**). The expected molecular weight of both PTK7 CARs, 54.7 kDa, is shown in a western blot of whole cell lysate against CD3ζ, and the expected band intensities increase with increasing MOI (**Figure 2.3C**), as do breakdown products. Altogether, the VH-L-VL CAR showed higher transduction efficiency and overall higher cell surface binding and expression. This CAR was selected for further studies, referred to as PTK7 CAR.

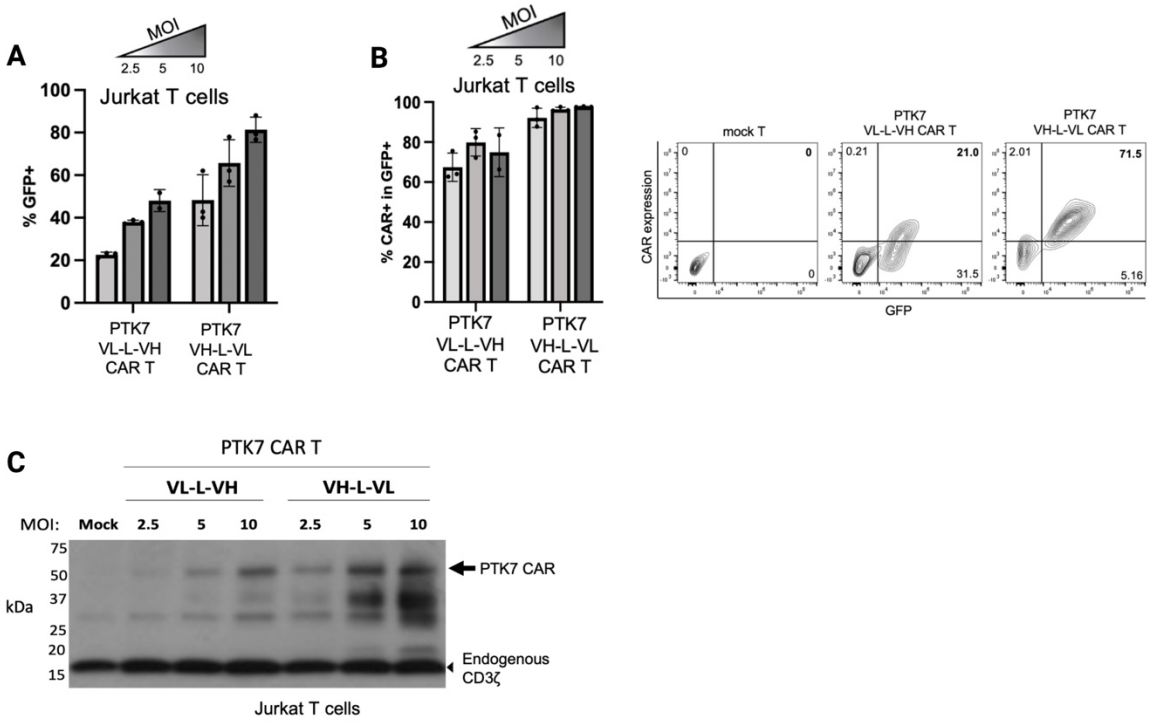

Figure 2. 3. VH-L-VL scFv orientation is superior to VL-L-VH

(A) %GFP+ Jurkat T cells transduced with PTK7 VL-L-VH CAR or PTK7 VH-L-VL CAR, gated on live cells, n = 3 biological replicates. **(B)** Left: %CAR+ (PTK7-Fc chimera+) Jurkat T cells transduced with PTK7 VL-L-VH CAR or PTK7 VH-L-VL CAR. Gated on live GFP+ cells, n = 3 biological replicates. Right: Representative flow plots showing GFP v. CAR expression in Jurkat T cells, gated on live cells. **(C)** CAR western blot from whole cell lysate of Jurkat T cells transduced with PTK7 VL-L-VH CAR or PTK7 VH-L-VL CAR, 3 days post-transduction. Western blot antibody against human CD3ζ. Expected molecular weight of CAR protein is 54.7 kDa.

PTK7 CAR T cells have antigen-specific activity

Jurkat PTK7 CAR T cells were then used to evaluate for on target T-cell activation in the presence of PTK7-positive NB cells. PTK7 CAR T cells were co-cultured with PTK7-positive or PTK7-negative NB cells or PTK7-negative CMK cells. After four hours of co-incubation, cell surface

CD69, an early T-cell activation marker, was measured within GFP+ effector CAR T cells. CD69 expression increased above baseline in Jurkat PTK7 CAR T cells when co-cultured with IMR5 NB cells but not with PTK7-negative CMK cells (**Figure 2.4A**). Jurkat T cells express low levels of PTK7, resulting in slightly elevated baseline CD69 expression due to Jurkat autoactivation by the PTK7 CAR (**Figure 2.4B**). Importantly, peripheral primary alpha beta T cells, that are used for CAR T-cell therapy clinically, lack PTK7 on their cell surface. CD69 increased on PTK7 CAR T cells co-cultured with SK-N-AS control cells but did not increase above baseline in two separate SK-N-AS cell lines with PTK7 genetically knocked out (KO) (**Figure 2.4C**). A CD19 CAR with the same backbone was used as an irrelevant-antigen CAR T-cell control as SK-N-AS cells do not express CD19. Collectively, our data show PTK7 CAR is expressed at the cell surface, able to bind PTK7, and is capable of activation in the presence of cells that are positive for cell surface PTK7.

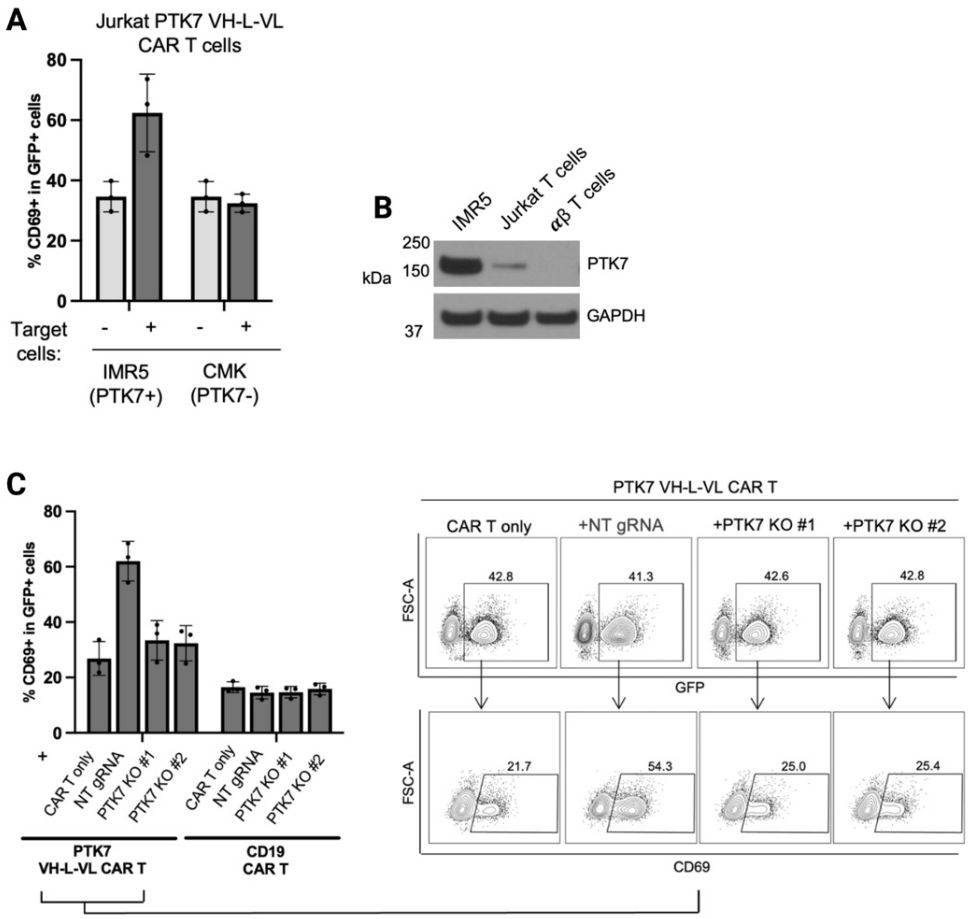

Figure 2. 4. PTK7 CAR T cells have antigen-specific activity

(A) %CD69+ Jurkat T cells cultured with (+) or without (-) target cells, gated on live GFP+ cells, n = 3 biological replicates. **(B)** PTK7 and GAPDH western blot of Jurkat T cell and primary T cell whole cell lysate. **(C)** Left: %CD69+ Jurkat T cells transduced with PTK7 VH-L-VL CAR or CD19 CAR co-cultured with target cells (SK-N-AS non targeting gRNA control or SK-N-AS PTK7 KO), gated on live GFP+ cells, n = 3 biological replicates. Right: Representative flow plots showing CD69 expression within GFP+ Jurkat CAR T cells.

EF1*α* promoter is required for optimal CAR expression in primary T cells

Although CAR expression and activation in Jurkat T cells showed specificity of the scFv, PTK7 CAR protein in primary T cells was not as highly expressed. We hypothesized that low CAR expression in primary T cells was due to a weak UBC promoter driving transcription and the upstream location of the eGFP transgene (**Figure 2.1A**). We therefore created a PTK7 CAR construct utilizing an EF1*α* promoter and removed the eGFP/P2A ribosomal skipping sequences (**Figure 2.1B**). Primary T cells from healthy donor PBMCs were transduced with PTK7 CAR lentiviral vector, expanded, and CAR expression was measured prior to downstream experiments (**Supplemental Figure 2.1**). Primary T-cell growth and viability following transduction and through expansion were comparable between UBC-based and EF1*α*-based constructs (**Figure 2.5A**). The EF1*α*-based PTK7 CAR is superior in both cell surface (**Figure 2.5B-C**) and total CAR expression (**Figure 2.5D**), so this construct was used in all subsequent studies.

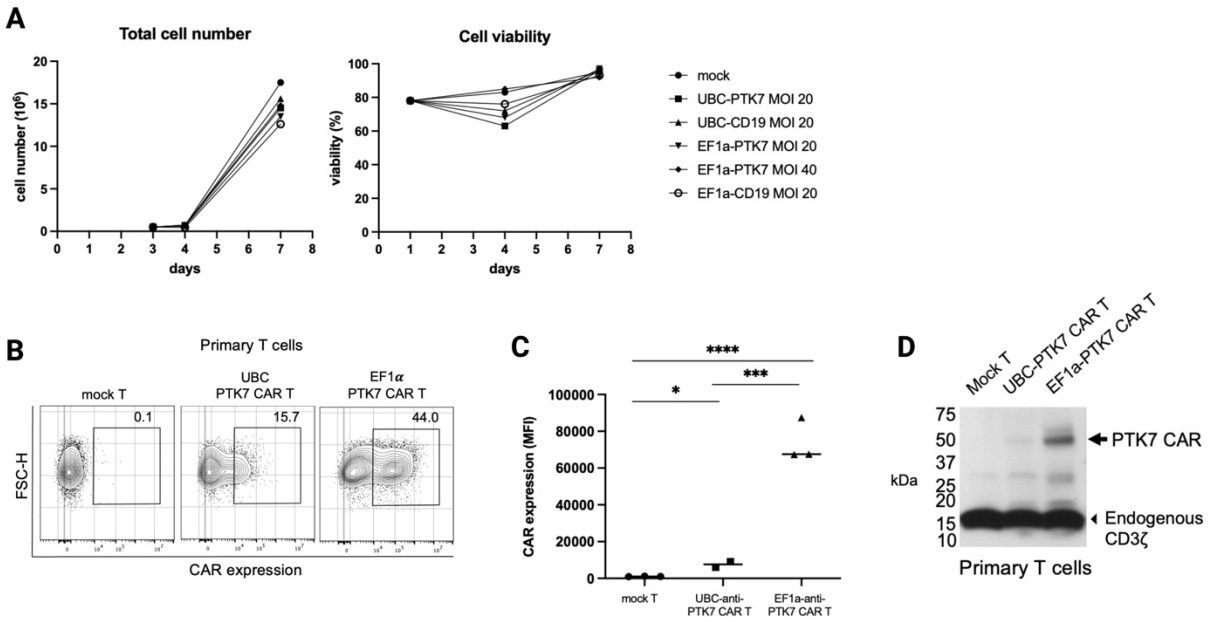

Figure 2. 5. EF1*α* promoter is required for optimal CAR expression in primary T cells

(A) Left: Total T cell count starting from Day 3 (Transduction) through expansion. Right: cell viability of T cells on Days 1, 4, and 7 of T cell timeline shown in Supplemental Figure 2.2. **(B)** Representative flow plot showing CAR expression (PTK7-Fc chimera) in primary T cells transduced with indicated CAR at MOI 20. **(C)** MFI expression of PTK7 CAR in primary T cells transduced with indicated CAR, n =2-3 biological replicates. **(D)** Western blot from whole cell lysate of primary T cells transduced with indicated CAR at MOI 20. Western blot antibody against human CD3ζ. Expected PTK7 CAR molecular weight is 54.7 kDa.

Characterization of PTK7 CAR

The PTK7 CAR was further characterized in comparison to the CD19 CAR with the same vector backbone. PTK7 CAR was expressed in 39% ± 5 T cells while CD19 CAR was expressed in 52% ± 9 T cells (**Figure 2.6A-C**). In addition, PTK7 T-cell differentiation was measured after expansion, 24 hours prior to use in downstream functional assays (**Figure 2.7A**). T cells were of mostly central memory (CD45RO+CCR7+) phenotype (56% ± 27), followed by effector memory (CD45RO+CCR7-) phenotype (32 ± 22), and minimally of naïve (CD45RO-CCR7+) phenotype (9 ± 9). No significant variance between the differentiation phenotypes or CD4/CD8 ratios were observed in mock T cells (**Figure 2.7A-B**). PTK7 CAR T cells expressed IL-2 upon interaction with IMR5 (**Figure 2.7C-D**) and both mock and PTK7 CAR T cells were mostly negative in co-expression of PD-1/TIM3 (**Figure 2.7E**). Co-expression of both markers could be indicative of severe CD8 T-cell exhaustion [92].

Altogether, the EF1***α***-based VH-L-VL PTK7 CAR showed the most promise to utilize in downstream *in vitro* cytotoxic and *in vivo* anti-tumor studies in Chapter 4.

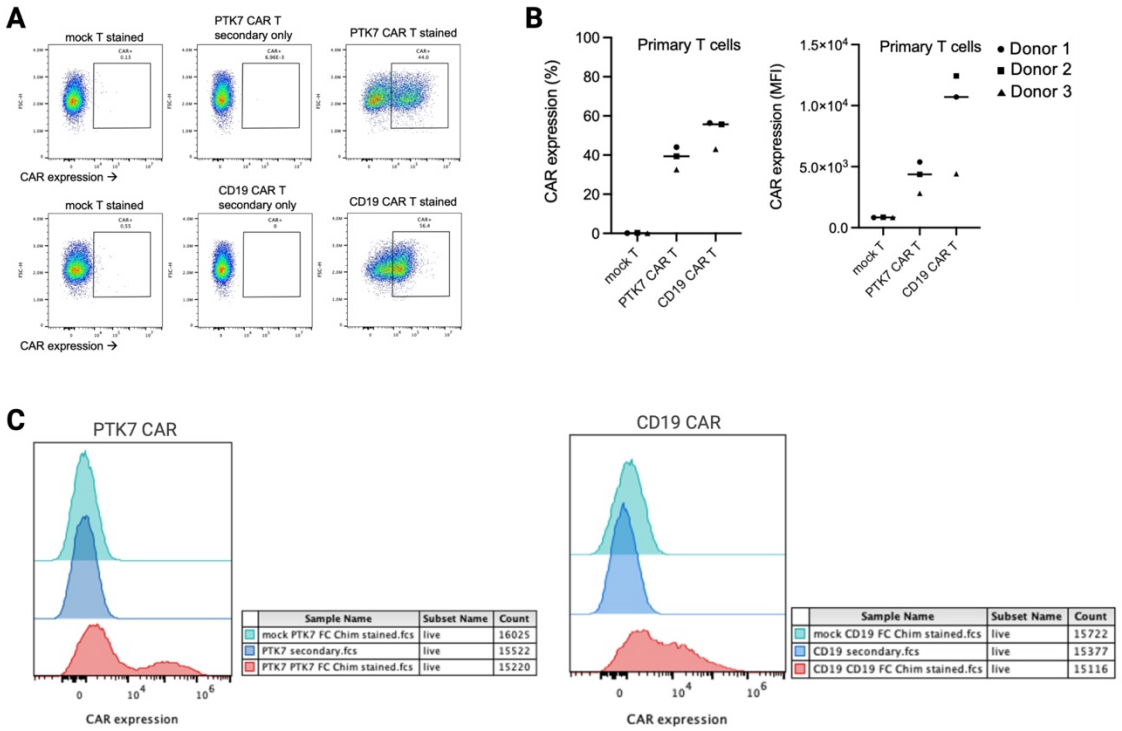

Figure 2. 6. CAR expression of PTK7 CAR T cells utilized in functional studies

(A) Representative flow plot showing PTK7 CAR or CD19 CAR expression in primary T cells. Showing Donor 2. **(B)** Left: %CAR expression in three donors used in functional studies in Figure 4.1. Right: MFI CAR expression in all three donors used in functional studies in Figure 4.2. **(C)** Representative histograms showing PTK7 CAR or CD19 CAR expression.

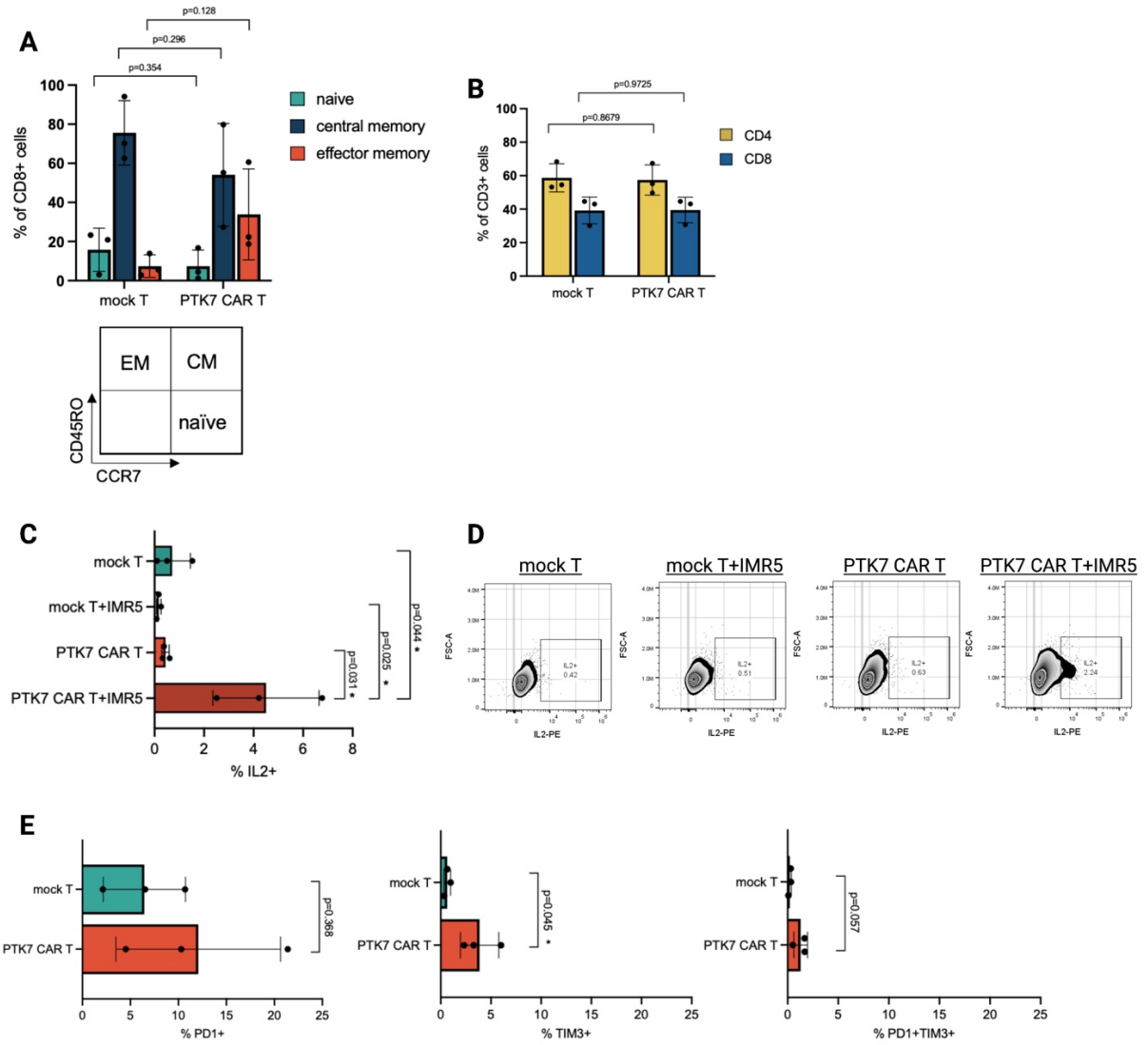

Figure 2. 7. T cell phenotype and function

(A) % of CD8 T cells that are naïve T (CCR7+CD45RO-), central memory (CCR7+CD45RO+), and effector memory (CCR7-CD45RO+) subsets, gated on live CD3+CD8+ cells. **(B)** %CD4+ or CD8+ cells in all three donors used in Figure 5 cytotoxicity assays, gated on live CD3+ cells. **(C)** %IL-2 expression in cells cultured with target cells for 4 hours, gated on primary T cells. **(D)** Representative flow plot of IL-2 expression in indicated cultures. **(E)** Left: %PD-1 expression, middle: %TIM-2 expression, and right: PD-1/TIM-3 co-expression in cells 24 hours before use in cytotoxic assays, gated on primary T cells. Statistical tests represent Student's t-test (*p<0.05; ns, p>0.05).

2.4 Discussion

CAR T-cell therapy is a form of adoptive cell therapy (ACT) that was developed to overcome the restrictions of tumor infiltrating lymphocyte (TIL)-based and T-cell receptor (TCR)-based therapies. CAR T cells mimic the effector T-cell signaling domains without the need for MHC presentation to recognize an antigen and allows the flexibility in designing an antigen binding domain against any known target. Importantly, remarkable success of CAR T cells has been shown in hematological cancers, but significant barriers exist in targeting solid tumors such as NB, with the same type of therapy, including the lack of tumor-specific antigens.

At present, investigators are engineering various evolutions of CAR constructs for T-cell therapy to a great extent [89-91]. CAR scFv's (antigen binding domain) are typically identified by conventional methods by noting high binding capacity to the target antigen through libraries of the immunoglobulin variable regions [93-96]. Moreover, the following domain, hinge domains, are optimized depending on epitope location on the antigen, thus should be customized to the specific CAR [97,98]. Lastly, the co-stimulatory domain has been shown to be critical for potent T-cell activity and persistence, therefore should be carefully tailored to determine the strength and longevity of the T-cell response. Discussed here are each of the components utilized in the PTK7 CAR.

We designed and tested various PTK7 CAR constructs, of which all contain the same scFv (of two different orientations) that others have previously identified as a part of a monoclonal antibody that moderately binds PTK7. We found this scFv effectively binds PTK7, allowing antigen-specific activation of T cells, showing the binding strength and duration is adequate to show a functional T-cell response of early activation. However, multiple variable region sequences that exist and others that have yet to be discovered should be tested. Investigations should include comparisons of multiple PTK7 scFv's with the readout being short- and long-term CAR T-cell capability, as the binding potential alone may not always correlate to CAR T-cell function [99-102]. Following the scFv in the PTK7 CAR construct is a hinge domain derived from the CD8 molecule,

and once more showed sufficient flexibility to determine PTK7 CAR T-cell efficacy. However, the hinge domain should be optimized for the specific epitope location and steric hindrance capacity.

Lastly, we utilized the CD28 co-stimulatory domain that provided adequate T-cell proliferation and IL-2 expression post-PTK7 antigen stimulation. Studies have shown that CAR T-cell persistence in NB is correlated with prolonged detection of CAR T cells and subsequent superior responses [103]. CAR T-cell persistence can vary by the T-cell subsets utilized, CAR architecture, cell culture media during expansion, introduction of exogenous cytokines, and metabolic reprograming. These variations and current findings in CAR architecture and persistence will be expanded on in Chapter 6 General Discussion. Currently, our future investigations include using 4-1BB or both CD28/4-1BB domains, as they have different functional and metabolic pathways that may influence CAR T-cell persistence [104].

In addition to CAR architecture, optimal viral-based CAR backbone components including the promoter should be determined for each individual CAR as variations in any of the transgene sequence may significantly change the transduction/transcription/translation efficiency. This was modeled by the need for a higher expressing promoter, EF1α, for PTK7 CAR, to get the optimal CAR expression, while the CD19 CAR utilized as control, needed only the lower expressing UBC-based construct to achieve an even higher CAR expression.

In conclusion of the chapter, our studies show a promising PTK7 CAR construct that specifically recognize and activates T cells in the presence of PTK7, to utilize in downstream functional assays to determine the feasibility of targeting PTK7 in NB tumor cells (see Chapter 4).

2.5 Materials and Methods

Cell lines and Primary T cells

Human-derived childhood cancer cell lines were obtained from the Children's Oncology Group (COG) Childhood Cancer Cell Line Repository (NB) or generously provided from the laboratory

of Dr. Robert Schnepp at Emory University (osteosarcoma, rhabdomyosarcoma) and cultured using RPMI1640 (Sigma) medium completed with 10% fetal bovine serum (Gemini) and 1% penicillin-streptomycin (Gemini) at 37°C in a humidified atmosphere with 5% CO_2 and 21% O_2 content. CMK cell lines were cultured in the same, except with 20% FBS. On a yearly basis, cell lines were authenticated using STR DNA genotyping (Texas Tech University Health Sciences Center). The identity of each cell line was confirmed to match the COG cell line database (cccells.org). Additionally, cell lines were routinely verified to be clean of mycoplasma contamination using the MycoAlert contamination kit (Lonza). Primary T cells were cultured at 2 million cells/mL (after the early cell dilution of ~100,000 cells/mL) in T cell media (X-VIVO 15 (Lonza), 10% fetal bovine serum (Gemini), 100 U/mL penicillin, 100 ug/mL streptomycin (Gemini), 100 IU/mL IL-2, and 5 ng/mL IL-7.

CRISPR-cas9 editing, plasmids and lentiviral delivery

PTK7-targeting CRISPR-cas9 knockout cell models were generated in SK-N-AS and NLF NB cell lines. Cas9 expression was first introduced through lentiviral infection and stable selection with blasticidin (VWR, #10191-146). Subsequently, commercially available scrambled sgRNA (5'-CGCGATAGCGCGAATATATT-3') or PTK7-targeted sgRNA CRISPR lentiviruses were transduced via spinoculation into each cas9 expressing cell line. sgRNAs targeting separate regions of PTK7 were included: sequence #1 (5'-GCGTCATCTCGAGTCACCC-3') and sequence #2 (5'-AGCGTACGACTGTGTACCA-3'). To create stable PTK7 knockout, antibiotic selection was performed with 0.5-2 μg/mL of puromycin (Gemini, #400-128P).

Design and cloning of PTK7 and CD19 CARs

UBC-based CARs: The variable light (VL) and variable heavy (VH) sequences of the PTK7 single-chain variable fragment (scFv) were taken from United States Patent 9102738 on human monoclonal antibodies to PTK7 (clone 12C6). Two different orientations connected by a (G4S)3

linker (VL-linker-VH and VH-linker-VL) were made. These sequences were ordered as a Gene Synthesis product flanked by AscI and NheI restriction enzyme sites in a pUC57 vector (GenScript). The pUC57-PTK7 scFv plasmids and a recipient plasmid with an AscI and NheI site upstream of the CD8, CD28, and CD3ζ were digested (New England BioLabs) and the PTK7 scFv was ligated to the recipient plasmid containing the downstream CAR components. UBC-CD19 CAR was made with the same CAR components and plasmid backbone as PTK7 CARs. The DNA sequence of all CAR components were codon optimized by a codon optimization table and all products were confirmed by Sanger sequencing (Genewiz).

EF1-a-based CARs: The following was ordered as a Gene Synthesis or GenePart product: DraIII-3'EF1-a-IL2ss-PTK7 VH-linker-VL CAR or CD19 CAR-SgrAI (GenScript). These products along with a standard EF1-a recipient plasmid (5'EF1-a-DraIII-3'EF1-a-SgrAI) were digested with DraIII and SgrAI restriction enzymes (New England BioLabs) and the PTK7 VH-linker-VL CAR or CD19 CAR was ligated to the recipient plasmid containing the 5' end of the EF1-a sequence. The DNA sequence of the CAR components were codon optimized and all products were confirmed by Sanger sequencing (Genewiz).

Lentiviral production

Lentiviral vectors were made and titers determined as previously described [105]. High-titer, recombinant, self-inactivating HIV lentiviral vectors were produced using a four-plasmid system including the expression (CAR) plasmid and packaging plasmids containing the gag, pol, and envelope (VSV-g) genes. HEK-293T cells were transiently transfected by calcium phosphate transfection. Vector supernatant was collected, filtered (0.22 um), and concentrated via centrifugation. Titering was performed on HEK 293T cells genomic DNA using quantitative polymerase chain reaction (qPCR).

Generation of PTK7 CAR T cells

Cryopreserved healthy donor peripheral blood mononuclear cells (PBMC) (AllCells) were defrosted and T cells negatively selected with EasySep Human T-cell Isolation Kit (Stemcell technologies), and stimulated with a 1:1 cell to bead ratio of CD3/CD28 Human T-Activator Dynabeads (ThermoFisher Scientific) for 48 hours. Jurkat T cells were used without stimulation. Beads were removed from primary T cells and 1x10^6 cells were transduced with indicated MOI (2.5, 5, and 10 for Jurkat T cells and 20 for primary T cells) of CAR lentiviral vectors with 10 ug/mL polybrene (EMD Millipore) for 18 hours. MOI was determined by the following calculation:

$$MOI = \frac{titer \times volume\ (mL)}{\#\ of\ cells}$$

After 18 hours, cells were resuspended in fresh primary T-cell media and diluted for an early cell dilution at 100,000 cells/mL and left to expand for 72 hours before cell surface CAR expression was determined and before use for cytotoxic assays. Cells were re-stimulated every 7 days, for a maximum of two stimulations total.

CAR expression Western blot

Cells were lysed with Cell Lysis Buffer (Cell Signaling Technologies) with cOmplete Protease Inhibitor Cocktail (Roche) for 30 minutes on ice. Cells debris were pelleted at 20,000 x g at 4 ☐C for 15 minutes and the supernatant was collected as lysate. Protein amount was determined with a Bradford assay using Protein Assay Dye (Bio-Rad) and resuspended in 2x Laemmli Sample Buffer (Bio-Rad) with 5% beta-mercaptoethanol as a reducing agent and heated at 100 ☐C for 10 minutes. Per sample, 25-50 ug protein was loaded into a 4-15% precast gel (Bio-Rad) with Precision Plus Protein Dual Color Standards (Bio-Rad), transferred to a 0.2 uM polyvinylidene fluoride (PVDF) membrane (Thermo Scientific), and detected with anti-CDζ primary (1:1000) (Biolegend) and goat anti-mouse HRP secondary (1:2000) (Biolegend), and imaged with Bio-Rad ChemiDoc XR+ Molecular Imager.

Measuring CAR expression

Jurkat or primary CAR T cells were stained with 3 ug Recombinant Human PTK7 Fc Chimera Protein (R&D Systems) or Mouse PTK7 Fc Chimera Protein (R&D Systems) and incubated on ice for 30 min. Cells were washed 2x FACS buffer (PBS + 2.5% FBS), stained with a R-Phycoerythrin F(ab')2 secondary antibody (Jackson ImmunoResearch Laboratories, INC.), washed 2x with FACS buffer, and detected by flow spectrometry (Aurora Cytek) and analyzed with FlowJo software (v10).

CAR activation assay

Jurkat CAR T or primary CAR T cells were incubated with VPD450 stained (BD Horizon) target cells at various effector to target ratios in 12x75mm flow cytometer tubes for four hours at 37 °C in 300 µL cell culture media. Cells were then washed with FACS buffer and stained with 3 µL anti-CD69-APC-Cy7 antibody (BD Pharmingen), washed 1x with FACS buffer, and detected by flow cytometry (Aurora Cytek) and analyzed by FlowJo software (v10).

2.6 Supplemental Figures, Tables, and Legends

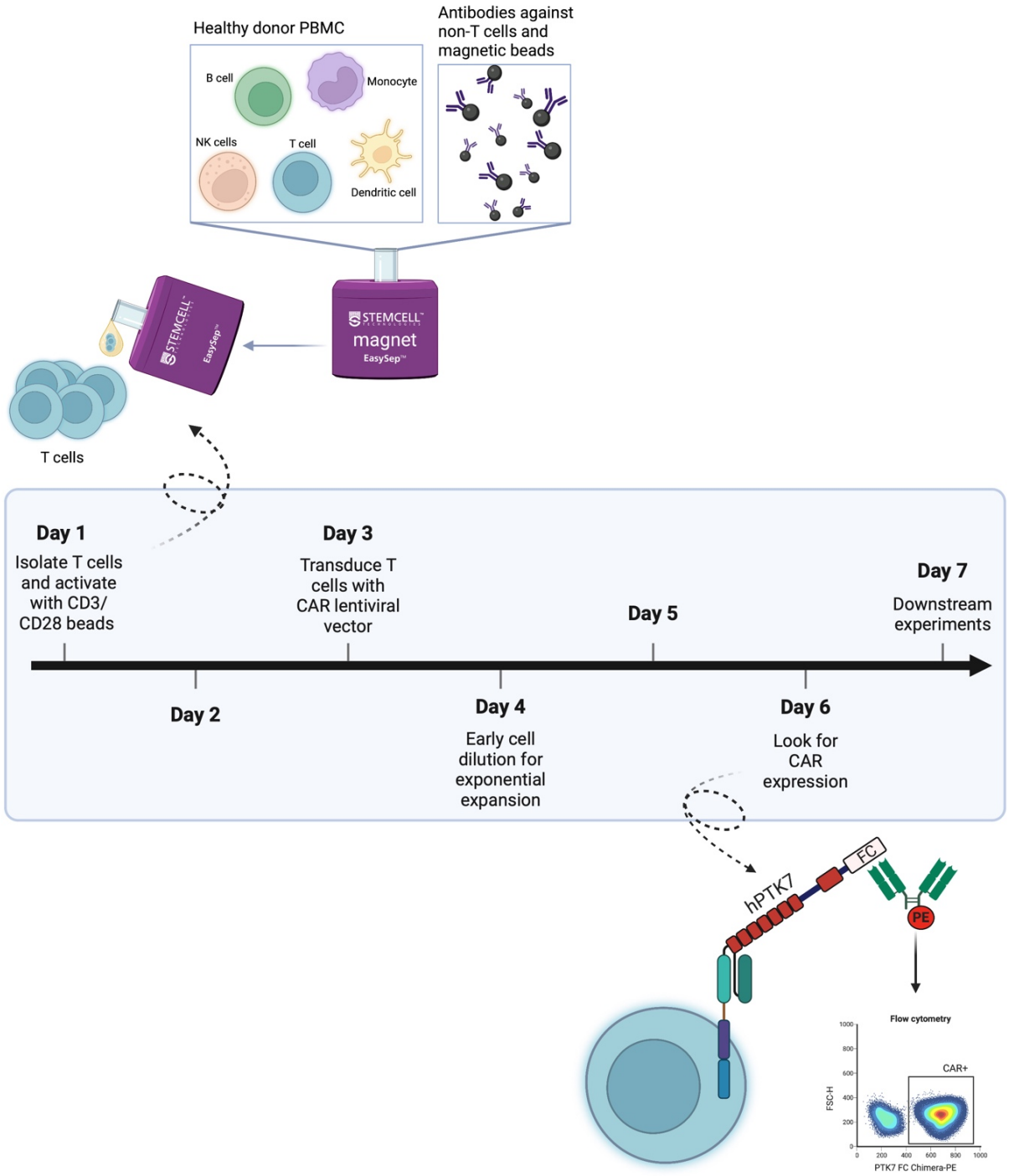

Supplemental Figure 2. 1. Timeline of isolation, transduction, and expansion of T cells utilized in functional experiments

T cells were isolated from healthy donor PBMC through negative selection, transduced with CAR lentiviral vector, and left to expand after an early cell dilution. CAR expression was observed a day prior to use in functional downstream assays.

Chapter 3: Method development of introducing PTK7 CAR expression in primary αβ T cells

Jasmine Y. Lee, Reginald Tran, Jordan S. Alexander, and H. Trent Spencer

Jasmine Y. Lee designed the column-based CAR+ selection method, conducted all experiments, and wrote this chapter

Reginald Tran designed and developed the proxim transduction method

Jordan S. Alexander designed the column-based CAR+ selection method

H. Trent Spencer provided oversight

The work presented in this chapter is unpublished.

3.1 Abstract

Current methods of introducing chimeric antigen receptor (CAR) transgene to primary T cells for preclinical and clinical use involves a traditional lentiviral/retroviral transduction protocol. Although these methods have been successful in introducing CAR transgene, improvements can be made to conserve viral vector. Here, we compared the traditional lentiviral transduction of PTK7 CAR transgene to a method that increases cell to virus contact named proxim transduction. We found a 10-fold decrease in the amount of lentiviral vector needed to achieve CAR expression through proxim. Both traditional and proxim transduced PTK7 CAR T cells induced similar cytotoxicity against a neuroblastoma cell line, IMR5. In addition to viral vector use, another downfall of traditional transduction is the resulting population is not 100% pure PTK7 CAR+ T cells. We therefore designed a positive column-based selection method that could be utilized post-transduction to isolate CAR+ cells. We show that this method is successful in isolating CAR+ T cells to a near pure population and release the direct binding protein, PTK7 Fc, used to bind the CAR+ T cells to the column, post-selection. PTK7 CAR+ T cells retain their antigen-specificity and cytotoxic potential. Future studies should determine the feasibility of incorporating both proxim transduction and positive column-based selection methods to utilize in additional functional studies.

3.2 Introduction

Two main variations of introducing CAR transgene are non-viral and viral systems, the latter being the most frequently utilized in the form of lentiviral or retroviral vectors. However, two main safety concerns lie with both vector systems. Vectors are designed to be self-inactivating, thus replication incompetent. However, an early study in 1992 reviled non-human primates that received transplantation with retroviral vector-transduced hematopoietic stem cells developed T-cell neoplasm due to replicating virus contamination [106]. This prompted the Food and Drug

Administration (FDA) to include guidance for testing of clinical vector lots, cell products, and post-infusion patients for replication-competent retrovirus or lentivirus (RCR/L) [107]. To date, RCR/L exposure has not been reported in humans. However, the other safety concern of viral-based systems, insertional oncogenesis, was seen after retroviral-mediated gene therapy of SCID-X1 human patients have been reported [108,109].

Given lentiviral vectors have not demonstrated oncogenic potential seen in retroviral vectors, we utilized this vector to introduce PTK7 CAR transgene to primary T cells. A substantial amount of lentiviral vector is needed for early phase clinical trials [110], and the process is non-standardized and labor-intensive. Here, we chose to apply a scalable tool designed by a biomedical engineer [111,112] to efficiently apply lentiviral transduction of PTK7 CAR transgene.

Equally important to cell and gene therapy, included within CAR constructs are markers such as murine CD variants, fluorescent protein EGFP, and nerve growth factor receptors and are co-introduced with CAR transgene for preclinical studies. However, these methods are not employed for clinical studies due to immune rejection of mouse origin molecules, marker release to extracellular space, physiological interference, and incompatibility with existing technology to allow enrichment of pure cells under good manufacturing practice (GMP) [113]. In more recent years, designer nuclease technology that allows for both positive and negative selection of CAR T cells during manufacturing or after infusion have been evaluated [114]. A CD34 splice variant, RQR8, has been shown to be a promising candidate to select CAR+ cells due to being GMP-compatible for an approved immunoaffinity-based enrichment method of CD34+ cells [113,115,116]. However, RQR8's influence in physiological functions is unknown and potential concern includes alterations of T-cell effector functions. We therefore tested a MACS column-based method of selecting a pure population of PTK7 CAR+ T cells, without the need of introducing an additional transgene. The MACS columns that were utilized here are from the same manufacturers of the FDA-approved CliniMACS CD34 Reagent System.

3.3 Results

Proxim transduction is an efficient method of introducing PTK7 CAR expression with reduced amount of viral vector

Proxim transduction was compared to a traditional transduction method of introducing CAR transgene to primary T cells (**Figure 3.1A**). Preliminary evidence shows traditional transduction gives 30.6% CAR expression in a single donor with a MOI of 20, and 37.7% CAR expression in the same donor with an MOI of 2, a 10-fold decrease in lentiviral vector used (**Figure 3.2A**). Percent CAR expression in proxim transduced T cells minimally changed with increased MOI at 36% (MOI 4), 40.7% (MOI 8), and 41.3% (MOI 16). In addition to percent CAR expression, the median fluorescence intensity (MFI) was measured. T cells transduced with an MOI 20 resulted in $3.9x10^5$ MFI CAR expression while proxim transduced cells more highly expressed CAR at $7.9x10^5$ (MOI 2), $9.6x10^5$ (MOI 4), $1.0x10^6$ (MOI 8), and $9.1x10^5$ (MOI 16) (Figure 3.2B). In a 4-hour cytotoxicity assay, a 5:1 effector to target ratio induced 54% cytotoxicity in IMR5 cells with traditionally transduced T cells, and a range of 51%-57% cytotoxicity with proxim transduced T cells (**Figure 3.2C**).

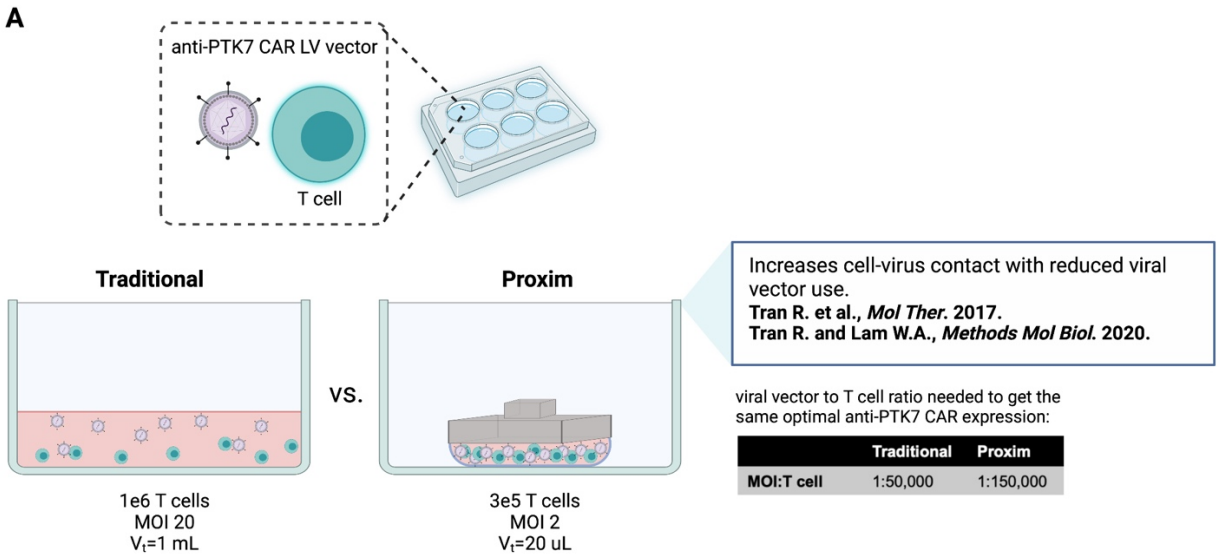

Figure 3. 1. Graphical design of traditional transduction v. proxim transduction

(A) Proxim transduction, a method to increase cell-virus contact, was designed by Reginald Tran. We tested this method in comparison to our traditional method of introducing PTK7 CAR transgene. The number of T cells to MOI and associated viral vector to T-cell ratio table was determined by results shown in Figure 3.2A-B.

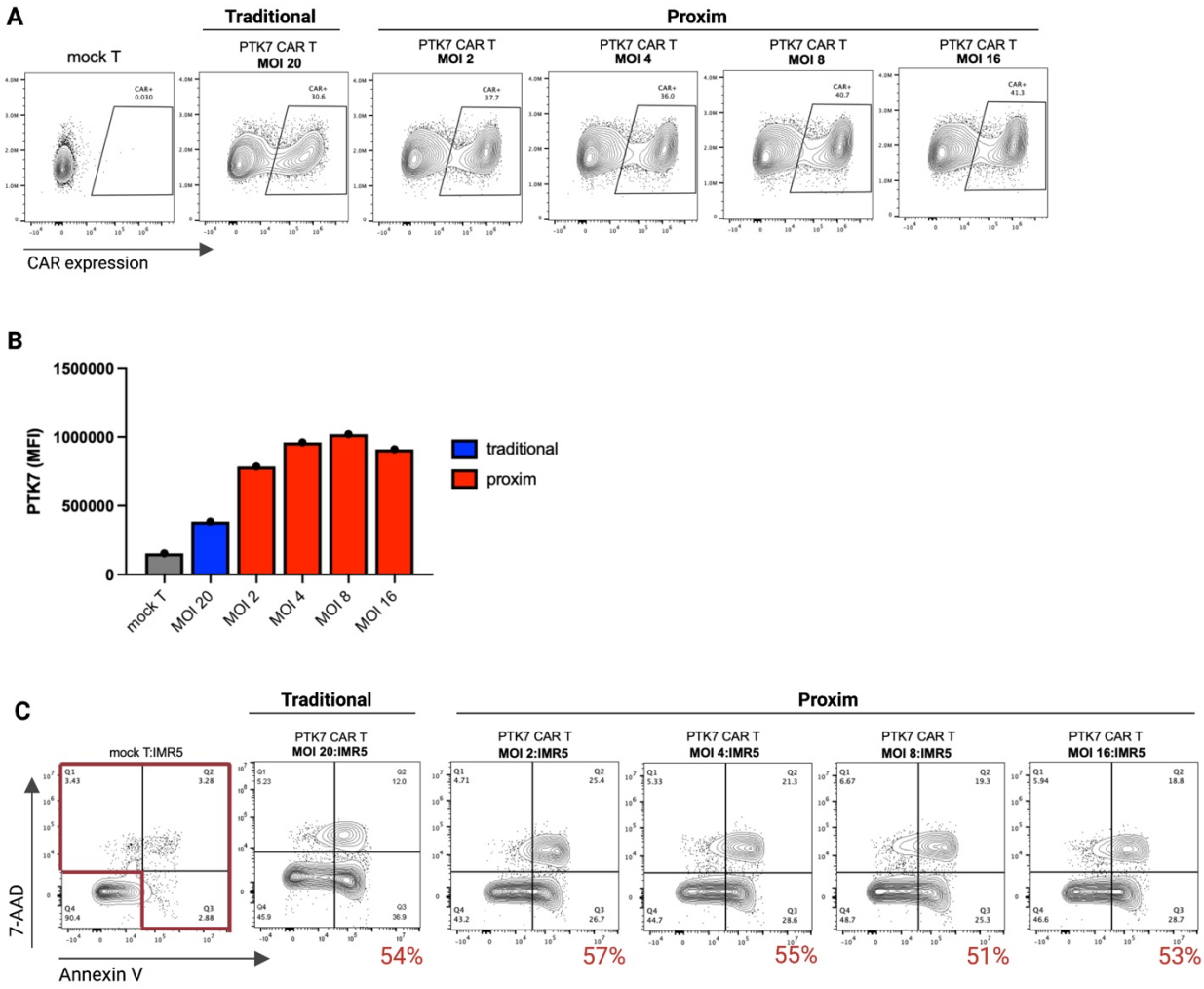

Figure 3. 2. Proxim transduction is an efficient method of introducing PTK7 CAR expression with reduced amount of viral vector

(A) Flow plots showing %CAR (PTK7 Fc+) of primary T cells transduced with traditional or proxim transduction at indicated MOI. **(B)** MFI CAR (PTK7 Fc+) of primary T cells transduced with traditional or proxim transduction at indicated MOI. **(C)** 4-hour flow cytometry cytotoxicity assay. % cytotoxicity in red = the sum of 7AAD+, Annexin V+, and double 7AAD+ Annexin V+ cells, gated on target cells only. N = 1 donor.

Development and testing of MACS column-based CAR-positive selection

To test the feasibility of selecting CAR+ cells through use of MACS columns, T cells transduced with PTK7 CAR transgene were utilized in the following assays. T cells expressing CARs were magnetically adhered to MACS columns through the following chain of molecules starting from the CAR side: PTK7 Fc chimera -> biotin anti-FC -> anti-biotin microbead (binds to column) (**Figure 3.3A**). Both the flow through cells and magnetic column-bound cells were collected and cell surface CAR expression was measured. The input cell population of 30.6% CAR expression resulted in 7.4% CAR+ flow through cells and 97.6% CAR+ column-bound cells.

Post-selected cells were then tested for release of PTK7 Fc and short term and long term cytotox potential (**Figure 3.4A-B**). To release any potential PTK7 Fc still being bound to the PTK7 CAR, column-bound CAR T cells were repeatedly resuspended in large amounts of 37 C media as described in the methods. Cells were then incubated with the $F(ab')_2$ secondary antibody that binds PTK7 Fc. If PTK7 CAR T column-bound cells were still bound to PTK7 Fc, cells would appear CAR+. The remaining binding protentional was ruled out as no significant population of cells appear CAR+ (**Figure 3.4A**). T cells were then assessed for cytotoxic potential both 24-hours and 7-days post-selection. At 24-hours selection, flow through (CAR-) cells induced 20% ± 1 cytotoxicity in IMR5 cells, which increased to 57% ± 4 with column-bound (CAR+) cells only after 4-hours of co-incubation (**Figure 3.4B**). These CAR+ cells remained cytotoxic (66% ± 6) after 7-days in culture post-selection.

Additionally, 7-day post-selected cells were phenotyped by activation potential, PD-1/TIM-3 expression, and T-cell differentiation (**Figure 3.5A-C**). In the presence of IMR5 cells, pre-selected T cells and flow through (CAR-) cells expressed 14.7% and 9.4% CD69 respectively, while column-bound (CAR+) cells expressed 31.9% (**Figure 3.5A**), showing post-selected CAR T cells retain antigen-specific activity long term. PD-1 and Tim-3 were observed as co-expression could be indicative of severe CD8 T-cell exhaustion [92]. T cells in all conditions without the introduction of IMR5 cells, remained mostly double-negative in PD-1/Tim-3 (**Figure 3.5B**). The

only trend in difference of expression was PD-1 upregulation in column-bound (CAR+) cells exposed to IMR5 cells (15.8%) compared to the same cells without IMR5 exposure (5.28%) of the overall population. In all by one condition, the pre-selected and post-selected cells remained primarily effector memory cells and secondarily central memory cells (**Figure 3.5C**). Column-bound (CAR+) cells cultured in the presence of IMR5 cells lost a majority of the central memory population (8.5%), to effector memory cells (83.7%).

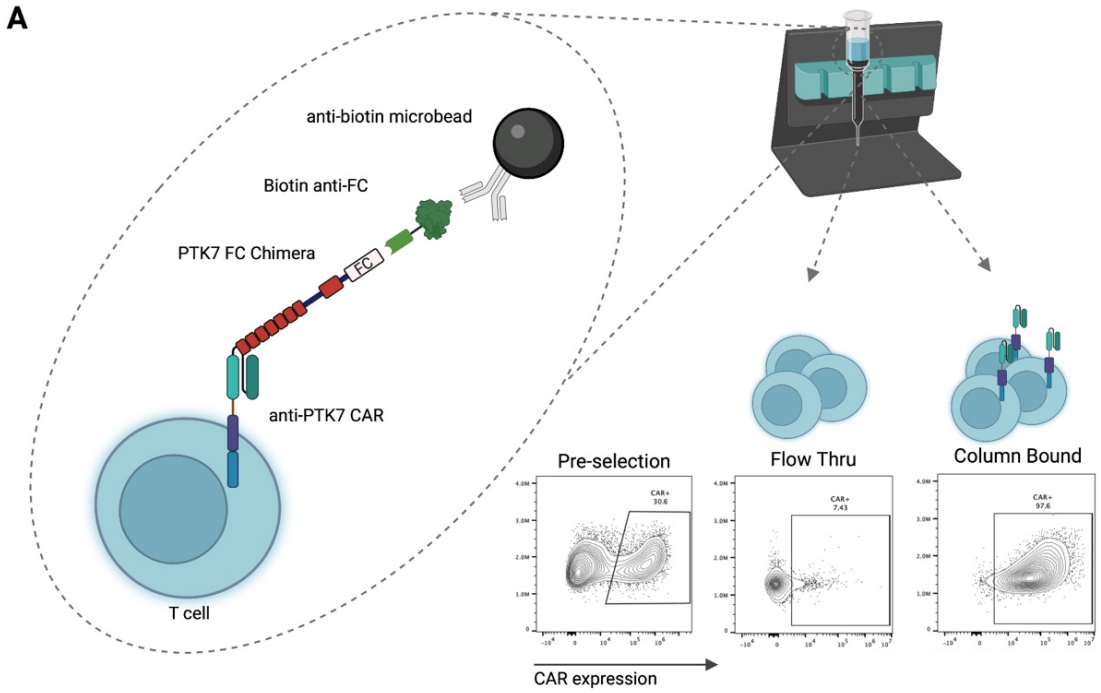

Figure 3. 3. Graphical design of MACS column-based CAR-positive selection method and resulting CAR+ expression

(A) This positive selection method was designed and utilized to select out only CAR+ T cells. Representative flow plots show CAR expression (PTK7 Fc) pre-selection, and post-selection (Flow through and column bound).

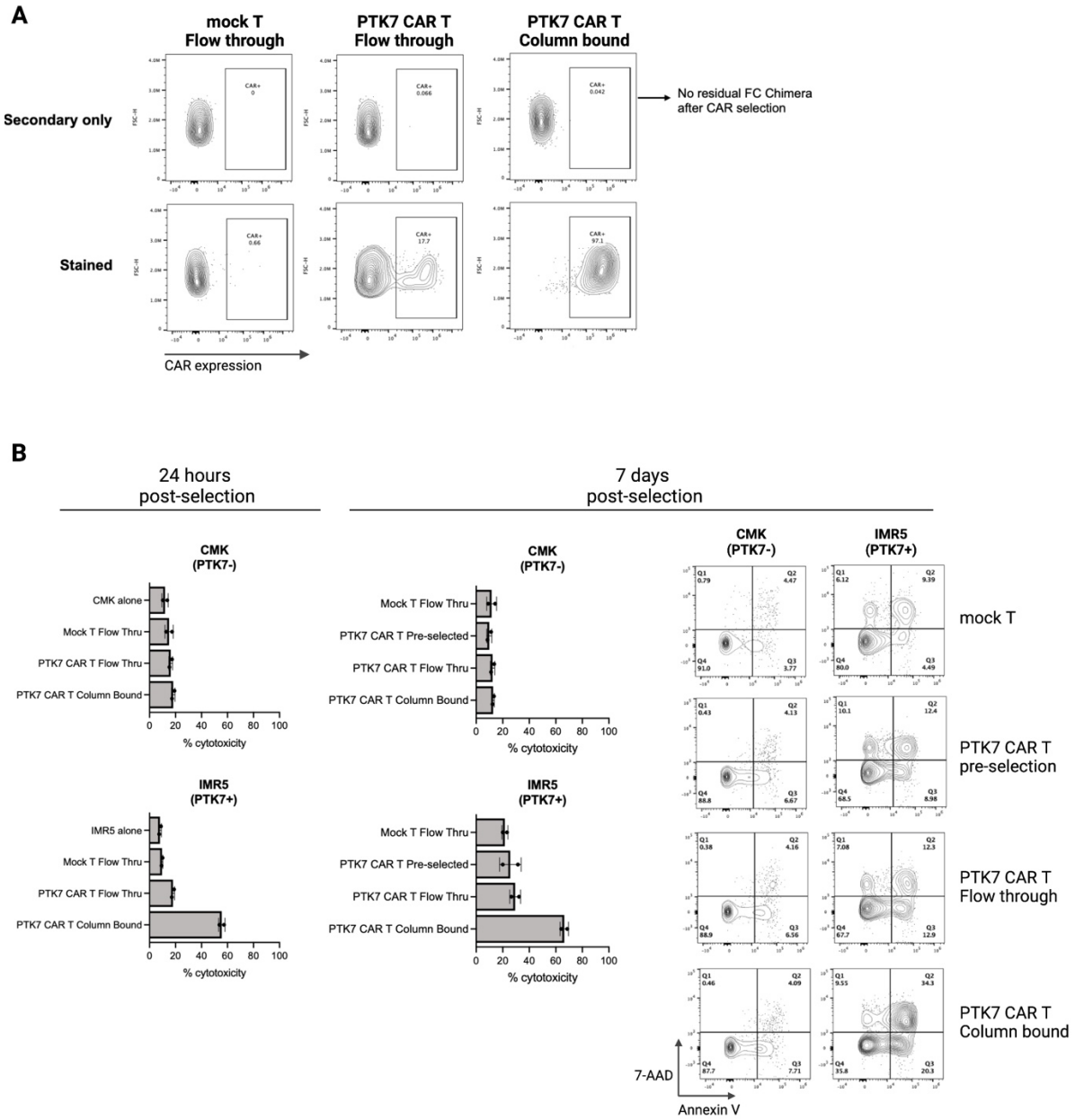

Figure 3. 4. Post-selected T cells: Fc chimera release and cytotoxic potential

(A) Flow plots showing CAR expression of post-selected T cells after repetitive resuspensions and washed to remove bound PTK7 Fc. Secondary is $F(ab)_2$ conjugated to PE, and Stained is PTK7 Fc plus $F(ab)_2$-PE. **(B)** 4-hr flow cytometry cytotoxicity assay. % cytotoxicity = the sum of 7AAD+, Annexin V+, and double 7AAD+ Annexin V+ cells, gated on target cells only. n = 1 donor with 2 experimental replicates. Left: 24-hour post-selection% cytotoxicity. Right: 7-day post-selection, % cytotoxicity and representative flow plots.

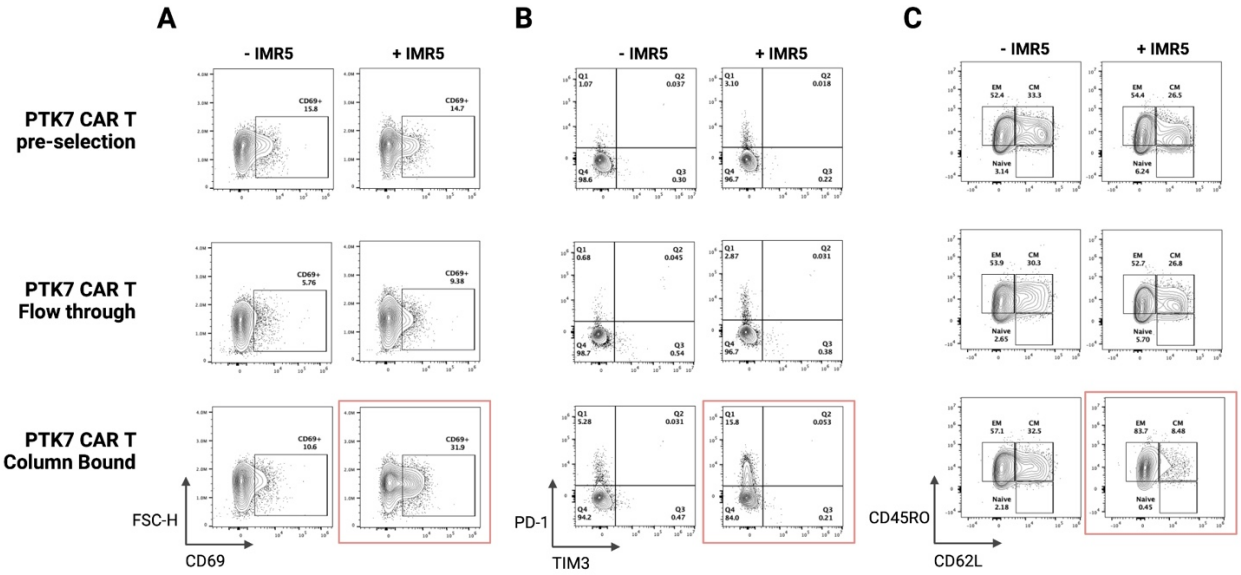

Figure 3. 5. Phenotype of post-selected T cells

Representative flow plots of **(A)** CD69 **(B)** PD-1/TIM-3 and **(C)** CD62L/CD45RO expression in T cells pre- and post-selection with or without IMR5 target cells.

Cryopreserved commercial AllCells PBMC product is superior to lab isolated Leukopak

Two cryopreserved healthy donor PBMC sources were compared for use in T-cell isolation and subsequent CAR T-cell functional analysis. One is a commercially available product (AllCells), the other from a neighboring lab (lab isolated). Both PBMCs are products from apheresis Leukopaks with differences in processing prior to preservation as well as the freezing media components which are listed in **Figure 3.6A**. The timeline for T-cell isolation, transduction, and expansion used for the following experiments were described previously (**Supplemental Figure 2.2**). A donor from pre-isolated AllCells PBMCs that started with 44% T cells were enriched to 96.7% T cells post-selection. Similarly, the lab filtered cells started with 29% T cells and were enriched to 94.9% T cells (**Figure 3.7A-B**). While the success of T-cell isolation of both donors were

comparable, notable differences lied in T-cell viability and cell number throughout expansion (**Figure 3.7B-C and Figure 3.8A-B**). T cells from a lab isolated donor contains a CD3+ population that lies much lower on the flow cytometry forward (FSC-A) scatter, compared to where they typically lie further up (**Figure 3.7B**). T cells that lie in this position, have been shown to be "unhealthy" T cells that express Annexin V (data not shown). In addition, it is well known that T-cell sizes are correlated to T-cell proliferation following activation [117-119]. The ability of these T cells to activate can also be visualized through T-cell:CD3/CD28 bead clusters. Directly after isolation, T cells were activated by CD3/CD28 beads and were imaged, 24-hours later (**Figure 3.7C**). Large clusters were observed in AllCells culture while considerably smaller clusters were present in lab isolated culture. While lab isolated T cells started 79% viable, which decreased to 71% viable prior to transduction on Day 3, AllCells T cells started 94% viable, and remained at a high viability of 93% on Day 3 (**Figure 3.8A**). The viability of lab filtered T cells improved by Days 6-7, however total T-cell numbers remained low at $5.0x10^6$ mock T cells and $4.6x10^6$ PTK7 CAR T cells at the end of expansion. In comparison, the viability of AllCells T cells remained high throughout expansion and total T-cell numbers of $26.0x10^6$ mock T cells and $20.4x10^6$-$27.6x10^6$ PTK7 CAR T cells were obtained, a 4-5-fold difference (**Figure 3.8B**).

Lastly, although transduction efficiency of AllCells and lab isolated cells were a similar 71.2% and 64.2% respectively (**Figure 3.8C**), the high viability and expanded total cell numbers made the AllCells T cells a notably superior product to use for downstream CAR T-cell functional assays.

A

	Cryopreservation
AllCells ®	Our cryopreserved MNCs are collected from fresh blood during apheresis in Leukopaks, which enriches lymphocytes and monocytes while depleting mature granulocytes. The mononuclear fraction is then further processed to eliminate red blood cells and platelets (we lyse the RBC and spin down to isolate the MNC). The cells are frozen in IMDM, FBS, DMSO, Hetastarch. We cannot provide the concentration for each component because it is proprietary. They then go through a 2-week Quality Control check to ensure that the lot meets our release criteria, and then they are made available for purchasing.
Lab filtered	To freeze PBMC, we use FBS to resuspend the cells first, then add 20% DMSO/FBS to make final 10% DMSO/FBS

Figure 3. 6. Cryopreservation method and materials for Commercial AllCells and lab filtered PBMC

(A) Cryopreservation method and materials for AllCells were provided by Emory University's AllCells Representative, and lab filtered cells were provided by the Emory University lab member that isolated and preserved the cells.

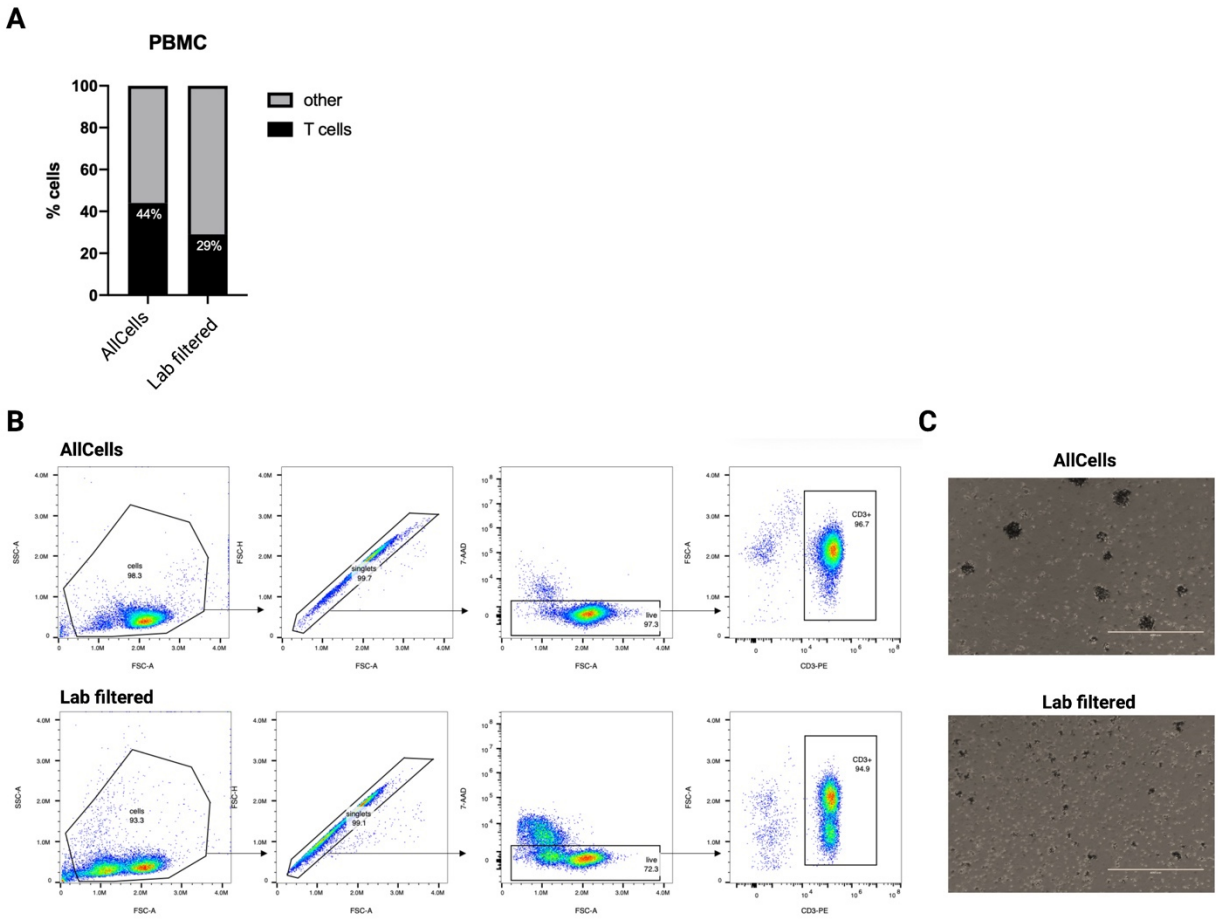

Figure 3. 7. T-cell isolation of AllCells and lab filtered PBMC

(A) Bar graph showing T cells (CD3+) as part of the whole PBMC population on Day 1, pre-isolation. **(B)** Gating strategy and CD3+ T cells post-isolation. **(C)** Representative images of activated T cells with CD3/CD28 beads 24-hours into activation.

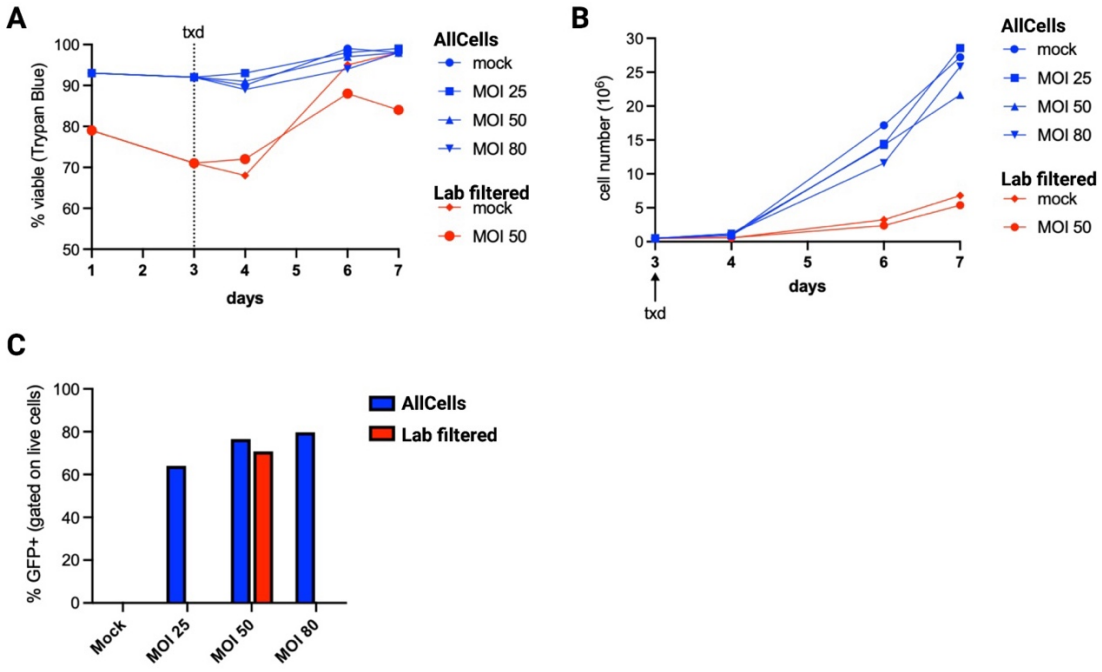

Figure 3. 8. Characterization of AllCells and lab filtered PBMC

(A) Viability and **(B)** Total live cell number throughout T cell isolation, transduction, and expansion. **(C)** GFP-only lentiviral vector was used to transduce isolated T cells, and transduction efficiency (GFP+) was measured. n = 1 donor AllCells, 1 donor lab filtered

3.4 Discussion

The current, traditional method of introducing CAR transgene to primary T cells includes lentiviral or retroviral transduction. However, production of viral vectors are typically labor-intensive and transfer from preclinical to clinical production is not easily scalable [111,120]. As a result, manufacturing timing and feasibility is one of the major barriers of introducing personalized cellular therapies with or without synthetic modification in the clinic, which is largely due to the diverse biological nature of the cells utilized for therapy. In addition to manufacturing, another limitation to CAR T-cell therapy is cost and as a result, patients' access to therapy. CAR T-cell therapies against CD19, axicabtagene ciloleucel and tisagenlecleucel, cost between $373,000-

$475,000 per patient [121], which increases to over an additional $30,000 to treat the common severe side effects. Therefore, efforts are currently underway to improve these obstacles.

To make the potential preclinical to clinical translation of PTK7 CAR T-cell therapy efficient, we tested a scalable method of lentiviral transduction that decreased the amount of vector needed to achieve similar cell surface CAR expression. Our preliminary tests showed proxim transduction impressively decreased the need for viral vector by 10-fold compared to traditional transduction. This not only shows promise for a reduced amount of vector needed therefore reduction in time and cost of therapy production, but also shows the feasibility of utilizing this method in which a preclinical scaling method has already shown promise for manufacturing of CD19-targeting CAR. However, this potential should be attested by direct experiments utilizing the scaled-up form for the PTK7 CAR specifically.

PTK7 CAR proxim transduced T cells remained as cytotoxic against PTK7-positive IMR5 cells compared to traditionally transduced T cells. However, further proxim studies are required to confirm the findings of decreased viral vector needed to achieve optimal CAR expression and its functional ability post-transduction. These studies should include multiple T-cell donors than was utilized in these studies, then subsequently determine the feasibility of utilizing donors derived from cancer patients.

In addition to testing scalable and cost-effective transduction methods, we aimed to improve a CAR selection method specific to our PTK7 CAR. The most commonly used preclinical markers are not utilized for patient products due to immune rejection, marker release to the extracellular area, functional barriers, and incompatibility with an existing technology [113]. We designed and tested a MACS column-based positive selection method that successfully isolated a pure positive (97.6%) population of CAR T cells. We found the PTK7 Fc, which is used to bind the CAR to the column is release post-isolation, freeing up the PTK7 CAR scFv to bind to PTK7 on target cells. The PTK7 CAR+ T cells retained their cytotoxic potential both short term (24-hours) and long term (7-days). It should be noted that future studies should include more donors to

understand selection success and retainment of cytotoxic potential trends. In all, both proxim transduction and MACS column-based PTK7 CAR selection, although requires more supporting evidence, shows promise as a scalable, efficient, and possible methods to utilize both pre-clinically and clinically.

3.5 Materials and Methods

See Chapter 2 Methods for:

Cell lines and primary T cells

Measuring CAR expression

CAR activation assay design and cloning of PTK7 CAR

Lentiviral production

Generation of PTK7 CAR T cells

Proxim transduction

This method was designed and developed by Reginald Tran [111,112]. Activated T cells were suspended with lentiviral vector in a total volume of 20 uL T cell media. The T cell/lentiviral vector suspension was transferred to the center well of 6-well plates. A proxim piston device was placed on top of the droplet to spread it out to a uniform height, while the outer edges were pressed down for a firm contact. The intermediate areas of the 6-well plate were filled with 10 mL PBS to prevent evaporation and cells were incubated at 37 °C for 18 hours. After 18 hours of transduction, T cells were carefully collected and used for downstream analysis.

MACS column-based CAR-positive selection

CAR T cells transduced with the traditional method as described in methods were used. ~20x10^6 T cells were washed with sterile FACS buffer (PBS + 2.5% FBS) and incubated with PTK7 fc

chimera on ice, end-to-end, for 30 minutes. Cells were then washed 2x with FACS buffer and incubated with 10 uL biotin anti-FC (Thermo Scientific) on ice, end-to-end, for 30 minutes, washed once with FACS buffer, and resuspended with 20 uL anti-biotin microbeads (Miltenyi Biotec). Cells were mixed well and incubated in the cold room for 15 minutes. Finally, cells were washed and resuspended in FACS buffer for separation with columns. MACS MS columns (Miltenyi Biotec) were placed in the magnetic field and rinsed with 500 uL FACS buffer. The labeled cell suspension was applied to the column and flow-through containing unlabeled cells were collected. Column was then washed 2x with FACS buffer, removed from the magnetic field, and placed on top of a 15 mL conical. The column which contains labeled cells were flushed with FACS buffer by firmly pushing the plunger into the column. All collected cells were resuspended and washed in 37 °C media 3X to remove potential PTK7 Fc chimera bound to the CAR.

Chapter 4: PTK7-targeting *αβ* CAR T cells induce NB cell death *in vitro* and in mouse metastasis NB model

Jasmine Y. Lee, Gianna M. Branella, Hunter C. Jonus, Christopher B. Doering, Kelly C. Goldsmith, and H. Trent Spencer

Jasmine Y. Lee conducted all *in vitro* and *in vivo* experiments and wrote this section of the paper.

Gianna M. Branella and Hunter C. Jonus conducted the *in vivo* experiment looking for PTK7 expression in recurrent tumor cells.

Kelly C. Goldsmith, H. Trent Spencer, and Christopher B. Doering provided oversight, feedback, and edited this section of the paper.

Parts of the work in this chapter was published in *Cell Reports Medicine* in 2023. See also Chapter 2 for work published in same paper.

Citation:

Jasmine Y. Lee, Hunter C. Jonus, Arhanti Sadanand, Gianna M. Branella, Victor Maximov, Suttipong Suttapitugsakul, Matthew J. Schniederjan, Jenny Shim, Andrew Ho, Kiran K. Parwani, Andrew Fedanov, Adeiye Pilgrim, Jordan Silva, Robert W. Schnepp, Christopher B. Doering, Ronghu Wu, H. Trent Spencer, and Kelly C. Goldsmith. Identification and targeting of protein tyrosine kinase 7 (PTK7) as an immunotherapy candidate for neuroblastoma cellular therapy. *Cell Rep Med*. 2023.

4.1 Abstract

To determine the feasibility of targeting a candidate marker identified to be highly expressed in neuroblastoma, we successfully designed and developed anti-PTK7 chimeric antigen receptors (CAR) in Chapter 2. Here, we tested the feasibility of targeting neuroblastoma (NB) cell lines and *in vivo* metastatic NB mouse models with this engineered CAR. We show that PTK7 CAR T cells prompt apoptotic-induced cell death in IMR5, NLF, and SK-N-AS NB cell lines, while the same cytotoxicity was not observed in PTK7 negative CMK and SK-N-AS PTK7 knock out (KO) cells. *In vivo*, PTK7 CAR T cells improved survival of mice bearing IMR5 metastatic disease, though response was not sustained. The evidence ruled out PTK7 antigen loss as a mechanism of resistance, suggesting multiple doses or further optimized CAR may be required for aa sustained response. Together, these data show our engineered $\alpha\beta$ PTK7 CAR T cells to be promising a candidate to treat NB.

4.2 Introduction

The recent addition of immunotherapies in high-risk NB patients improved overall survival by 20% [9]. Dinutuximab is a monoclonal antibody currently used to treat high-risk NB and several pitfalls of this therapy due to antigen choice were recognized [82,122-124]. To overcome the pitfalls of targeting GD2, we have identified a novel target, protein tyrosine kinase 7 (PTK7), that is highly expressed on NB tumor cells with low normal tissue expression (Chapter 1.3) and designed and developed a second-generation chimeric antigen receptor (CAR) against this target antigen (Chapter 2). Here, we test out the feasibility of using PTK7 CAR T-cell therapy as a safe and effective method of inducing NB cell death and controlling tumor burden *in vivo*.

4.3 Results

PTK7-targeting CAR T cells induce NB cell death *in vitro*

To determine the cytotoxic potential, primary PTK7 CAR T cells were co-cultured with PTK7-positive or negative cells at various E:T ratios. Given the high expression of PTK7 on all wildtype NB models, we used PTK7 negative CMK cells as well as SK-N-AS PTK7 KO cells as PTK7-negative controls. T cells were characterized for CAR expression, T-cell differentiation, and checkpoint markers, 24-hours prior to cytotoxic assays (**Figure 2.6, Figure 2.7**). NB specific cytotoxicity was measured via Annexin V/7-AAD staining after 4 hours and 12 hours of co-culture (**Figure 4.1A**). PTK7 CAR T cells induced cytotoxicity of IMR5 NB after 4 hours, which further increased to an average of 1:1 (29% ± 8), 5:1 (63% ± 6), and 10:1 (74% ± 10) E:T ratio after 12 hours. Similar cytotoxicity was seen in NLF that was augmented with increasing E:T ratios and increased incubation time. CD69 upregulation was also observed at the indicated time points in these co-cultures (**Figure 4.1B**). Of note, NLF cells have higher PTK7 MFI expression (**Figure 4.2A**) and induce significantly higher CD69 activation in CAR T cells at 4 hours with a trend for higher CD69 activation at 12 hours, suggesting there may be a correlation between PTK7 expression levels and CAR T-cell killing potential. While clustering of CAR T cells on the tumor target may lead to tonic T-cell activation and potential exhaustion, others have shown that CAR T-cell clustering promotes tumor-cell killing [125]. Clustering of PTK7 CAR T cell cocultures with IMR5 cells was observed where potent anti-NB cytotoxicity occurred (**Figure 4.2B**), while neither clustering nor CD69 activation was observed when IMR5 cells were co-cultured with mock T cells or CD19 CAR T cells. Caspase 3/7 activity was also measured in a live cell-based cytotoxicity assay using SK-N-AS non-targeting gRNA control and SK-N-AS PTK7 KO target cells, which showed similar antigen specific induction of NB cell death (**Figure 4.2C-D**). Importantly, PTK7 CAR T-cell-mediated tumor cell death was not observed in PTK7 negative CMK cells (**Figure 4.1A**) nor in SK-N-AS PTK7 KO cells

compared to SK-N-AS gRNA control cells (**Figure 4.2D**). The combined data support PTK7 CAR T cells induce PTK7-*specific* cytotoxicity of PTK7 positive NB cells *in vitro*.

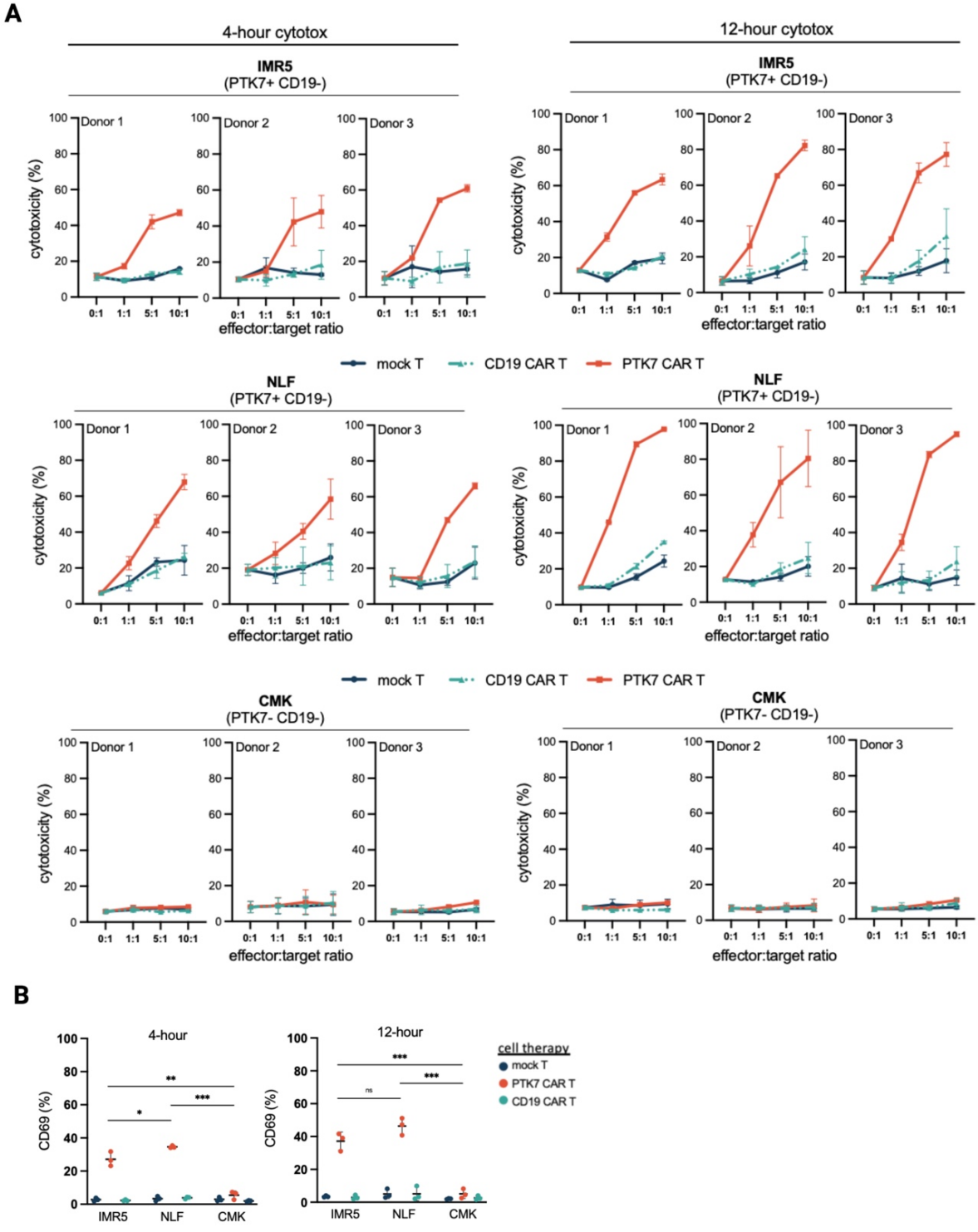

Figure 4. 1. PTK7 CAR T cells induce antigen-specific cytotoxicity of NB cells, *in vitro*

(A) 4-hour and 12-hour flow cytometry cytotoxicity assay. %cytotoxicity = the sum of 7AAD+, Annexin V+, and 7AAD+Annexin V+ cells, gated on target cells only. N = 3 donors with n = 2 biological replicates. **(B)** %CD69 expression in mock T cells or CAR T cells co-cultured with indicated target cells from 4-hour cytotoxicity assay, gated on live primary T cells. N = 3 donors, statistical analysis represents Student's t-test (***p < 0.001, **p < 0.01, ⁎p < 0.05; ns, p > 0.05).

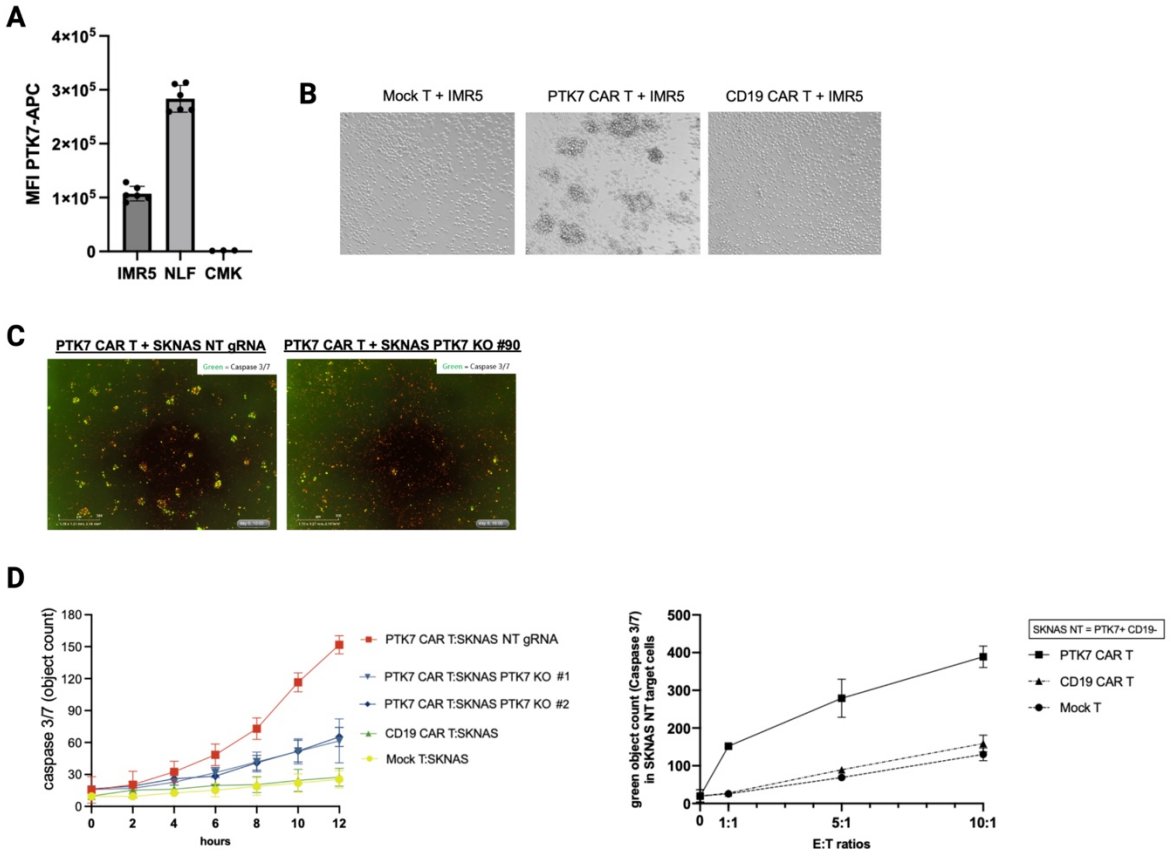

Figure 4. 2. PTK7 CAR T cells induce antigen-specific cytotoxicity of NB cells, *in vitro continued*

(A) PTK7 MFI expression in IMR5, NLF, and CMK target cells, n = 6 biological replicates. **(B)** Representative image of mock T or CAR T cells with IMR target cell co-culture at 4-hours. **(C)** IncuCyte (caspase 3/7) image captured 10 hours into co-incubation. **(D)** Left: Target cells and CAR T cells or mock T cell control were incubated with Caspase-3/7 dye and live cell analysis was

performed at the indicated time points. Processing definitions of caspase 3/7 activity (green object count) on target cells were determined. n = 1 donor. Right: Caspase 3/7 activity in SK-N-AS NT gRNA (non-targeting gRNA) incubated with indicated mock T or CAR T cells at indicated effector to target ratios. Error bars represent SD of 4 technical replicates.

PTK7-targeting CAR T cells induce NB cell death in an *in vivo* metastasis model

To evaluate the efficacy of PTK7 CAR T cells in an *in vivo* high-risk disease model [126], $3x10^5$ luciferase expressing IMR5 (*MYCN* amplified) cells were injected intravenously into NOD-*scid* IL2Rgamma^{null} (NSG) and a single dose of $5x10^6$ mock T cells or PTK7 CAR T cells were delivered intravenously 24 hours later. Mice were imaged with IVIS bioluminescence imaging 1-3 times per week until tumor burden endpoint (**Figure 4.3A**). Untreated mice and mock T-cell treated mice had an endpoint range of D31-35, while PTK7 CAR T-cell treated mice had an endpoint range of D35-48, leading to a significant survival advantage in PTK7 CAR T-cell treated mice (**Figure 4.3B**). In addition, PTK7 CAR T cells were also tested in a *MYCN* non-amplified cell line, CHLA-255. CHLA-255 cells are positive for PTK7 expression at the cell surface (data not shown) and although not significant, there was a trend toward improved survival in CHLA-255 bearing mice treated with PTK7 CAR T cells compared to mock T cells (**Figure 4.4A-B**). Although we found our CAR to bind murine PTK7 using murine PTK7 Fc (**Figure 4.5A-B**), no significant changes in weight nor cytopenias were observed in PTK7 CAR T cell treated mice (**Figure 4.5C, Figure 4.5D**). While tumors recurred in mice following PTK7 CAR T cell treatment, flow cytometry of the recurrent metastatic NB cells demonstrated PTK7 expression is retained and high on the relapsed NB cell surface (**Figure 4.5E**).

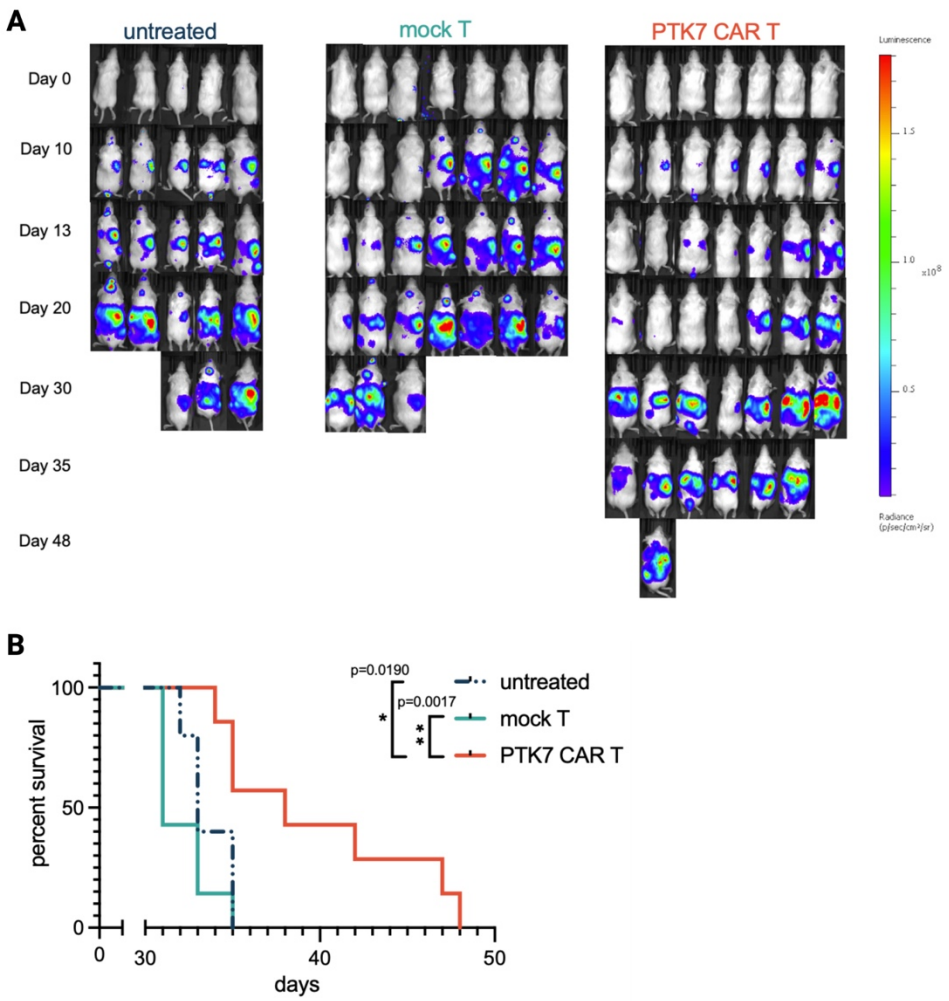

Figure 4. 3. PTK7 CAR T cells improve survival in a NB MYCN-amplified metastatic mouse model

(A-B) NSG mice were injected with $3x10^5$ IMR5 cells on Day -1 IV, then treated with $5x10^6$ mock T cells or PTK7 CAR T cells on Day 0 IV. **(A)** Bioluminescence images and **(B)** Kalpan-Meier survival analysis of arms. N = 5 untreated, n = 7 mock T cell, n = 7 PTK7 CAR T cell. Statistical analysis represents log-rank (Mantel-Cox) test (**p < 0.01, *p < 0.05; ns, p > 0.05).

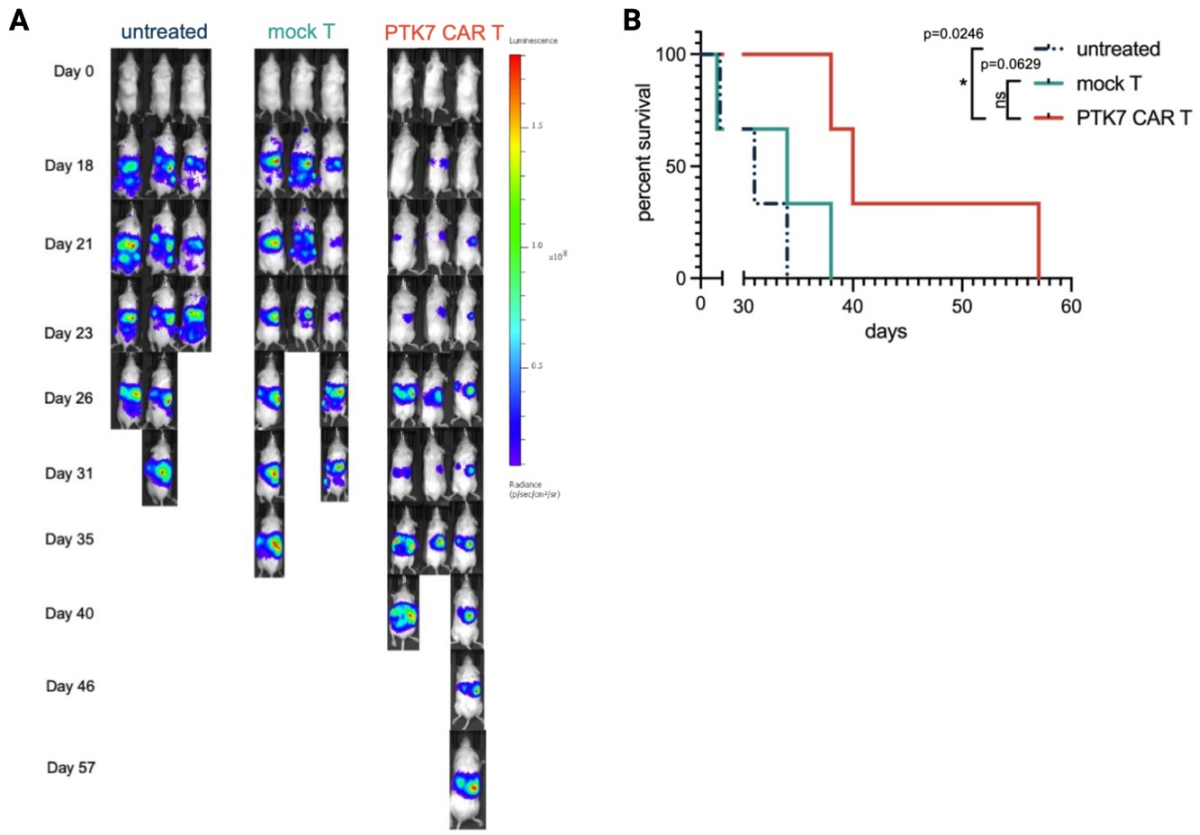

Figure 4. 4. PTK7 CAR T-cell treated mice bearing MYCN-non amplified metastatic tumor cells trend toward improved survival

(A-B) NSG mice were injected with $3x10^5$ IMR5 cells on Day -1 IV, then treated with $5x10^6$ mock T cells or PTK7 CAR T cells on Day 0 IV. **(A)** Bioluminescence images and **(B)** Kalpan-Meier survival analysis of arms. N = 3 per arm. Statistical analysis represents log-rank (Mantel-Cox) test (**p < 0.01, *p < 0.05; ns, p > 0.05).

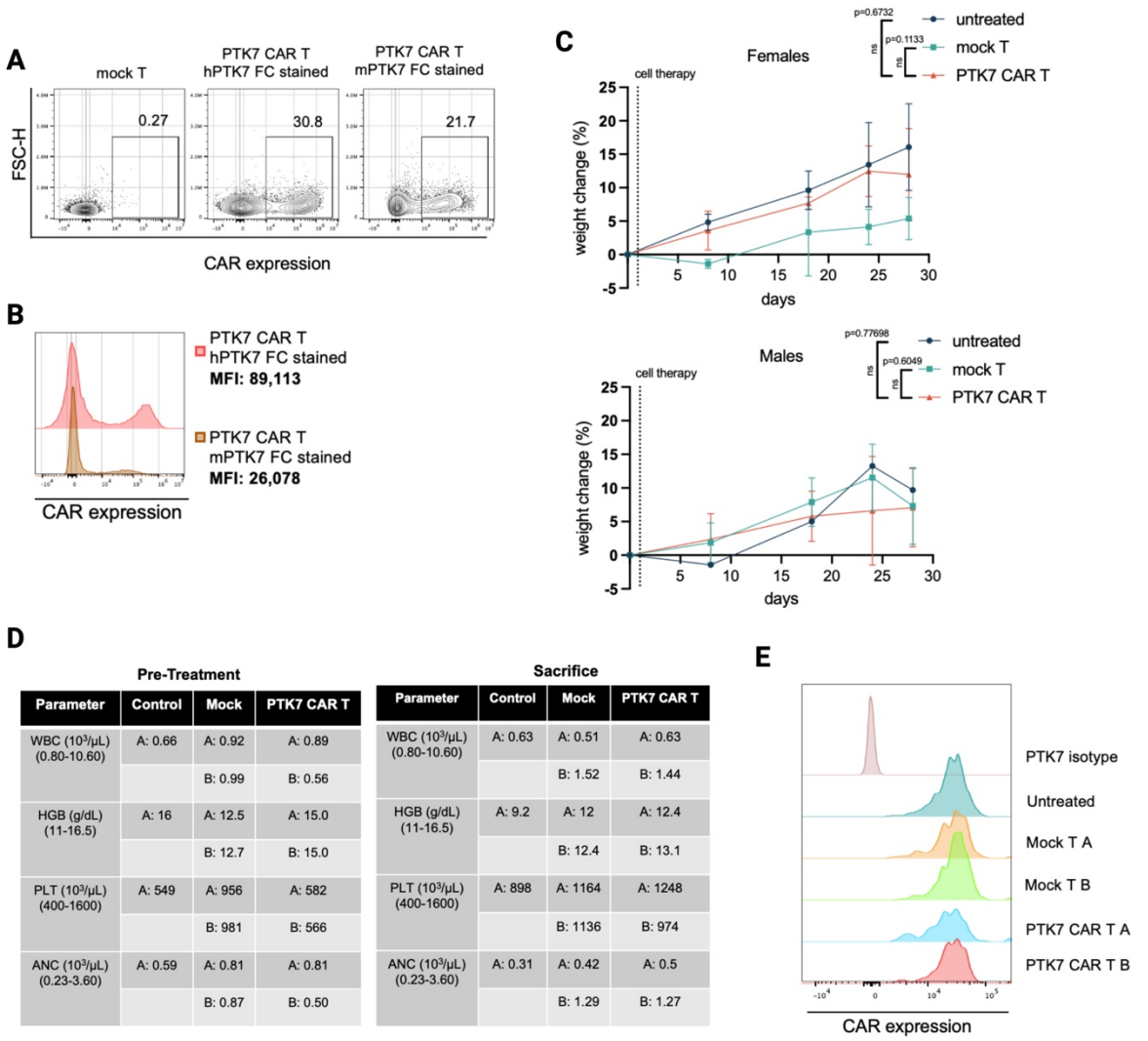

Parameter	Control	Mock	PTK7 CAR T
WBC (10^3/µL) (0.80-10.60)	A: 0.66	A: 0.92	A: 0.89
		B: 0.99	B: 0.56
HGB (g/dL) (11-16.5)	A: 16	A: 12.5	A: 15.0
		B: 12.7	B: 15.0
PLT (10^3/µL) (400-1600)	A: 549	A: 956	A: 582
		B: 981	B: 566
ANC (10^3/µL) (0.23-3.60)	A: 0.59	A: 0.81	A: 0.81
		B: 0.87	B: 0.50

Pre-Treatment

Parameter	Control	Mock	PTK7 CAR T
WBC (10^3/µL) (0.80-10.60)	A: 0.63	A: 0.51	A: 0.63
		B: 1.52	B: 1.44
HGB (g/dL) (11-16.5)	A: 9.2	A: 12	A: 12.4
		B: 12.4	B: 13.1
PLT (10^3/µL) (400-1600)	A: 898	A: 1164	A: 1248
		B: 1136	B: 974
ANC (10^3/µL) (0.23-3.60)	A: 0.31	A: 0.42	A: 0.5
		B: 1.29	B: 1.27

Sacrifice

Figure 4. 5. No significant changes in weight nor cytopenias post PTK7 CAR T-cell treatment

(A) Representative flow plot showing %PTK7 CAR binding/expression to human and mouse PTK7-FC Chimera. **(B)** histogram and MFI of CAR binding/expression. **(C)** Weight change (%) of mice in IMR5-bearing mice treated in Figure 4.3 Top: Females. Bottom: Males. **(D)** Select blood counts of NSG mice injected with 3x105 IMR5 cells on Day -1 IV, then treated with 5x106 mock T cells or PTK7 CAR T cells on Day 0 IV. Blood counts are presented for D-1 (Pre-Treatment) and 16 days post immunotherapy (Sacrifice). Values for white blood cells (WBC), hemoglobin (HGB), platelets (PLT), and absolute neutrophil counts (ANC) are provided for control (n = 1, NSG grafted with IMR5), mock T (n = 2, NSG grafted with IMR5 + Mock T cells) and PTK7 CAR

T (n = 2, NSG grafted with IMR5 + PTK7 CAR T cells). **(E)** Flow cytometry histogram of PTK7 expression in IMR5 cells in the liver of mice with indicated treatment on Day 16.

4.4 Discussion

Dinutuximab, a monoclonal antibody against GD2, improved survival of high-risk NB patients by 20% [9]. However, several pitfalls of GD2 targeting exist. To overcome the drawbacks of targeting GD2, other immunotherapy antigen candidates were identified through a glycoproteomics discovery platform. Included is PTK7, which is highly and stably expressed on the cell surface of NB cell lines, primary tumor cells, and PDX's (Chapter 1.3). We showed previously in Chapter 2 that lentiviral vector EF1α-based PTK7 VH-L-VL CAR T cells are antigen-specific and show the most promise for use in determining the *in vitro* and *in vivo* efficacy of targeting PTK7 in NB.

Severe toxicities are associated with CAR T-cell therapies; thus, efforts should be made to eliminate any off-tumor off-target toxicities due to non-specific binding of CARs. To test this, we first showed PTK7 CAR T-cells induce direct apoptosis (Annexin V/7AAD/Caspase 3/7) in only PTK7-expressing NB cell lines, while sparing cell lines that don't express PTK7, owing to the specificity and safety of the PTK7 CAR. In addition to *in vitro* efficacy, we determined the *in vivo* effect by utilizing a metastasis model most utilized in the NB CAR T-cell preclinical field. We show PTK7 CAR T cells demonstrated potent anti-NB activity *in vivo*, where survival was significantly prolonged in cell line xenograft (CDX) models representing the potentially more aggressive adrenergic NB phenotype, IMR5, which was recently shown to be less amenable to immunotherapy than NB tumors that fall into the mesenchymal, more dedifferentiated type of NB [127-129]. Important to determining off-tumor on-target toxicities, our mouse and human PTK7-binding CAR T-cell treated mice showed no significant difference in weight nor cytopenia. However, in future investigations, off-tumor on-target toxicities should be seriously considered given there is low PTK7 expression in some pediatric normal tissue (Chapter 1.3).

While the results are encouraging, especially considering the aggressive phenotype of the *in vivo* models that were used, there remains room for optimization of our CAR-based approach. For example, our design utilized a CD28-based co-stimulatory domain, which has not shown to be as successful in NB or other solid tumors preclinically compared to 4-1BB or dual 4-1BB/CD28 signaling [130-133]. In fact, the most recent promising clinical trial results utilized a third-generation dual CD28/4-1BB co-stimulatory domain-based CAR, in which CAR T cells were detected in the bone marrow up to 2 years post-infusion [44].

An additional optimization strategy of CAR T-cell therapy includes utilizing different T-cell subsets. This can include expanding $\alpha\beta$ T cells to achieve specific differentiation states or using other lymphocytes such as NK cells or $\gamma\delta$ T cells. We chose to test PTK7 CAR in $\gamma\delta$ T cells to take advantage of their inherent anti-tumorigenic ability, which is further described in the following chapter.

4.5 Materials and Methods

Flow-based cytotoxicity assay

NB target cells were stained with VPD450 (BD Horizon) and plated onto 48-well cell culture plates at 50,000 cells/well and left to adhere overnight. Suspension target cells (697 and CMK's) were also stained with VPD450 and re-plated into T25 flasks overnight and re-counted and plated into 48-well cell culture plates at 50,000 cells/well the next day. Primary CAR T cells were added at various effector to target ratios in a total volume of 300 uL and incubated at 37 □C for 4 hours or 12 hours. Suspension cell wells were harvested and added to flow tubes, while adherent cell suspensions were collected, and adherent cells gently taken off the wells with Accutase (Stemcell Technologies) to prevent spontaneous flipping of phosphatidylserine and added to corresponding flow tubes. Cells were washed 1x with Annexin V Binding Buffer (BioLegend), stained with 3 uL Annexin V-APC (BioLegend) and 3 uL anti-CD69-APC-Cy7 (BD Pharmingen), and washed 1x with Annexin V Binding Buffer. 7-AAD Viability Dye (BioLegend) was added 2 minutes before flow

cytometry analysis. Detection was done by flow cytometry (Auora Cytek) and analyzed with FlowJo software (v10). Percent cytotoxicity was measured by adding Annexin V+, 7AAD+, and Annexin V+7AAD+ target cells.

IncuCyte-based cytotoxicity assays

Target cells were plated in a flat bottom 96-well cell culture plate at 7,000 cells/well and left to adhere overnight. Primary CAR T cells were added at indicated effector to target ratios in a total volume of 200 uL (total ratio of 1:1000 IncuCyte Caspase-3/7 Green Dye (Sartorius)) and placed into IncuCyte Live Cell Analysis System (IncuCyte ZOOM) over the indicated number of hours. Processing definitions of Caspase 3/7 activity (green object count) on target cells were determined and quantified using the IncuCyte ZOOM software.

Animal Study Ethics

All animal studies were conducted in accordance with policies set forth by the Emory University Institutional Animal Care and Use Committee (IACUC) under an approved animal use protocol (PROTO201700089, PROTO201800202).

In vivo metastasis model for αβ CAR T-cell therapy

4-week-old NSG mice were engrafted with $3x10^5$ GFP/luciferase-tagged IMR5 cells via tail vein injection. $5x10^6$ total Mock T cells or PTK7 CAR T cells (35-45% CAR+ cells) were injected via retroorbital injection 24 hours later. Mice were injected with D-luciferin (PerkinElmer) at 10 µL/g of body weight via intraperitoneal injection and were imaged with IVIS bioluminescence (PerkinElmer) 1-3x a week. Mice were sacrificed at a predefined endpoint of tumor burden, which considered changes in weight, scruff, movement, and hunched state. Alternatively, mice were sacrificed 16 days after immunotherapy treatment and biopsied for residual tumor burden. Based on IVIS imaging, primary focus was placed on liver as a heavily tumor populated organ.

Chapter 5: PTK7-targeting *γδ* CAR T cells and bispecific T-cell engagers enhance NB cell death *in vitro* and in mouse metastasis NB model.

Jasmine Y. Lee and H. Trent Spencer

Jasmine Y. Lee designed and conducted all experiments and wrote this chapter

H. Trent Spencer provided oversight and feedback

Acknowledgment: I would like to thank Expression Therapeutics, specifically Brian Petrich and David Schofield, for providing the PTK7 bispecific T-cell engager

The work presented in this chapter is unpublished.

5.1 Abstract

$\gamma\delta$ T cells are a small subset of T cells in the peripheral blood that recognize stressed cells independent of antigen processing and MHC presentation. They have both adaptive and innate like properties and can induce rapid and potent tumor cell death. Our lab has previously shown that ex-vivo expanded $\gamma\delta$ T cells are capable of inducing NB tumor cell death and is further exemplified with the addition of Dinutuximab. We modified $\gamma\delta$ T cells to express PTK7 CAR to improve NB cell-killing potential of these cells. In addition to CAR modification, we separately modified $\gamma\delta$ T cells to secrete a soluble molecule, a bispecific engager, that binds CD3 and PTK7 to engage the endogenous signaling pathway through T-cell redirection. Our delivery method of choice, mRNA electroporation, resulted in a high 65.6%-76.9% PTK7 CAR expression. We found PTK7 $\gamma\delta$ CAR T cells to induce donor-dependent cytotoxicity of NB cells, and $\gamma\delta$ CD3-PTK7 bispecific engager to induce similar cytotoxicity. In a limited *in vivo* study of n = 2/arm, we found both PTK7 $\gamma\delta$ CAR T cells and $\gamma\delta$ CD3-PTK7 bispecific engager to control early tumor growth until Day 21. Additional *in vitro* and *in vivo* studies should be performed to determine the feasibility of utilizing modified $\gamma\delta$ T cells to target PTK7 in NB.

5.2 Introduction

$\gamma\delta$ T cells make up a small percentage of circulating blood cells in adults where they only account for around 1-10% of CD3+ T cells [134]. Unlike classical $\alpha\beta$ T cells, $\gamma\delta$ T cells recognize target cells in an MHC-independent manner and have innate immune cell receptors such as NKG2D, NKp30, and NKp44 [49,66,135]. A specific subtype of $\gamma\delta$ T cells, Vg9V2dT, have been shown to be effectively cytotoxic against several solid tumors and leukemia/lymphoma cells [67,136]. Advantages of utilizing $\gamma\delta$ T cells as a form of therapy is the possibility of 3rd party donors due to the MHC independence of these cells and the flexibility to give multiple doses over time as $\gamma\delta$ T cells don't form memory.

Our lab has previously shown that ex-vivo expanded, non-modified $\gamma\delta$ T cells have anti-tumor effects on NB tumors [68]. To enhance the antitumor efficacy of these T cells, we modified these cells to express CARs against PTK7.

In addition to CAR T cells, bispecific engagers have been utilized to stimulate a T-cell response in both pre-clinical and clinical settings [137]. Most currently tested bispecific engagers don't include a co-infusion with effector cells but have shown some promising clinical results on their own [138]. Here, we propose to electroporate CD3-PTK7 bispecific engager mRNA to $\gamma\delta$ T cells, then utilize both the $\gamma\delta$ T-cell population plus the secreted engagers as a candidate therapy for NB.

5.3 Results

PTK7-targeting $\gamma\delta$ CAR T cells and bispecific engager induce NB cell death *in vitro*

$\gamma\delta$ T cells were isolated from healthy donor PBMCs, in which almost the entire population is $\gamma\delta$ TCR+ by the last day of expansion (Day 12) (**Figure 5.1A-B**). mRNA was electroporated into $\gamma\delta$ T cells by mRNA electroporation for transient expression of PTK7 CAR (**Figure 5.2A**). Additionally, a mRNA bispecific engager against PTK7 and CD3 was electroporated into T cells to both secrete and bind the engager (**Figure 5.2B**). Electroporation resulted in high cell surface PTK7 CAR expression (65.6%-76.9%) (**Figure 5.3A and Supplemental Figure 5.1A-C**). Expression of the bispecific engager was not determined.

To determine cytotoxic potential, PTK7 $\gamma\delta$ CAR T cells were co-cultured with PTK7-positive or negative cells (**Figure 5.4A-B**). NB cytotoxicity was measured with Annexin V/7-AAD flow cytometry after 4 hours of co-culture. Unmodified $\gamma\delta$ T cells Donor 4 induced 81% ± 1 cytotoxicity of IMR5 cells, which only slightly increased to 84% ± 1 with PTK7 CAR modification (**Figure 5.4A**). However, unmodified $\gamma\delta$ T cells of Donors 5 and 6 induced 41% ± 0 and 34% ± 2, and notably increased to 87% ± 9 and 71% ± 1 with PTK7 CAR modification. A similar notable

increase in cytotoxicity of PTK7 CAR modified $\gamma\delta$ T cells of Donors 5 and 6 were seen in NLF and CHLA-255 cells. Altogether, the data show PTK7 CAR modification induces a donor dependent increase in cytotoxicity of NB cells. The antigen specificity of the increased cytotoxicity was discerned in SK-N-AS PTK7 KO model where a marked difference in cytotoxicity of modified and CAR modified $\gamma\delta$ T cells was shown (**Figure 5.4B**).

To determine the feasibility of targeting PTK7 through endogenous T-cell mechanism, a bispecific engager against CD3 and PTK7 was transiently expressed in $\gamma\delta$ T cells. The cytotoxicity of CD3-PTK7 $\gamma\delta$ T cells was comparable to PTK7 CAR T-cell induced cytotoxicity (**Figure 5.4C**). Further downstream experiments are required to determine the advantages and disadvantages of both therapies.

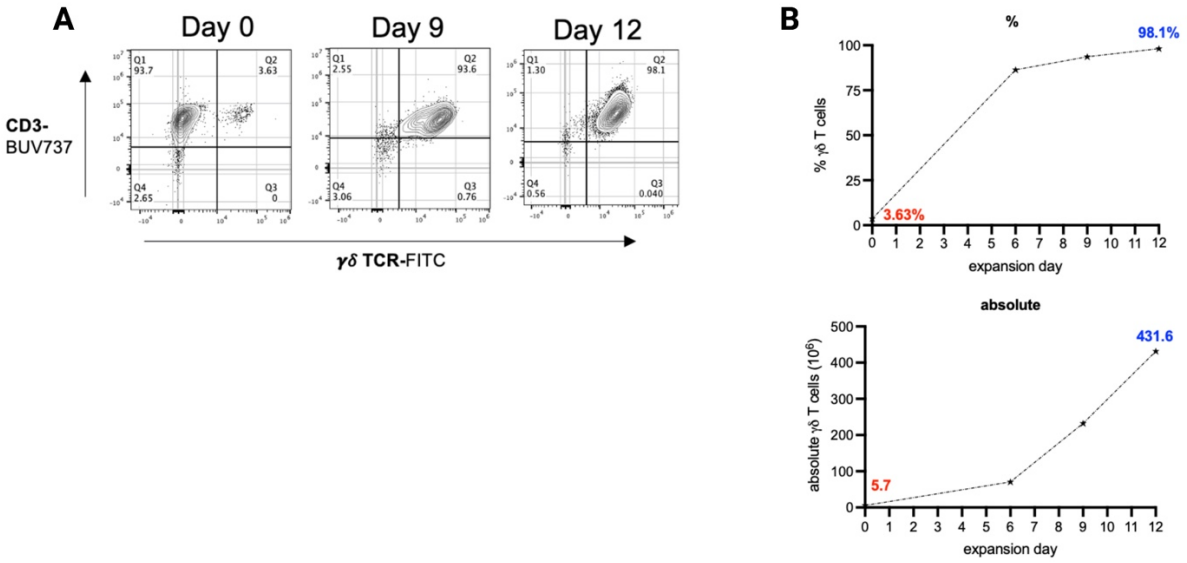

Figure 5. 1. $\gamma\delta$ T cell expansion

$\gamma\delta$ T cells were isolated from healthy donor PBMCs as described in methods. **(A)** Representative flow cytometry plot of $\gamma\delta$ TCR and CD3 expression on indicated day of expansion, gated on live cells **(B)** Top: % $\gamma\delta$ T cells ($\gamma\delta$ TCR+CD3+) Bottom: Total live $\gamma\delta$ T cell number by trypan blue

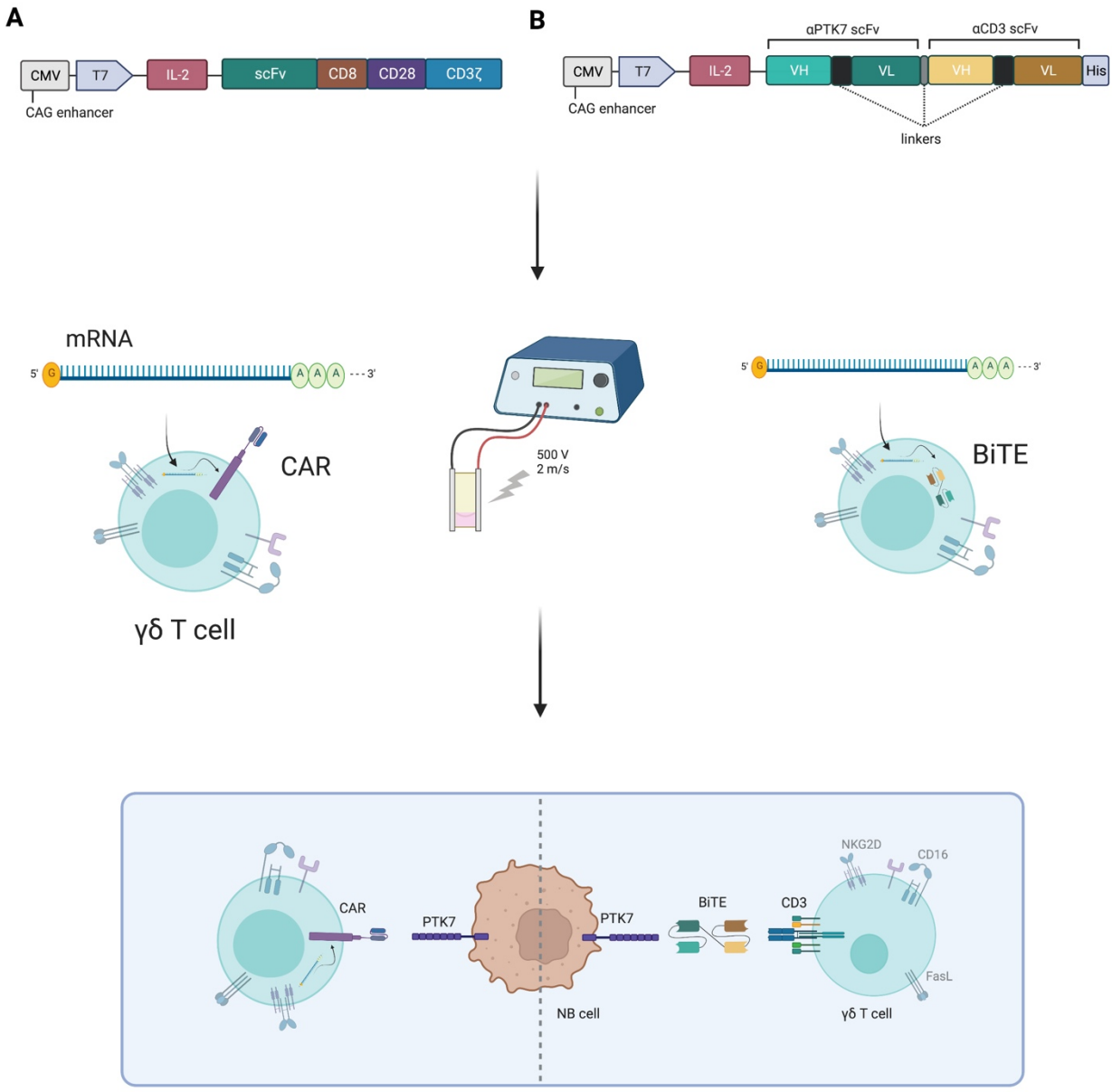

Figure 5. 2. Graphical design of PTK7 CAR and CD3-PTK7 bispecific engager constructs and introduction to *γδ* T cells

(A) T7 mRNA promoter-based PTK7 CAR and **(B)** CD3-PTK7 bispecific engager mRNA were electroporated into *γδ* T cells

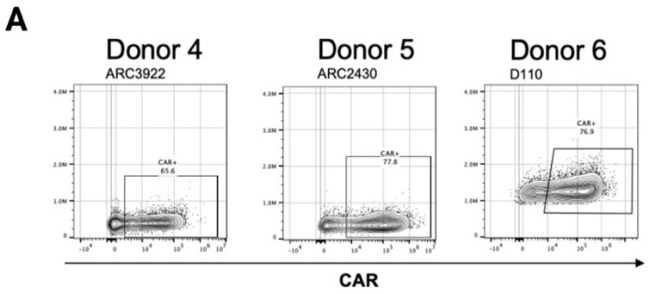

Figure 5. 3. PTK7 CAR T-cell expression in $\gamma\delta$ T cells

(A) PTK7 CAR expression (PTK7-Fc) in $\gamma\delta$ T cells 24-hours post-electroporation of CAR mRNA

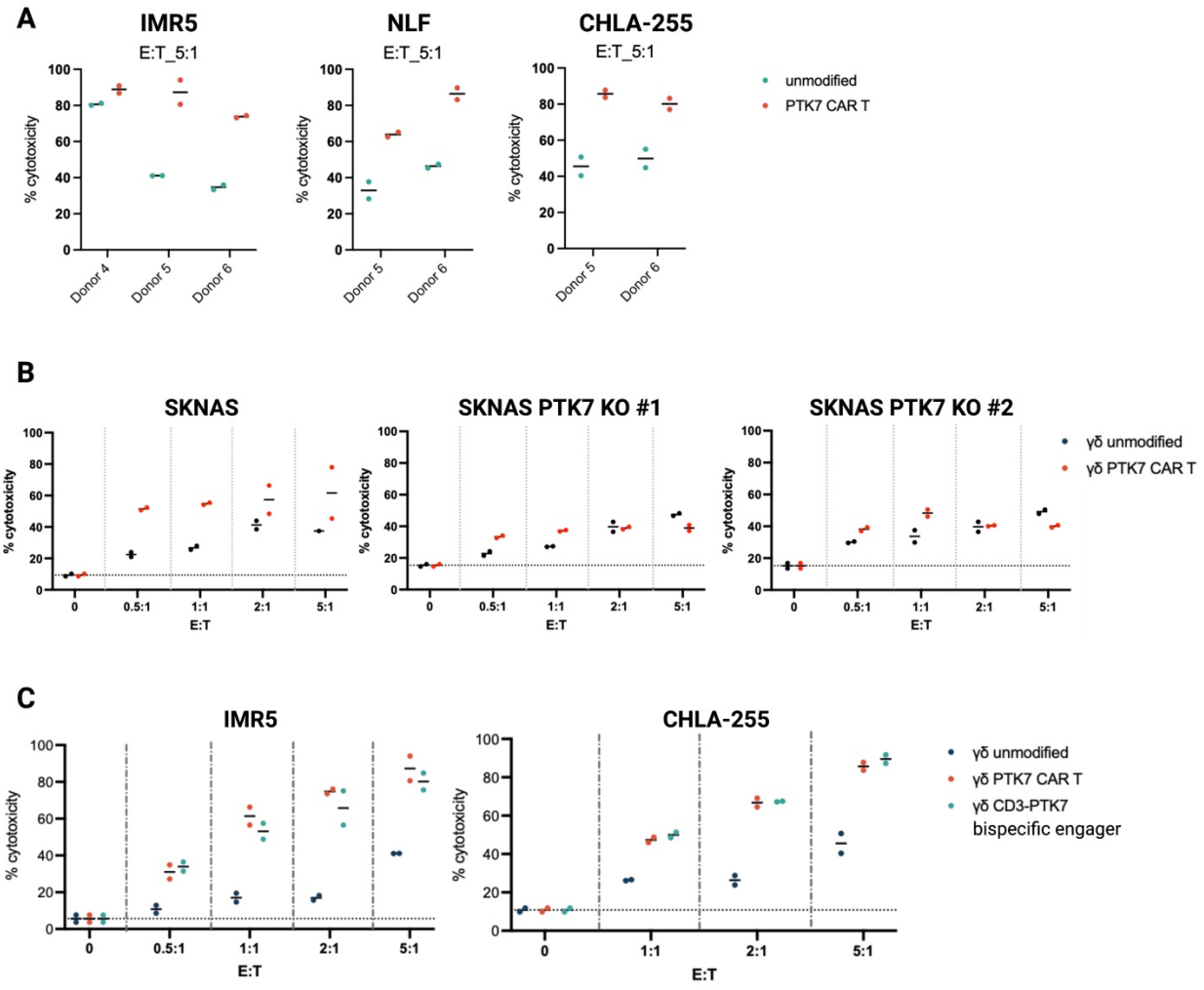

Figure 5. 4. PTK7 *γδ* CAR T cells and CD3-PTK7 bispecific engagers induce donor dependent cytotoxicity of NB cells *in vitro*

PTK7 *γδ* CAR T cells in 4-hour flow cytometry cytotoxicity assays of indicated **(A)** IMR5, NLF, and CHLA-255, **(B)** SK-N-AS or SK-N-AS with PTK7 knocked out. **(C)** PTK7 *γδ* CAR T cells and CD3-PTK7 bispecific engagers in 4-hour flow cytometry cytotoxicity assays. n = 2 experimental replicates. %cytotoxicity = the sum of 7AAD+, Annexin V+, and 7AAD+Annexin V+ cells, gated on target cells only.

PTK7-targeting $\gamma\delta$ CAR T cells and bispecific engager delays NB tumor cell growth in an *in vivo* metastasis model

To evaluate the efficacy of PTK7 $\gamma\delta$ CAR or CD3-PTK7 bispecific T cells in an *in vivo* high-risk disease model [126], 1x10^6 luciferase expressing IMR5 cells were injected intravenously into NOD-*scid* IL2Rgamma^{null} (NSG) mice on Day -1. Others have shown that $\gamma\delta$ CAR T cells have limited persistence in mice [139]. In addition, we found that *ex vivo* expanded unmodified $\gamma\delta$ T cells are detectable in peripheral blood up to 72 hours post-injection in NSG mice (data not shown). Based on the limited persistence, mice were treated with multiple doses of 10x10^6 $\gamma\delta$ T cell therapy on Day 0, 3, 7, and 10. Mice were imaged with IVIS bioluminescence imaging 2-3 times per week until tumor burden endpoint (**Figure 5.5A**). Mice treated with either PTK7-targeting CAR or bispecific engager delayed tumor formation in mice up to Day 24 (**Figure 5.5B**). However, no notable differences in survival were observed (**Figure 5.5C**). The small sample size should be taken into consideration and further experiments should be performed to determine the anti-tumor cell efficacy of modified $\gamma\delta$ T-cell therapy.

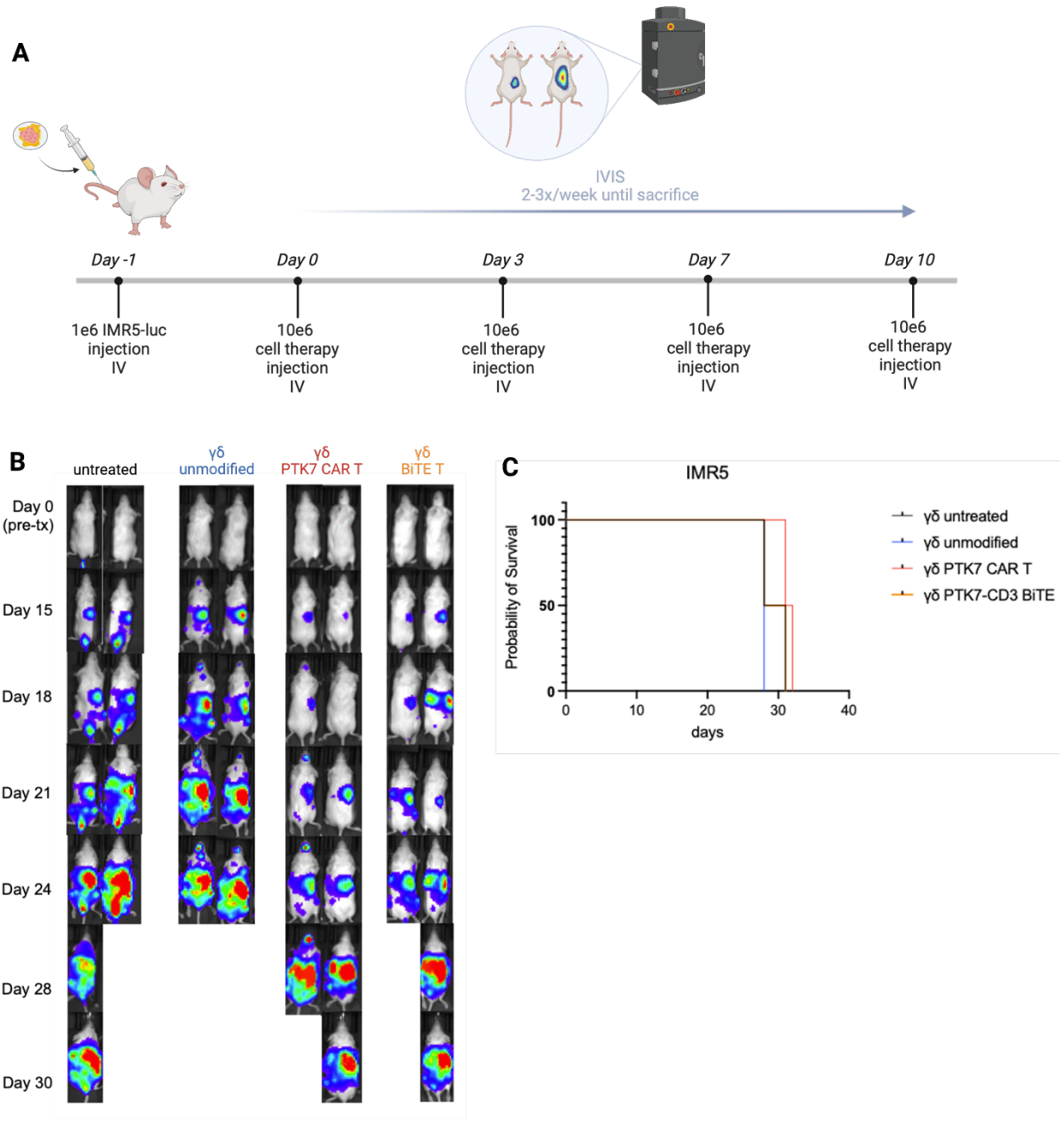

Figure 5. 5. PTK7 *γδ* CAR T cells and bispecific engager delays NB tumor cell growth

(A) Graphical timeline of mouse model and treatment with cell therapy **(B)** Bioluminescence images **(C)** Kalpan-Meier survival analysis of arms. N = 2 per arm. Statistical analysis represents log-rank (Mantel-Cox) test (∗∗$p < 0.01$, ∗$p < 0.05$; ns, $p > 0.05$).

5.4 Discussion

$\gamma\delta$ T cells are an attractive candidate for cellular therapy due to their independence from MHC molecules and historical clinical studies show they have an ideal safety profile (NCT03183232, NCT03183219). Investigators examining associations between tumor-associated lymphocytes and patient prognosis found that intratumoral $\gamma\delta$ T-cell signatures were the most significantly correlated with favorable outcome [140]. Our lab has also recently shown that non-modified $\gamma\delta$ T cells in combination with dinutuximab and temozolomide, were capable of inducing NB tumor cell death, *in vivo* [68]. We showed in Chapter 4 that PTK7 $\alpha\beta$ CAR T cells were an effective method of targeting NB *in vitro* and *in vivo*. Given their inherent ability to induce rapid and potent tumor cell death, we chose to modify Vγ9Vδ2 T cells with PTK7 CAR to determine the feasibility of treating NB.

Two main subtypes, Vδ1+ and Vδ2+ cells have been tested both preclinically and clinically. However, Vδ2+ cells make up 60-95% of $\gamma\delta$ T cells in adult peripheral blood, and selective stimulation can result in expansion of Vγ9Vδ2 T cells *ex vivo* [59,60], rendering them easier to expand than Vδ1+ cells which lie in small numbers in the blood but mostly present in mucosal tissues. *In vitro*, we found PTK7 $\gamma\delta$ CAR T cells to induce donor-dependent cytotoxicity of NB cells. As cytotoxicity of $\gamma\delta$ T cells varies by donor, we consequently saw increased cytotoxicity with PTK7 CAR modification only if the donor showed minimal to moderate cytotoxicity in their unmodified form. $\gamma\delta$ T cells from donors that are considered highly cytotoxic, did not increase in cytotoxicity with added PTK7 CAR modification. Variation in $\gamma\delta$ T-cell potency expanded with the same GMP-compliant protocol utilized in these studies has been attributed to presence of NK cells within the expanded product [141]. However, NK cell presence was not determined in all donors utilized in these studies, minimizing the ability to confirm those findings in this setting.

In addition to CAR T-cell therapy, we employed a $\gamma\delta$ T-cell bispecific engager combination to target PTK7. There is pre-clinical evidence that show bispecific engagers lead to tumor cell lysis, selective activity, and recruitment of Vγ9Vδ2 T cells in blood and solid tumors [73-77]. In $\alpha\beta$ T cells, a subclass of bispecific engagers termed BiTE, showed promising clinical results in hematopoietic cancers [142,143]. These studies utilize synthetic production of engagers as a single therapy, while here, we proposed to combine cellular therapy with engager therapy by utilizing bispecific engager-expressing $\gamma\delta$ T cells against CD3 and PTK7. The hypothesis of utilizing this method is to increase the potency and flexibility of bispecific engagers with $\gamma\delta$ T cells and vise versa. *In vitro*, CD3-PTK7 bispecific engager expressing $\gamma\delta$ T cells induced similar toxicity to PTK7 $\gamma\delta$ CAR T cells. Lastly, in a limited *in vivo* study, we found both $\gamma\delta$ T cell modified therapies to control early tumor cell growth, until Day 21, post-first infusion.

In conclusion, we showed CAR or bispecific engager-modified $\gamma\delta$ T cells specifically target NB cells in certain donors. Future *in vitro* studies should include determining the NK cell population within the expanded donor cells, in addition to determining the level of expression of innate cell killing-associated ligands and receptors expressed on $\gamma\delta$ T-cells, FASL, NKG2D, CD16. These studies will begin to determine which donor characteristics would best as biomarkers of anti-tumor cell killing-enhancement potential by gene modification. Lastly, additional *in vivo* studies should be performed to determine the feasibility of targeting PTK7 utilizing these therapies in an aggressive metastatic NB model, starting with modification of the treatment schedule, or enhancement of $\gamma\delta$ T cells to increase *in vivo* persistence.

5.5 Materials and Methods

See Chapter 2 Methods for:

Cell lines

Measuring CAR expression

See Chapter 3 Methods for:

Flow-based cytotoxicity assay

Animal Study Ethics

Cloning of T7-PTK7 CAR

A codon optimized AscI-PTK7 VH scFv-5'CD8-BlpI gBlock (Integrated DNA Technologies) insert and T7-IL2ss-AscI-scFv-5'CD8-BlpI-3'CD8-CD28-CD3z plasmid were digested with AscI and BlpI (New England BioLabs) and complementary ends ligated together. The cloning product was confirmed by Sanger sequencing (Genewiz).

mRNA production

PTK7 CAR or CD3-PTK7 bispecific engager construct was linearized with XhoI (New England BioLabs) and mRNA produced with mMESSAGE mMACHINE® T7 Ultra Kit (Life Technologies) using the manufacturer protocol. mRNA tailing was confirmed by RNA gel electrophoresis. mRNA was stored at -80 °C for up to 6 months.

$\gamma\delta$ T-cell isolation and expansion

On Day 0, cryopreserved 100M PBMC vials (AllCells) were activated with 500 IU/mL of IL-2 and 5 mM zoledronic acid in OpTmizer media (Gibco) for 48-hours. After incubation, media was replaced and fresh 500 IU/mL IL-2 and 5 mM zoledronic acid OpTmizer media. On Day 6, $\alpha\beta$ T cells were depleted and remaining almost pure T cells were incubated with 1000 IU/mL IL-2. Media was replaced with fresh media on Day 9, and $\gamma\delta$ T cells continued to expand through Day 12.

Electroporation of mRNA into γδ T cells

Fresh or cryopreserved $\gamma\delta$ T cells were resuspended in complete OpTimizer (Gibco) and 1000 IU/mL IL-2 and left to rest at 37 °C for 2 hours. 4x106 cells and 15 ug mRNA was placed in a 4 mm cuvette and electroporated (Bio-Rad) with the following settings: square wave, gene pulzerx, pulse length = 5 ms, 500 V, 1 pulse, pulse interval = 0, cuvette = 4. Cells were then resuspended in OpTimizer (Gibco) and 1000 IU/mL IL-2 and left to rest at 37 °C for 24-hours before CAR expression and use in functional studies.

In vivo metastasis model

4-week-old NSG mice were engrafted with $1x10^6$ GFP/luciferase-tagged IMR5 cells via tail vein injection on Day -1. $10x10^6$ total unmodified, PTK7 CAR modified, or CD3-PTK7 bispecific engager modified $\gamma\delta$ T cells were injected via retroorbital injection on Day 0, 3, 7, and 10. Mice were injected with D-luciferin (PerkinElmer) at 10 μL/g of body weight via intraperitoneal injection and were imaged with IVIS bioluminescence (PerkinElmer) 2-3x a week. Mice were sacrificed at a predefined endpoint of tumor burden, which considered changes in weight, scruff, movement, and hunched state.

5.6 Supplemental Figures, Tables, and Legends

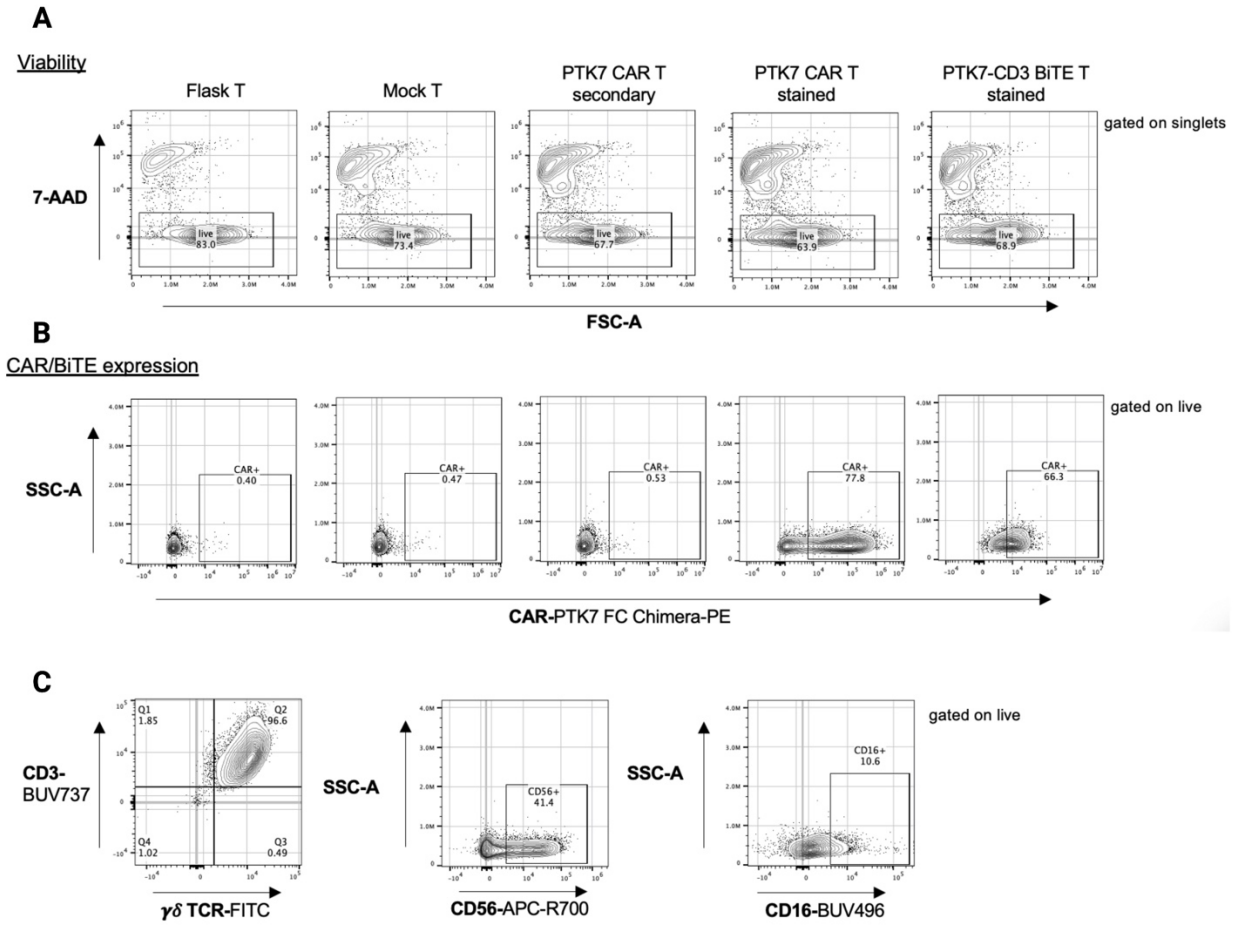

Supplemental Figure 5. 1. Characterization of *γδ* CAR/bispecific T cells utilized in functional studies

(A) Live/Dead gating on electroporated or control *γδ* T cells **(B)** CAR expression (PTK7 Fc) (C) *γδ* T-cell population in final modified products

Chapter 6: General Discussion

6.1 Summary of Results

PTK7 was identified as a promising NB target through a discovery platform that identifies N-glycoproteins in a model that represents post-chemotherapy refractory/recurrent patient population. Here, we determined the feasibility of targeting PTK7 through cellular-based therapies. We first engineered and tested various PTK7 CAR lentivirus vector constructs and the transgene components from extracellular to intracellular included were scFv-CD8 hing-CD28 transmembrane-CD3z. We obtained the scFv sequence from an existing monoclonal antibody VH/VL sequence that moderately binds PTK7. We determined VH-L-VL orientation is more efficiently expressed and better binds PTK7 compared to VL-L-VH. Lastly, PTK7 CAR T cells became specifically activated in the presence of several NB cell lines, while similar activation was not observed in CAR T cells in presence of PTK7-negative cells. Altogether demonstrating specific activation of PTK7 CAR T cells to antigen-positive cells only.

Simultaneous to PTK7 CAR engineering, we performed method development of introducing CAR expression in primary $\alpha\beta$ T cells. We applied a method termed proxim transduction that increases cell to virus contact. Lentiviral proxim transduction of PTK7 CAR resulted in a 10-fold decrease in the amount of viral vector needed to achieve CAR expression. Lentiviral/retroviral transduction are the most utilized tools to deliver CAR transgene. However, neither is capable of transducing 100% of the primary T cell population. We therefore designed and tested the feasibility of selecting PTK7 CAR+ T cells using transduced primary T cells with a positive selection column-based method. We showed that this selection method is successful in isolating PTK7 CAR+ T cells to a near pure population and release the direct binding protein, PTK7 Fc, used to bind CAR+ T cells to the column. Importantly, PTK7 CAR+ T cells also retain antigen-specificity and cytotoxic potential. However, additional experiments are needed to determine the feasibility of incorporating both proxim transduction and column-based selection methods to utilize in PTK7 CAR T-cell functional studies.

We then focused our efforts on determining cytotoxic potential of our engineering PTK7 CAR T cells. PTK7 CAR T cells demonstrated potent cytotoxicity against NB cell lines IMR5, NLF, and SK-N-AS, while ineffective at inducing cell death in PTK7 negative cell lines, CMK, and SK-N-AS PTK7 KO. *In vivo*, survival was significantly prolonged in NSG mice bearing metastatic IMR5 disease that were treated with a single dose of PTK7 CAR T-cell therapy. The response was however not sustained long-term, and disease recurred.

Finally, in addition to PTK7 CAR T cells utilizing $\alpha\beta$ T cells, we explored targeting PTK7 in NB through PTK7 $\gamma\delta$ T cells and $\gamma\delta$ CD3-PTK7 bispecific engagers. We found these modified $\gamma\delta$ T cells to induce donor-dependent cytotoxicity of NB cell lines. In a limited in vivo study, we found both PTK7 $\gamma\delta$ CAR T cells and $\gamma\delta$ CD3-PTK7 bispecific engager able to control tumor cell growth through Day 21. Additional *in vitro* and *in vivo* studies should be performed to determine the feasibility of utilizing modified $\gamma\delta$ T cells to target PTK7 in NB.

6.2 Implication of Findings

Patient survival of high-risk NB has been significantly improved with addition of combination immunotherapy that includes a monoclonal antibody against GD2, GM-CSF, and IL-2 [9]. This successful addition of immunotherapy to the standard of care for high-risk patients started multiple clinical trials against the same antigen, GD2, most notably, CAR T-cell therapy [82,123,124]. Most recent and notable thus far are the clinical trial results for GD2-CART01 therapy for relapsed or refractory high-risk NB (NCT03373097), with an overall response rate of 63% (17/27) [44]. Despite the interim success, not all patients respond to anti-GD2 immunotherapy [9,144,145]. Thus, past investigations identified new targets based on differential transcription expression of NB antigens compared to normal tissue (e.g. GPC2, B7H3, and ALK) [146-148]. Most recently, neuroblastoma experts, the Goldsmith Lab of Emory University, identified a new target, PTK7,

through sensitive and specific cell surface glycoproteomics technology. PTK7 is an inactive receptor tyrosine kinase involved in both canonical and non-conical Wnt signaling and plays a role in embryonic development and tissue homeostasis [149,150]. They found PTK7 was not required for proliferation, cell survival, or therapy response in NB cell lines, however, PTK7 expression is correlated with poor survival in patient survival data so future investigations in functional roles are being tested, such as cell motility, tumor initiation, and metastasis, which play a role in adult cancers [151-153].

Here, our main objective was to design a sufficient CAR against PTK7 to determine the feasibility of targeting it in NB. We tested multiple engineered PTK7 CAR constructs for specific cytotoxic potential and *in vivo* efficacy. Our preclinical investigation defines PTK7 as targetable through $\alpha\beta$ CAR T cell, $\gamma\delta$ CAR T cell, and $\gamma\delta$ bispecific engager therapy both *in vitro* and *in vivo*. These therapies may be especially beneficial for NB patients that progress through the current immunotherapy against GD2. Given the inherent persistence potential over $\gamma\delta$'s, $\alpha\beta$ CAR T-cell therapy may be the superior option to target PTK7 for an effective and sustained response. However, NB patients that enroll in phase I/II clinical trials have refractory or relapsed disease after exhausting current treatment options, including multiple high doses of chemotherapy that have been shown to impair T-cell function. We therefore propose utilizing PTK7 CAR-modified allogenic $\gamma\delta$ T cells expanded from healthy donors may be the better choice for these patients, while $\alpha\beta$ T cells expanded from patients may be best utilized prior to chemotherapy treatment in patients.

Our secondary objective was method development of introducing lentiviral PTK7 CAR in addition to a CAR+ T-cell selection method. Lentiviral vectors haven't demonstrated the same oncogenic potential as retroviral vectors [108,109]. However, problems still lie with the use of lentiviral vectors, such as the substantial amount needed for early phase clinical trials [110], in addition to being non-standardized and labor-intensive. Lentiviral CAR delivery through proxim transduction decreased the amount of vector needed by 10-fold and has the potential to scale up

to manufacturing protocol. Pre-clinical designs of CAR constructs include markers that can't be employed for clinical studies due to immune rejection of mouse origin molecules, marker release to extracellular space, physiological interference, as well as incompatibility with technology currently employed to allow enrichment of cells under GMP [113]. Thus, technology that allows positive selection of CAR T cells during manufacturing have been tested with a splice variant of CD34, RQR8 [113,115,116]. However, influence in physiological functions is still being tested [113]. Our column-based method allows selection of pure PTK7 CAR+ T cells without additional transgenes and use of columns that are from the manufacturers of the FDA-approved CliniMACS CD34 Reagent System, making this method more clinically relevant and translatable for introduction to patients.

6.3 Limitations and Future Directions

CAR design components

There are many preclinically tested CAR components that show specific advantages and disadvantages of each functional domain. So much so, the task of identifying the appropriate outfit for each CAR T-cell therapy can be daunting. As a result, many variations can theoretically and perhaps will eventually be introduced and tested in the clinic. However, today, only the same few variations of CARs have been utilized in clinical trials. This can be subjectively attributed to the following. Compared to chemotherapies or other targeted therapies, CAR T-cell therapy is relatively new, and as with any new type of therapies, time and multiple trials are needed to iron out various kinks associated with the therapy. In addition, one of the main barriers of CAR T-cell therapy is determining an optimal target antigen. Once a target is identified, efforts to validate the antigen as a promising candidate should be prioritized, prior to optimization of the downstream CAR components.

Given PTK7 was newly identified and characterized as highly expressed in NB, our efforts focused on determining the feasibility of targeting this specific antigen with immunotherapies, in

which we found it was. However, it can be presumed that further optimization of the CAR components may drastically improve the efficacy of the therapy. The PTK7 CAR constructs tested were all of the same VH/VL scFv sequence others have identified as a part of a monoclonal antibody that others have found binds PTK7. Although this scFv was effective in binding and specifically activating the CAR T-cell function, this is an empirical method and does not determine the best sequence for CAR T-cell targeting of PTK7. Multiple VH and VL sequences that exist, or have yet to be discovered, should be tested to truly determine the best scFv for optimal short- and long-term CAR T-cell function, as binding potential alone doesn't always positively correlate to CAR T-cell function [99-102]. An effort to test other CAR components such as the hinge and transmembrane domains are currently underway. The scFv binding potential to an antigen may be highly dependent on the ability of the hinge molecule to provide the optimal steric hindrance and distance from the cellular membrane [91], thus should be customized to the specific antigen/scFv. Lastly, co-stimulatory domains have been the main topic of determinates of CAR T-cell persistence, and one of the main downfalls of this therapy in solid tumors is lack of persistence. Therefore, other co-stimulatory domains should be compared to the CD28 domain utilized in our studies, such as 4-1BB or dual 4-1BB/CD28 domains that have been more successful clinically [130-133].

Potential resistance mechanisms to PTK7 CAR T-cell therapy

Although successful, trials utilizing CAR T-cell therapies against CD19 reviled mechanisms of resistance in patient populations that initially responded to the therapy then relapsed with CD19 antigen loss or modulation [154]. Target modulation is one of the most common described mechanisms of disease relapse following CAR T-cell therapy and a complete loss of expression is not always necessary as CD22 cell surface downregulation was enough to evade CAR T cells in leukemia patients [155]. This idea of antigen escape was first noticed in preclinical research where a positive correlation between antigen density and CAR-T cell induced activity occurred [156,157]. One

potential major limitation to targeting PTK7 in NB, is its lack of necessity in NB cell proliferation or response to chemotherapy. Transformed cells have evolved to not only survive but thrive in harsh conditions such as hypoxic environments or evade the innate and adaptive immune system over time. This hallmark of cancer easily translates to one of the major downfalls of all therapies, which is acquired resistance and subsequent relapse. Cancer cells may undergo various mechanisms of resistance including downregulation of gene or protein expression, slight modification to the protein structure to escape recognition, direct contact inactivation or efflux of the therapy. Rarely is a single protein responsible for the survival of these transformed cells, thus are more likely able to "spare" the expression or functionality of the antigen to overcome therapy. In our *in vivo* metastatic model, disease eventually recurred post PTK7 CAR T-cell therapy. Promisingly, IMR5 cells residing in the liver at recurrence show high PTK7 expression; however, this was determined only within days of the first signs of recurrence, thus lacks conclusion of PKT7 expression at a later point nor any potential slight modification of the protein structure. Future studies should include *in vitro* or *ex vivo* repeated challenge assays to evaluate CAR T-cell-mediated cell death over time. Preemptively, to address the potential PTK7 loss, we are investigating multi-antigen targeting by determining the feasibility of dual PTK7 and GD2 targeting. Targeting GD2 alone with CAR T cells has recently shown great efficacy in a clinical trial for relapsed or refractory NB, however long-term response or potential relapse to therapy has yet to be defined [44].

CAR T-cell persistence

One critical component to $\alpha\beta$ CAR T-cell therapy that was alluded to yet be optimized in our current studies is persistence. A major population of patients with poor response to CAR T-cell therapy has been attributed to the lack of persistence of T cells and even patients who initially respond to the therapy are at risk of relapse due to limited persistence. Several known variables have been preclinically and clinically modified to increase CAR T-cell persistence and they are

mainly altering T-cell differentiation state, CAR architecture, and supplements in *ex vivo* expansion media.

T-cell subsets are classified by the expression or lack of expression of cell surface markers that are related to migratory and functional roles, and each subset differs in proliferation and survival. In general, both preclinical and clinical evidence show less differentiated T cells, which include naïve T cells (T_N), stem cell memory T cells (T_{SCM}), and central memory T cells (T_{CM}), proliferate and persist longer *in vivo* [158] and is associated with long-term remission in patients [159] compared to the more differentiated effector memory T cells (T_{EM}) and effector T cells (T_{EFF}). T_{SCM} cells are an attractive cell type to test in ACT's due to their ability of regeneration and continued proliferative ability. However, they retain a naïve T-cell phenotype that renders them incapable of inducing potent anti-tumor activity. This knowledge combined with the appreciation of later stages of T-cell differentiated cells being less persist, suggests a goldilocks T-cell subtype for use for CAR T-cell therapies, in which they are stem cell-like enough to proliferate, yet differentiated enough to effectively kill tumor cells. We found our expanded mock T cells and PTK7 CAR T cells to be mostly of T_{CM} phenotype (CCR7+CD45RO+). However, PTK7 CAR T cells contained a notable higher percentage of more differentiated T_{EM} cells (CCR7-CD45RO+) compared to mock T cells. Given primary T cells don't express PTK7 and they have yet to be exposed to outside antigen, we hypothesize that our transduction method induces a stress response leading to a more rapid differentiation state. Therefore, this therapy may benefit from future studies that optimize lentiviral transduction to retain the T_{CM} phenotype seen in mock T cells, or perhaps introduce the use of specific cytokines that have shown to conserve stem cell memory-like phenotype.

First-generation CARs lack a co-stimulatory domain and rely solely on the CD3ζ domain to prime and activate T cells upon antigen binding. These initial CAR T cells lacked the required cytokine release for a potent and sustained response, therefore triggered the introduction of co-stimulatory signaling domains. These second-generation CARs are more efficient at activating and promoting an efficient expansion of T cells. The most utilized co-stimulatory domains are

CD28 and 4-1BB and both preclinical [160,161] and clinical [162,163] evidence show CAR T's with CD28-based co-stimulatory domains persist less than 4-1BB domains [164]. Therefore, efforts to draw a comparison between the two co-stimulatory domains should be made for the PTK7 CAR, including looking at variances in cellular metabolism, as the addition of 4-1BB demonstrated both increased respiratory capacity and mitochondrial biogenesis in T cells.

Lastly, persistence of $\gamma\delta$ T cells is not as well studied compared to traditional $\alpha\beta$ T cells, however in preclinical studies, persistence was shown to be limited *in vivo* [139]. In addition, evidence shows Vγ1+ cells have a decreased susceptibility for activation-induced cell death over Vγ9Vδ2+ cells [165], insinuating increased persistence *in vivo*.

PTK7 targetable in other cancers

In addition to NB, PTK7 is expressed in other pediatric and adult solid tumors. In point, PTK7 has been recently pre-clinically targeted for the first time by CAR T cells in adult lung cancer [166] with *in vitro* and *in vivo* efficacy. In addition to NB and lung cancer, PTK7 transcript is highly expressed in cancer cell lines, including pediatric bone cancers, sarcomas, brain cancers, and leukemias (**Figure 6.1A-B**). Given high PTK7 gene expression, PTK7 protein expression was then validated in tissue of two osteosarcoma PDXs and primary patient tumor and paired PDX and shown to be highly expressed (IHC score >2) (**Figure 6.2.A**). Given the elevated protein expression, we preliminarily determined the cytotoxic potential of our primary PTK7 CAR T cells in osteosarcoma and rhabdomyosarcoma and found these cell lines, like NB, were susceptible to PTK7 CAR-T cell induced cell death (**Figure 6.2B**). Current investigations are underway to further determine the feasibility of targeting PTK7 in osteosarcoma and rhabdomyosarcoma.

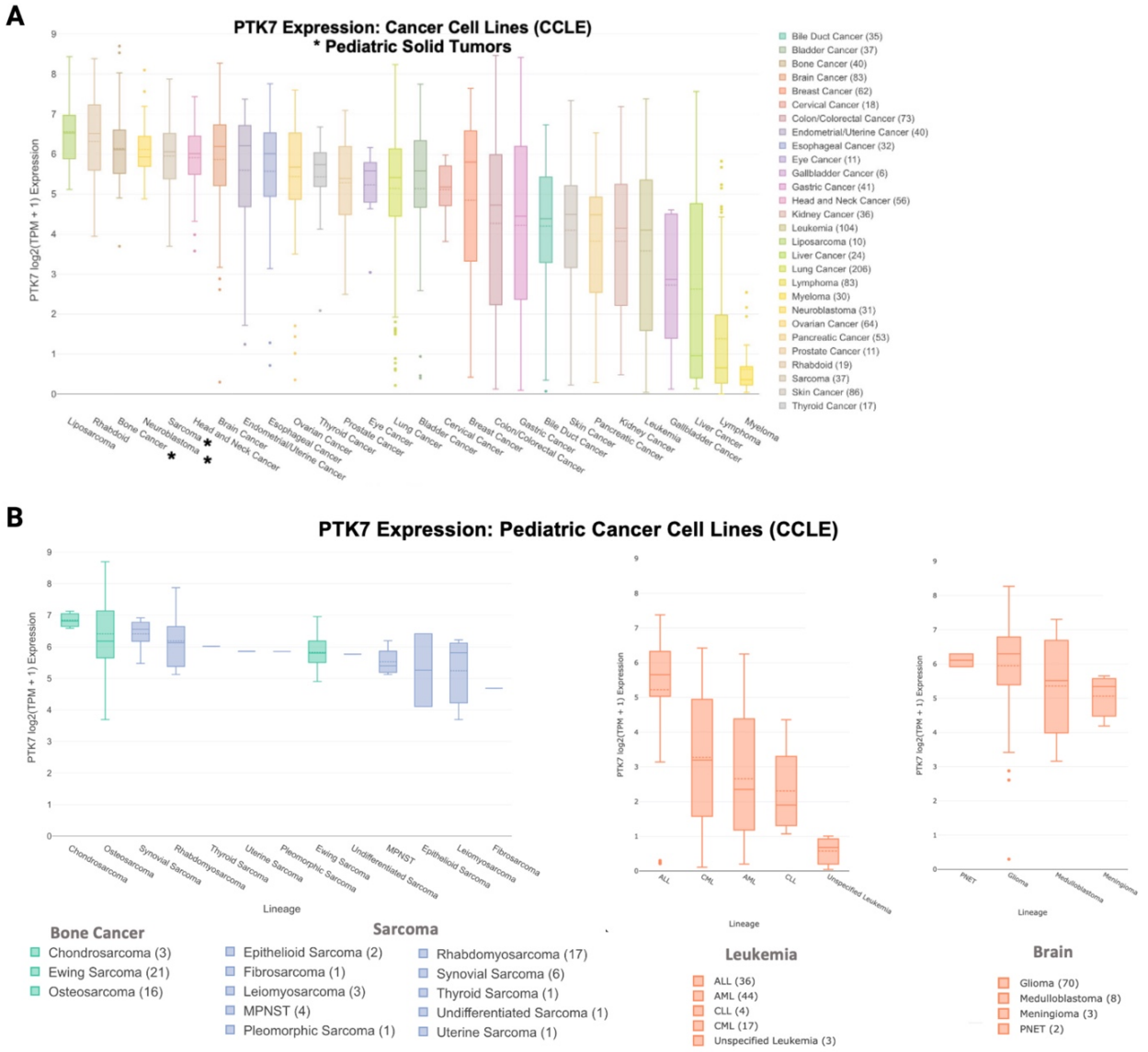

Figure 6. 1. PTK7 is targetable beyond NB

(A) Box and whisker plots show PTK7 expression from Cancer Cell Line Encyclopedia (CCLE, sites.broadinstitute.org/ccle/). Dotted line represents the mean. Solid line represents the median. Dots represent outliers. Error bars represent SD. **(B)** PTK7 expression in cancers further classified into subtypes. Left to right: bone cancer, sarcoma, leukemia, brain cancer. Normalized transcript data was taken from CCLE and plots generated in RStudio with the package: Plotly Technologies Inc. Collaborative data science. Montréal, QC, 2015. https://plot.ly. Plots are published in Lee J.Y. and Jonus H.C. *et al. Cell Rep. Med.*, 2023.

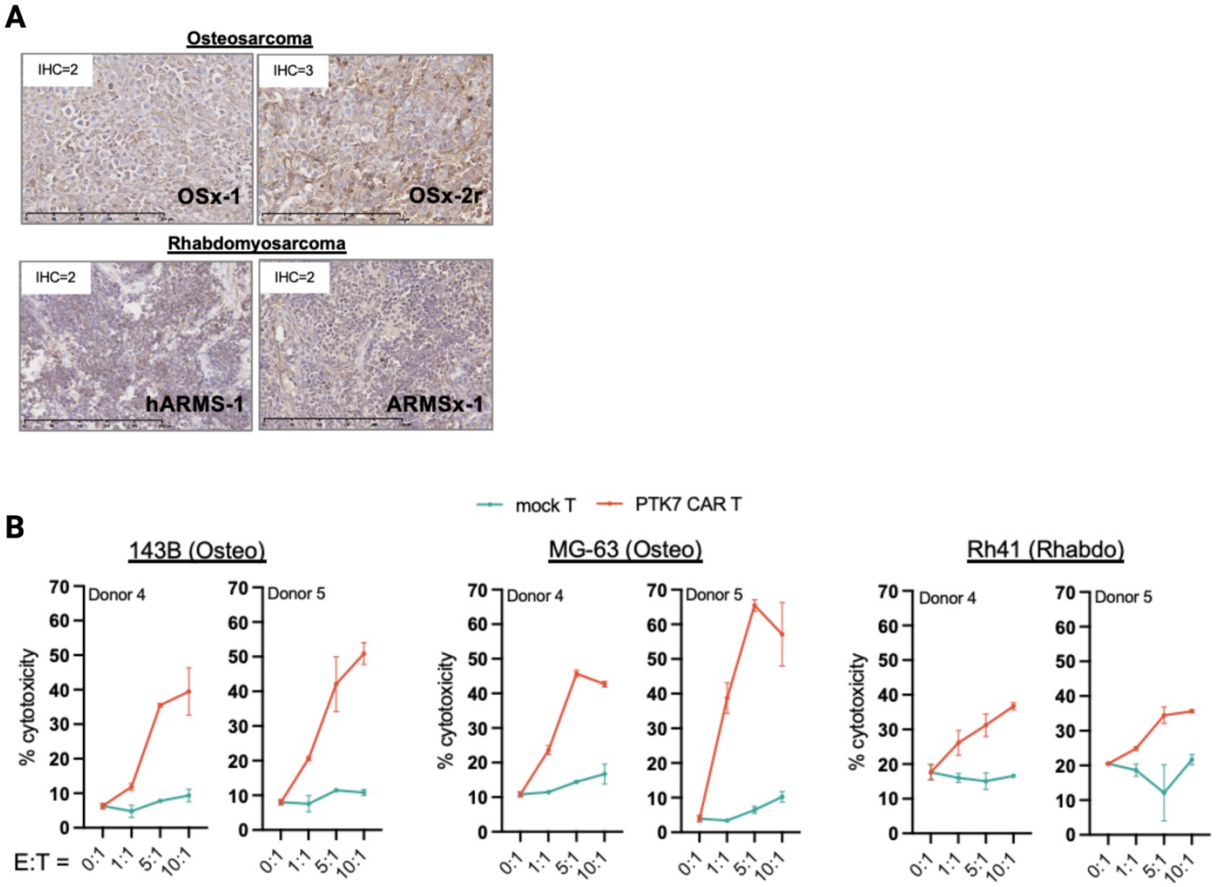

Figure 6. 2. PTK7 CAR T cells are effective against osteosarcoma and rhabdomyosarcoma tumor cells

(A) IHC demonstrating PTK7 expression in osteosarcoma PDX tissue and rhabdomyosarcoma primary and paired PDX tissue. Scores of IHC staining for each tissue are provided in top left. Figure curtesy of the Goldsmith Lab. **(B)** 4-hour flow cytometry cytotoxicity assay of PTK7 CAR modified T cells against PTK7 expressing osteosarcoma and rhabdomyosarcoma cell lines compared to mock T cell controls. % cytotoxicity = the sum of 7AAD+, Annexin V+, and 7AAD+ Annexin V+ cells, gated on target cells. N = 2 donors with n = 3 biological replicates. Data represented as mean and error bars as SD. Published in Lee J.Y. and Jonus H.C. *et al. Cell Rep. Med.*, 2023.

6.4 Conclusions

In conclusion, our investigation shows PTK7 is targetable through cellular immunotherapies in NB and likely other pediatric cancers. Ongoing and future research focus on optimization of genetically engineered immune cells to target PTK7 for translation into clinical studies.

Citations

1. London, W.B., Castleberry, R.P., Matthay, K.K., Look, A.T., Seeger, R.C., Shimada, H., Thorner, P., Brodeur, G., Maris, J.M., Reynolds, C.P., and Cohn, S.L. (2005). Evidence for an age cutoff greater than 365 days for neuroblastoma risk group stratification in the Children's Oncology Group. J Clin Oncol *23*, 6459-6465. 10.1200/JCO.2005.05.571.
2. Matthay, K.K., Maris, J.M., Schleiermacher, G., Nakagawara, A., Mackall, C.L., Diller, L., and Weiss, W.A. (2016). Neuroblastoma. Nat Rev Dis Primers *2*, 16078. 10.1038/nrdp.2016.78.
3. Maris, J.M., Hogarty, M.D., Bagatell, R., and Cohn, S.L. (2007). Neuroblastoma. Lancet *369*, 2106-2120. 10.1016/S0140-6736(07)60983-0.
4. Dubois, S.G., Geier, E., Batra, V., Yee, S.W., Neuhaus, J., Segal, M., Martinez, D., Pawel, B., Yanik, G., Naranjo, A., et al. (2012). Evaluation of Norepinephrine Transporter Expression and Metaiodobenzylguanidine Avidity in Neuroblastoma: A Report from the Children's Oncology Group. Int J Mol Imaging *2012*, 250834. 10.1155/2012/250834.
5. Bresler, S.C., Weiser, D.A., Huwe, P.J., Park, J.H., Krytska, K., Ryles, H., Laudenslager, M., Rappaport, E.F., Wood, A.C., McGrady, P.W., et al. (2014). ALK mutations confer differential oncogenic activation and sensitivity to ALK inhibition therapy in neuroblastoma. Cancer Cell *26*, 682-694. 10.1016/j.ccell.2014.09.019.
6. Seeger, R.C., Brodeur, G.M., Sather, H., Dalton, A., Siegel, S.E., Wong, K.Y., and Hammond, D. (1985). Association of multiple copies of the N-myc oncogene with rapid progression of neuroblastomas. N Engl J Med *313*, 1111-1116. 10.1056/NEJM198510313131802.
7. Brodeur, G.M., Hayes, F.A., Green, A.A., Casper, J.T., Wasson, J., Wallach, S., and Seeger, R.C. (1987). Consistent N-myc copy number in simultaneous or consecutive neuroblastoma samples from sixty individual patients. Cancer Res *47*, 4248-4253.
8. Sharp, S.E., Gelfand, M.J., and Shulkin, B.L. (2011). Pediatrics: diagnosis of neuroblastoma. Semin Nucl Med *41*, 345-353. 10.1053/j.semnuclmed.2011.05.001.
9. Yu, A.L., Gilman, A.L., Ozkaynak, M.F., London, W.B., Kreissman, S.G., Chen, H.X., Smith, M., Anderson, B., Villablanca, J.G., Matthay, K.K., et al. (2010). Anti-GD2 antibody with GM-CSF, interleukin-2, and isotretinoin for neuroblastoma. N Engl J Med *363*, 1324-1334. 10.1056/NEJMoa0911123.
10. Otte, J., Dyberg, C., Pepich, A., and Johnsen, J.I. (2020). MYCN Function in Neuroblastoma Development. Front Oncol *10*, 624079. 10.3389/fonc.2020.624079.
11. Ogawa, S., Takita, J., Sanada, M., and Hayashi, Y. (2011). Oncogenic mutations of ALK in neuroblastoma. Cancer Sci *102*, 302-308. 10.1111/j.1349-7006.2010.01825.x.
12. Busch, W. (1868). Aus der Sitzung der medicinischen Section vom 13 November 1867. Berlin Klin Wochenschr *5:137*.
13. Fehleisen, F. (1882). Ueber die Züchtung der Erysipelkokken auf künstlichem Nährboden und ihre Übertragbarkeit auf den Menschen. Dtsch Med Wochenschr *8:553–554*.
14. Starnes, C.O. (1992). Coley's toxins. Nature *360*, 23. 10.1038/360023b0.
15. Starnes, C.O. (1992). Coley's toxins in perspective. Nature *357*, 11-12. 10.1038/357011a0.
16. McCarthy, E.F. (2006). The toxins of William B. Coley and the treatment of bone and soft-tissue sarcomas. Iowa Orthop J *26*, 154-158.

17. Dobosz, P., and Dzieciatkowski, T. (2019). The Intriguing History of Cancer Immunotherapy. Front Immunol *10*, 2965. 10.3389/fimmu.2019.02965.
18. Isaacs, A., and Lindenmann, J. (1957). Virus interference. I. The interferon. Proc R Soc Lond B Biol Sci *147*, 258-267. 10.1098/rspb.1957.0048.
19. Decker, W.K., da Silva, R.F., Sanabria, M.H., Angelo, L.S., Guimaraes, F., Burt, B.M., Kheradmand, F., and Paust, S. (2017). Cancer Immunotherapy: Historical Perspective of a Clinical Revolution and Emerging Preclinical Animal Models. Front Immunol *8*, 829. 10.3389/fimmu.2017.00829.
20. Old, L.J. (1977). Cancer immunology. Sci Am *236*, 62-70, 72-63, 76, 79. 10.1038/scientificamerican0577-62.
21. Burnet, F.M. (1970). The concept of immunological surveillance. Prog Exp Tumor Res *13*, 1-27. 10.1159/000386035.
22. Miller, J.F., Mitchell, G.F., and Weiss, N.S. (1967). Cellular basis of the immunological defects in thymectomized mice. Nature *214*, 992-997. 10.1038/214992a0.
23. van der Bruggen, P., Traversari, C., Chomez, P., Lurquin, C., De Plaen, E., Van den Eynde, B., Knuth, A., and Boon, T. (1991). A gene encoding an antigen recognized by cytolytic T lymphocytes on a human melanoma. Science *254*, 1643-1647. 10.1126/science.1840703.
24. Winau, F., Westphal, O., and Winau, R. (2004). Paul Ehrlich--in search of the magic bullet. Microbes Infect *6*, 786-789. 10.1016/j.micinf.2004.04.003.
25. Lindenmann, J. (1984). Origin of the terms 'antibody' and 'antigen'. Scand J Immunol *19*, 281-285. 10.1111/j.1365-3083.1984.tb00931.x.
26. Rudnicka, D., Oszmiana, A., Finch, D.K., Strickland, I., Schofield, D.J., Lowe, D.C., Sleeman, M.A., and Davis, D.M. (2013). Rituximab causes a polarization of B cells that augments its therapeutic function in NK-cell-mediated antibody-dependent cellular cytotoxicity. Blood *121*, 4694-4702. 10.1182/blood-2013-02-482570.
27. Krummel, M.F., and Allison, J.P. (1995). CD28 and CTLA-4 have opposing effects on the response of T cells to stimulation. J Exp Med *182*, 459-465. 10.1084/jem.182.2.459.
28. Leach, D.R., Krummel, M.F., and Allison, J.P. (1996). Enhancement of antitumor immunity by CTLA-4 blockade. Science *271*, 1734-1736. 10.1126/science.271.5256.1734.
29. Waldmann, T.A. (2018). Cytokines in Cancer Immunotherapy. Cold Spring Harb Perspect Biol *10*. 10.1101/cshperspect.a028472.
30. Baldo, B.A. (2014). Side effects of cytokines approved for therapy. Drug Saf *37*, 921-943. 10.1007/s40264-014-0226-z.
31. Rosenberg, S.A., Mule, J.J., Spiess, P.J., Reichert, C.M., and Schwarz, S.L. (1985). Regression of established pulmonary metastases and subcutaneous tumor mediated by the systemic administration of high-dose recombinant interleukin 2. J Exp Med *161*, 1169-1188. 10.1084/jem.161.5.1169.
32. Rosenberg, S.A., Lotze, M.T., Muul, L.M., Leitman, S., Chang, A.E., Ettinghausen, S.E., Matory, Y.L., Skibber, J.M., Shiloni, E., Vetto, J.T., and et al. (1985). Observations on the systemic administration of autologous lymphokine-activated killer cells and recombinant interleukin-2 to patients with metastatic cancer. N Engl J Med *313*, 1485-1492. 10.1056/NEJM198512053132327.
33. Italian Cooperative Study Group on Chronic Myeloid, L., Tura, S., Baccarani, M., Zuffa, E., Russo, D., Fanin, R., Zaccaria, A., and Fiacchini, M. (1994). Interferon alfa-2a as compared

with conventional chemotherapy for the treatment of chronic myeloid leukemia. N Engl J Med *330*, 820-825. 10.1056/NEJM199403243301204.

34. Kirkwood, J.M., Strawderman, M.H., Ernstoff, M.S., Smith, T.J., Borden, E.C., and Blum, R.H. (2023). Interferon Alfa-2b Adjuvant Therapy of High-Risk Resected Cutaneous Melanoma: The Eastern Cooperative Oncology Group Trial EST 1684. J Clin Oncol *41*, 425-435. 10.1200/JCO.22.02264.
35. Rini, B.I., Weinberg, V., Bok, R., and Small, E.J. (2003). Prostate-specific antigen kinetics as a measure of the biologic effect of granulocyte-macrophage colony-stimulating factor in patients with serologic progression of prostate cancer. J Clin Oncol *21*, 99-105. 10.1200/JCO.2003.04.163.
36. Spitler, L.E., Grossbard, M.L., Ernstoff, M.S., Silver, G., Jacobs, M., Hayes, F.A., and Soong, S.J. (2000). Adjuvant therapy of stage III and IV malignant melanoma using granulocyte-macrophage colony-stimulating factor. J Clin Oncol *18*, 1614-1621. 10.1200/JCO.2000.18.8.1614.
37. Guo, C., Manjili, M.H., Subjeck, J.R., Sarkar, D., Fisher, P.B., and Wang, X.Y. (2013). Therapeutic cancer vaccines: past, present, and future. Adv Cancer Res *119*, 421-475. 10.1016/B978-0-12-407190-2.00007-1.
38. Waldman, A.D., Fritz, J.M., and Lenardo, M.J. (2020). A guide to cancer immunotherapy: from T cell basic science to clinical practice. Nat Rev Immunol *20*, 651-668. 10.1038/s41577-020-0306-5.
39. Southam, C.M., Brunschwig, A., Levin, A.G., and Dizon, Q.S. (1966). Effect of leukocytes on transplantability of human cancer. Cancer *19*, 1743-1753. 10.1002/1097-0142(196611)19:11<1743::aid-cncr2820191143>3.0.co;2-u.
40. Rosenberg, S.A., Yannelli, J.R., Yang, J.C., Topalian, S.L., Schwartzentruber, D.J., Weber, J.S., Parkinson, D.R., Seipp, C.A., Einhorn, J.H., and White, D.E. (1994). Treatment of patients with metastatic melanoma with autologous tumor-infiltrating lymphocytes and interleukin 2. J Natl Cancer Inst *86*, 1159-1166. 10.1093/jnci/86.15.1159.
41. Rosenberg, S.A., Yang, J.C., Sherry, R.M., Kammula, U.S., Hughes, M.S., Phan, G.Q., Citrin, D.E., Restifo, N.P., Robbins, P.F., Wunderlich, J.R., et al. (2011). Durable complete responses in heavily pretreated patients with metastatic melanoma using T-cell transfer immunotherapy. Clin Cancer Res *17*, 4550-4557. 10.1158/1078-0432.CCR-11-0116.
42. Jensen, M.C., Popplewell, L., Cooper, L.J., DiGiusto, D., Kalos, M., Ostberg, J.R., and Forman, S.J. (2010). Antitransgene rejection responses contribute to attenuated persistence of adoptively transferred CD20/CD19-specific chimeric antigen receptor redirected T cells in humans. Biol Blood Marrow Transplant *16*, 1245-1256. 10.1016/j.bbmt.2010.03.014.
43. Brocker, T. (2000). Chimeric Fv-zeta or Fv-epsilon receptors are not sufficient to induce activation or cytokine production in peripheral T cells. Blood *96*, 1999-2001.
44. Del Bufalo, F., De Angelis, B., Caruana, I., Del Baldo, G., De Ioris, M.A., Serra, A., Mastronuzzi, A., Cefalo, M.G., Pagliara, D., Amicucci, M., et al. (2023). GD2-CART01 for Relapsed or Refractory High-Risk Neuroblastoma. N Engl J Med *388*, 1284-1295. 10.1056/NEJMoa2210859.
45. Born, W., Miles, C., White, J., O'Brien, R., Freed, J.H., Marrack, P., Kappler, J., and Kubo, R.T. (1987). Peptide sequences of T-cell receptor delta and gamma chains are identical to predicted X and gamma proteins. Nature *330*, 572-574. 10.1038/330572a0.

46. Hayday, A.C., Saito, H., Gillies, S.D., Kranz, D.M., Tanigawa, G., Eisen, H.N., and Tonegawa, S. (1985). Structure, organization, and somatic rearrangement of T cell gamma genes. Cell *40*, 259-269. 10.1016/0092-8674(85)90140-0.
47. Chien, Y., Becker, D.M., Lindsten, T., Okamura, M., Cohen, D.I., and Davis, M.M. (1984). A third type of murine T-cell receptor gene. Nature *312*, 31-35. 10.1038/312031a0.
48. Sheridan, B.S., Romagnoli, P.A., Pham, Q.M., Fu, H.H., Alonzo, F., 3rd, Schubert, W.D., Freitag, N.E., and Lefrancois, L. (2013). gammadelta T cells exhibit multifunctional and protective memory in intestinal tissues. Immunity *39*, 184-195. 10.1016/j.immuni.2013.06.015.
49. Silva-Santos, B., Serre, K., and Norell, H. (2015). gammadelta T cells in cancer. Nat Rev Immunol *15*, 683-691. 10.1038/nri3904.
50. Mokuno, Y., Matsuguchi, T., Takano, M., Nishimura, H., Washizu, J., Ogawa, T., Takeuchi, O., Akira, S., Nimura, Y., and Yoshikai, Y. (2000). Expression of toll-like receptor 2 on gamma delta T cells bearing invariant V gamma 6/V delta 1 induced by Escherichia coli infection in mice. J Immunol *165*, 931-940. 10.4049/jimmunol.165.2.931.
51. Kabelitz, D., Kalyan, S., Oberg, H.H., and Wesch, D. (2013). Human Vdelta2 versus non-Vdelta2 gammadelta T cells in antitumor immunity. Oncoimmunology *2*, e23304. 10.4161/onci.23304.
52. Holtmeier, W., Pfander, M., Hennemann, A., Zollner, T.M., Kaufmann, R., and Caspary, W.F. (2001). The TCR-delta repertoire in normal human skin is restricted and distinct from the TCR-delta repertoire in the peripheral blood. J Invest Dermatol *116*, 275-280. 10.1046/j.1523-1747.2001.01250.x.
53. Kalyan, S., and Kabelitz, D. (2013). Defining the nature of human gammadelta T cells: a biographical sketch of the highly empathetic. Cell Mol Immunol *10*, 21-29. 10.1038/cmi.2012.44.
54. Mensurado, S., Blanco-Dominguez, R., and Silva-Santos, B. (2023). The emerging roles of gammadelta T cells in cancer immunotherapy. Nat Rev Clin Oncol *20*, 178-191. 10.1038/s41571-022-00722-1.
55. Carding, S.R., and Egan, P.J. (2002). Gammadelta T cells: functional plasticity and heterogeneity. Nat Rev Immunol *2*, 336-345. 10.1038/nri797.
56. Khairallah, C., Dechanet-Merville, J., and Capone, M. (2017). gammadelta T Cell-Mediated Immunity to Cytomegalovirus Infection. Front Immunol *8*, 105. 10.3389/fimmu.2017.00105.
57. Farnault, L., Gertner-Dardenne, J., Gondois-Rey, F., Michel, G., Chambost, H., Hirsch, I., and Olive, D. (2013). Clinical evidence implicating gamma-delta T cells in EBV control following cord blood transplantation. Bone Marrow Transplant *48*, 1478-1479. 10.1038/bmt.2013.75.
58. Willcox, C.R., Davey, M.S., and Willcox, B.E. (2018). Development and Selection of the Human Vgamma9Vdelta2(+) T-Cell Repertoire. Front Immunol *9*, 1501. 10.3389/fimmu.2018.01501.
59. Wang, H., Fang, Z., and Morita, C.T. (2010). Vgamma2Vdelta2 T Cell Receptor recognition of prenyl pyrophosphates is dependent on all CDRs. J Immunol *184*, 6209-6222. 10.4049/jimmunol.1000231.
60. Tanaka, Y., Kobayashi, H., Terasaki, T., Toma, H., Aruga, A., Uchiyama, T., Mizutani, K., Mikami, B., Morita, C.T., and Minato, N. (2007). Synthesis of pyrophosphate-containing

compounds that stimulate Vgamma2Vdelta2 T cells: application to cancer immunotherapy. Med Chem *3*, 85-99. 10.2174/157340607779317544.

61. Wang, R.N., Wen, Q., He, W.T., Yang, J.H., Zhou, C.Y., Xiong, W.J., and Ma, L. (2019). Optimized protocols for gammadelta T cell expansion and lentiviral transduction. Mol Med Rep *19*, 1471-1480. 10.3892/mmr.2019.9831.
62. Hoeres, T., Smetak, M., Pretscher, D., and Wilhelm, M. (2018). Improving the Efficiency of Vgamma9Vdelta2 T-Cell Immunotherapy in Cancer. Front Immunol *9*, 800. 10.3389/fimmu.2018.00800.
63. Rincon-Orozco, B., Kunzmann, V., Wrobel, P., Kabelitz, D., Steinle, A., and Herrmann, T. (2005). Activation of V gamma 9V delta 2 T cells by NKG2D. J Immunol *175*, 2144-2151. 10.4049/jimmunol.175.4.2144.
64. Wrobel, P., Shojaei, H., Schittek, B., Gieseler, F., Wollenberg, B., Kalthoff, H., Kabelitz, D., and Wesch, D. (2007). Lysis of a broad range of epithelial tumour cells by human gamma delta T cells: involvement of NKG2D ligands and T-cell receptor- versus NKG2D-dependent recognition. Scand J Immunol *66*, 320-328. 10.1111/j.1365-3083.2007.01963.x.
65. Angelini, D.F., Borsellino, G., Poupot, M., Diamantini, A., Poupot, R., Bernardi, G., Poccia, F., Fournie, J.J., and Battistini, L. (2004). FcgammaRIII discriminates between 2 subsets of Vgamma9Vdelta2 effector cells with different responses and activation pathways. Blood *104*, 1801-1807. 10.1182/blood-2004-01-0331.
66. Correia, D.V., Lopes, A., and Silva-Santos, B. (2013). Tumor cell recognition by gammadelta T lymphocytes: T-cell receptor vs. NK-cell receptors. Oncoimmunology *2*, e22892. 10.4161/onci.22892.
67. Kunzmann, V., and Wilhelm, M. (2005). Anti-lymphoma effect of gammadelta T cells. Leuk Lymphoma *46*, 671-680. 10.1080/10428190500051893.
68. Zoine, J.T., Knight, K.A., Fleischer, L.C., Sutton, K.S., Goldsmith, K.C., Doering, C.B., and Spencer, H.T. (2019). Ex vivo expanded patient-derived gammadelta T-cell immunotherapy enhances neuroblastoma tumor regression in a murine model. Oncoimmunology *8*, 1593804. 10.1080/2162402X.2019.1593804.
69. Wilhelm, M., Kunzmann, V., Eckstein, S., Reimer, P., Weissinger, F., Ruediger, T., and Tony, H.P. (2003). Gammadelta T cells for immune therapy of patients with lymphoid malignancies. Blood *102*, 200-206. 10.1182/blood-2002-12-3665.
70. Dieli, F., Vermijlen, D., Fulfaro, F., Caccamo, N., Meraviglia, S., Cicero, G., Roberts, A., Buccheri, S., D'Asaro, M., Gebbia, N., et al. (2007). Targeting human gammadelta T cells with zoledronate and interleukin-2 for immunotherapy of hormone-refractory prostate cancer. Cancer Res *67*, 7450-7457. 10.1158/0008-5472.CAN-07-0199.
71. Kobayashi, H., Tanaka, Y., Yagi, J., Minato, N., and Tanabe, K. (2011). Phase I/II study of adoptive transfer of gammadelta T cells in combination with zoledronic acid and IL-2 to patients with advanced renal cell carcinoma. Cancer Immunol Immunother *60*, 1075-1084. 10.1007/s00262-011-1021-7.
72. De Gassart, A., Le, K.S., Brune, P., Agaugue, S., Sims, J., Goubard, A., Castellano, R., Joalland, N., Scotet, E., Collette, Y., et al. (2021). Development of ICT01, a first-in-class, anti-BTN3A antibody for activating Vgamma9Vdelta2 T cell-mediated antitumor immune response. Sci Transl Med *13*, eabj0835. 10.1126/scitranslmed.abj0835.
73. Oberg, H.H., Peipp, M., Kellner, C., Sebens, S., Krause, S., Petrick, D., Adam-Klages, S., Rocken, C., Becker, T., Vogel, I., et al. (2014). Novel bispecific antibodies increase

gammadelta T-cell cytotoxicity against pancreatic cancer cells. Cancer Res *74*, 1349-1360. 10.1158/0008-5472.CAN-13-0675.

74. de Weerdt, I., Lameris, R., Ruben, J.M., de Boer, R., Kloosterman, J., King, L.A., Levin, M.D., Parren, P., de Gruijl, T.D., Kater, A.P., and van der Vliet, H.J. (2021). A Bispecific Single-Domain Antibody Boosts Autologous Vgamma9Vdelta2-T Cell Responses Toward CD1d in Chronic Lymphocytic Leukemia. Clin Cancer Res *27*, 1744-1755. 10.1158/1078-0432.CCR-20-4576.
75. de Weerdt, I., Lameris, R., Scheffer, G.L., Vree, J., de Boer, R., Stam, A.G., van de Ven, R., Levin, M.D., Pals, S.T., Roovers, R.C., et al. (2021). A Bispecific Antibody Antagonizes Prosurvival CD40 Signaling and Promotes Vgamma9Vdelta2 T cell-Mediated Antitumor Responses in Human B-cell Malignancies. Cancer Immunol Res *9*, 50-61. 10.1158/2326-6066.CIR-20-0138.
76. Ganesan, R., Chennupati, V., Ramachandran, B., Hansen, M.R., Singh, S., and Grewal, I.S. (2021). Selective recruitment of gammadelta T cells by a bispecific antibody for the treatment of acute myeloid leukemia. Leukemia *35*, 2274-2284. 10.1038/s41375-021-01122-7.
77. de Bruin, R.C.G., Veluchamy, J.P., Lougheed, S.M., Schneiders, F.L., Lopez-Lastra, S., Lameris, R., Stam, A.G., Sebestyen, Z., Kuball, J., Molthoff, C.F.M., et al. (2017). A bispecific nanobody approach to leverage the potent and widely applicable tumor cytolytic capacity of Vgamma9Vdelta2-T cells. Oncoimmunology *7*, e1375641. 10.1080/2162402X.2017.1375641.
78. Xu, Y., Xiang, Z., Alnaggar, M., Kouakanou, L., Li, J., He, J., Yang, J., Hu, Y., Chen, Y., Lin, L., et al. (2021). Allogeneic Vgamma9Vdelta2 T-cell immunotherapy exhibits promising clinical safety and prolongs the survival of patients with late-stage lung or liver cancer. Cell Mol Immunol *18*, 427-439. 10.1038/s41423-020-0515-7.
79. Rischer, M., Pscherer, S., Duwe, S., Vormoor, J., Jurgens, H., and Rossig, C. (2004). Human gammadelta T cells as mediators of chimaeric-receptor redirected anti-tumour immunity. Br J Haematol *126*, 583-592. 10.1111/j.1365-2141.2004.05077.x.
80. Lammie, G., Cheung, N., Gerald, W., Rosenblum, M., and Cordoncardo, C. (1993). Ganglioside gd(2) expression in the human nervous-system and in neuroblastomas - an immunohistochemical study. Int J Oncol *3*, 909-915. 10.3892/ijo.3.5.909.
81. Wu, Z.L., Schwartz, E., Seeger, R., and Ladisch, S. (1986). Expression of GD2 ganglioside by untreated primary human neuroblastomas. Cancer Res *46*, 440-443.
82. Sait, S., and Modak, S. (2017). Anti-GD2 immunotherapy for neuroblastoma. Expert Rev Anticancer Ther *17*, 889-904. 10.1080/14737140.2017.1364995.
83. Postow, M.A., Chesney, J., Pavlick, A.C., Robert, C., Grossmann, K., McDermott, D., Linette, G.P., Meyer, N., Giguere, J.K., Agarwala, S.S., et al. (2015). Nivolumab and ipilimumab versus ipilimumab in untreated melanoma. N Engl J Med *372*, 2006-2017. 10.1056/NEJMoa1414428.
84. Reck, M., Rodriguez-Abreu, D., Robinson, A.G., Hui, R., Csoszi, T., Fulop, A., Gottfried, M., Peled, N., Tafreshi, A., Cuffe, S., et al. (2016). Pembrolizumab versus Chemotherapy for PD-L1-Positive Non-Small-Cell Lung Cancer. N Engl J Med *375*, 1823-1833. 10.1056/NEJMoa1606774.
85. Maude, S.L., Laetsch, T.W., Buechner, J., Rives, S., Boyer, M., Bittencourt, H., Bader, P., Verneris, M.R., Stefanski, H.E., Myers, G.D., et al. (2018). Tisagenlecleucel in Children

and Young Adults with B-Cell Lymphoblastic Leukemia. N Engl J Med *378*, 439-448. 10.1056/NEJMoa1709866.

86. Neelapu, S.S., Locke, F.L., Bartlett, N.L., Lekakis, L.J., Miklos, D.B., Jacobson, C.A., Braunschweig, I., Oluwole, O.O., Siddiqi, T., Lin, Y., et al. (2017). Axicabtagene Ciloleucel CAR T-Cell Therapy in Refractory Large B-Cell Lymphoma. N Engl J Med *377*, 2531-2544. 10.1056/NEJMoa1707447.
87. Raffaghello, L., Prigione, I., Bocca, P., Morandi, F., Camoriano, M., Gambini, C., Wang, X., Ferrone, S., and Pistoia, V. (2005). Multiple defects of the antigen-processing machinery components in human neuroblastoma: immunotherapeutic implications. Oncogene *24*, 4634-4644. 10.1038/sj.onc.1208594.
88. Anderson, J., Majzner, R.G., and Sondel, P.M. (2022). Immunotherapy of Neuroblastoma: Facts and Hopes. Clin Cancer Res *28*, 3196-3206. 10.1158/1078-0432.CCR-21-1356.
89. Young, R.M., Engel, N.W., Uslu, U., Wellhausen, N., and June, C.H. (2022). Next-Generation CAR T-cell Therapies. Cancer Discov *12*, 1625-1633. 10.1158/2159-8290.CD-21-1683.
90. Hossian, A., Hackett, C.S., Brentjens, R.J., and Rafiq, S. (2022). Multipurposing CARs: Same engine, different vehicles. Mol Ther *30*, 1381-1395. 10.1016/j.ymthe.2022.02.012.
91. Rafiq, S., Hackett, C.S., and Brentjens, R.J. (2020). Engineering strategies to overcome the current roadblocks in CAR T cell therapy. Nat Rev Clin Oncol *17*, 147-167. 10.1038/s41571-019-0297-y.
92. Jin, H.T., Anderson, A.C., Tan, W.G., West, E.E., Ha, S.J., Araki, K., Freeman, G.J., Kuchroo, V.K., and Ahmed, R. (2010). Cooperation of Tim-3 and PD-1 in CD8 T-cell exhaustion during chronic viral infection. Proc Natl Acad Sci U S A *107*, 14733-14738. 10.1073/pnas.1009731107.
93. Ochi, T., Maruta, M., Tanimoto, K., Kondo, F., Yamamoto, T., Kurata, M., Fujiwara, H., Masumoto, J., Takenaka, K., and Yasukawa, M. (2021). A single-chain antibody generation system yielding CAR-T cells with superior antitumor function. Commun Biol *4*, 273. 10.1038/s42003-021-01791-1.
94. Jespers, L.S., Roberts, A., Mahler, S.M., Winter, G., and Hoogenboom, H.R. (1994). Guiding the selection of human antibodies from phage display repertoires to a single epitope of an antigen. Biotechnology (N Y) *12*, 899-903. 10.1038/nbt0994-899.
95. Frenzel, A., Kugler, J., Helmsing, S., Meier, D., Schirrmann, T., Hust, M., and Dubel, S. (2017). Designing Human Antibodies by Phage Display. Transfus Med Hemother *44*, 312-318. 10.1159/000479633.
96. Marks, J.D., Hoogenboom, H.R., Bonnert, T.P., McCafferty, J., Griffiths, A.D., and Winter, G. (1991). By-passing immunization. Human antibodies from V-gene libraries displayed on phage. J Mol Biol *222*, 581-597. 10.1016/0022-2836(91)90498-u.
97. Jensen, M.C., and Riddell, S.R. (2015). Designing chimeric antigen receptors to effectively and safely target tumors. Curr Opin Immunol *33*, 9-15. 10.1016/j.coi.2015.01.002.
98. Hudecek, M., Sommermeyer, D., Kosasih, P.L., Silva-Benedict, A., Liu, L., Rader, C., Jensen, M.C., and Riddell, S.R. (2015). The nonsignaling extracellular spacer domain of chimeric antigen receptors is decisive for in vivo antitumor activity. Cancer Immunol Res *3*, 125-135. 10.1158/2326-6066.CIR-14-0127.
99. Chmielewski, M., Hombach, A., Heuser, C., Adams, G.P., and Abken, H. (2004). T cell activation by antibody-like immunoreceptors: increase in affinity of the single-chain

fragment domain above threshold does not increase T cell activation against antigen-positive target cells but decreases selectivity. J Immunol *173*, 7647-7653. 10.4049/jimmunol.173.12.7647.

100. Drent, E., Themeli, M., Poels, R., de Jong-Korlaar, R., Yuan, H., de Bruijn, J., Martens, A.C.M., Zweegman, S., van de Donk, N., Groen, R.W.J., et al. (2017). A Rational Strategy for Reducing On-Target Off-Tumor Effects of CD38-Chimeric Antigen Receptors by Affinity Optimization. Mol Ther *25*, 1946-1958. 10.1016/j.ymthe.2017.04.024.
101. Maus, M.V., Plotkin, J., Jakka, G., Stewart-Jones, G., Riviere, I., Merghoub, T., Wolchok, J., Renner, C., and Sadelain, M. (2016). An MHC-restricted antibody-based chimeric antigen receptor requires TCR-like affinity to maintain antigen specificity. Mol Ther Oncolytics *3*, 1-9. 10.1038/mto.2016.23.
102. Liu, X., Jiang, S., Fang, C., Yang, S., Olalere, D., Pequignot, E.C., Cogdill, A.P., Li, N., Ramones, M., Granda, B., et al. (2015). Affinity-Tuned ErbB2 or EGFR Chimeric Antigen Receptor T Cells Exhibit an Increased Therapeutic Index against Tumors in Mice. Cancer Res *75*, 3596-3607. 10.1158/0008-5472.CAN-15-0159.
103. Louis, C.U., Savoldo, B., Dotti, G., Pule, M., Yvon, E., Myers, G.D., Rossig, C., Russell, H.V., Diouf, O., Liu, E., et al. (2011). Antitumor activity and long-term fate of chimeric antigen receptor-positive T cells in patients with neuroblastoma. Blood *118*, 6050-6056. 10.1182/blood-2011-05-354449.
104. Kawalekar, O.U., RS, O.C., Fraietta, J.A., Guo, L., McGettigan, S.E., Posey, A.D., Jr., Patel, P.R., Guedan, S., Scholler, J., Keith, B., et al. (2016). Distinct Signaling of Coreceptors Regulates Specific Metabolism Pathways and Impacts Memory Development in CAR T Cells. Immunity *44*, 712. 10.1016/j.immuni.2016.02.023.
105. Raikar, S.S., Fleischer, L.C., Moot, R., Fedanov, A., Paik, N.Y., Knight, K.A., Doering, C.B., and Spencer, H.T. (2018). Development of chimeric antigen receptors targeting T-cell malignancies using two structurally different anti-CD5 antigen binding domains in NK and CRISPR-edited T cell lines. Oncoimmunology *7*, e1407898. 10.1080/2162402X.2017.1407898.
106. Donahue, R.E., Kessler, S.W., Bodine, D., McDonagh, K., Dunbar, C., Goodman, S., Agricola, B., Byrne, E., Raffeld, M., Moen, R., and et al. (1992). Helper virus induced T cell lymphoma in nonhuman primates after retroviral mediated gene transfer. J Exp Med *176*, 1125-1135. 10.1084/jem.176.4.1125.
107. Marcucci, K.T., Jadlowsky, J.K., Hwang, W.T., Suhoski-Davis, M., Gonzalez, V.E., Kulikovskaya, I., Gupta, M., Lacey, S.F., Plesa, G., Chew, A., et al. (2018). Retroviral and Lentiviral Safety Analysis of Gene-Modified T Cell Products and Infused HIV and Oncology Patients. Mol Ther *26*, 269-279. 10.1016/j.ymthe.2017.10.012.
108. Hacein-Bey-Abina, S., Garrigue, A., Wang, G.P., Soulier, J., Lim, A., Morillon, E., Clappier, E., Caccavelli, L., Delabesse, E., Beldjord, K., et al. (2008). Insertional oncogenesis in 4 patients after retrovirus-mediated gene therapy of SCID-X1. J Clin Invest *118*, 3132-3142. 10.1172/JCI35700.
109. Hacein-Bey-Abina, S., von Kalle, C., Schmidt, M., Le Deist, F., Wulffraat, N., McIntyre, E., Radford, I., Villeval, J.L., Fraser, C.C., Cavazzana-Calvo, M., and Fischer, A. (2003). A serious adverse event after successful gene therapy for X-linked severe combined immunodeficiency. N Engl J Med *348*, 255-256. 10.1056/NEJM200301163480314.

110. MacGregor, R.R. (2001). Clinical protocol. A phase 1 open-label clinical trial of the safety and tolerability of single escalating doses of autologous CD4 T cells transduced with VRX496 in HIV-positive subjects. Hum Gene Ther *12*, 2028-2029.
111. Tran, R., and Lam, W.A. (2020). Microfluidic Approach for Highly Efficient Viral Transduction. Methods Mol Biol *2097*, 55-65. 10.1007/978-1-0716-0203-4_3.
112. Tran, R., Myers, D.R., Denning, G., Shields, J.E., Lytle, A.M., Alrowais, H., Qiu, Y., Sakurai, Y., Li, W.C., Brand, O., et al. (2017). Microfluidic Transduction Harnesses Mass Transport Principles to Enhance Gene Transfer Efficiency. Mol Ther *25*, 2372-2382. 10.1016/j.ymthe.2017.07.002.
113. Fehse, B., Richters, A., Putimtseva-Scharf, K., Klump, H., Li, Z., Ostertag, W., Zander, A.R., and Baum, C. (2000). CD34 splice variant: an attractive marker for selection of gene-modified cells. Mol Ther *1*, 448-456. 10.1006/mthe.2000.0068.
114. Mosti, L., Langner, L.M., Chmielewski, K.O., Arbuthnot, P., Alzubi, J., and Cathomen, T. (2021). Targeted multi-epitope switching enables straightforward positive/negative selection of CAR T cells. Gene Ther *28*, 602-612. 10.1038/s41434-021-00220-6.
115. Krause, D.S., Fackler, M.J., Civin, C.I., and May, W.S. (1996). CD34: structure, biology, and clinical utility. Blood *87*, 1-13.
116. Schumm, M., Lang, P., Taylor, G., Kuci, S., Klingebiel, T., Buhring, H.J., Geiselhart, A., Niethammer, D., and Handgretinger, R. (1999). Isolation of highly purified autologous and allogeneic peripheral CD34+ cells using the CliniMACS device. J Hematother *8*, 209-218. 10.1089/106161299320488.
117. Jiang, X., Dudzinski, S., Beckermann, K.E., Young, K., McKinley, E., O, J.M., Rathmell, J.C., Xu, J., and Gore, J.C. (2020). MRI of tumor T cell infiltration in response to checkpoint inhibitor therapy. J Immunother Cancer *8*. 10.1136/jitc-2019-000328.
118. Pollizzi, K.N., Waickman, A.T., Patel, C.H., Sun, I.H., and Powell, J.D. (2015). Cellular size as a means of tracking mTOR activity and cell fate of CD4+ T cells upon antigen recognition. PLoS One *10*, e0121710. 10.1371/journal.pone.0121710.
119. Teague, T.K., Munn, L., Zygourakis, K., and McIntyre, B.W. (1993). Analysis of lymphocyte activation and proliferation by video microscopy and digital imaging. Cytometry *14*, 772-782. 10.1002/cyto.990140710.
120. Vormittag, P., Gunn, R., Ghorashian, S., and Veraitch, F.S. (2018). A guide to manufacturing CAR T cell therapies. Curr Opin Biotechnol *53*, 164-181. 10.1016/j.copbio.2018.01.025.
121. Hernandez, I., Prasad, V., and Gellad, W.F. (2018). Total Costs of Chimeric Antigen Receptor T-Cell Immunotherapy. JAMA Oncol *4*, 994-996. 10.1001/jamaoncol.2018.0977.
122. Keyel, M.E., and Reynolds, C.P. (2019). Spotlight on dinutuximab in the treatment of high-risk neuroblastoma: development and place in therapy. Biologics *13*, 1-12. 10.2147/BTT.S114530.
123. Park, J.A., and Cheung, N.V. (2020). Targets and Antibody Formats for Immunotherapy of Neuroblastoma. J Clin Oncol *38*, 1836-1848. 10.1200/JCO.19.01410.
124. Whittle, S.B., Smith, V., Doherty, E., Zhao, S., McCarty, S., and Zage, P.E. (2017). Overview and recent advances in the treatment of neuroblastoma. Expert Rev Anticancer Ther *17*, 369-386. 10.1080/14737140.2017.1285230.

125. Wang, X., Scarfo, I., Schmidts, A., Toner, M., Maus, M.V., and Irimia, D. (2019). Dynamic Profiling of Antitumor Activity of CAR T Cells Using Micropatterned Tumor Arrays. Adv Sci (Weinh) *6*, 1901829. 10.1002/advs.201901829.
126. Li, N., Torres, M.B., Spetz, M.R., Wang, R., Peng, L., Tian, M., Dower, C.M., Nguyen, R., Sun, M., Tai, C.H., et al. (2021). CAR T cells targeting tumor-associated exons of glypican 2 regress neuroblastoma in mice. Cell Rep Med *2*, 100297. 10.1016/j.xcrm.2021.100297.
127. Wolpaw, A.J., Grossmann, L.D., Dessau, J.L., Dong, M.M., Aaron, B.J., Brafford, P.A., Volgina, D., Pascual-Pasto, G., Rodriguez-Garcia, A., Uzun, Y., et al. (2022). Epigenetic state determines inflammatory sensing in neuroblastoma. Proc Natl Acad Sci U S A *119*. 10.1073/pnas.2102358119.
128. van Groningen, T., Koster, J., Valentijn, L.J., Zwijnenburg, D.A., Akogul, N., Hasselt, N.E., Broekmans, M., Haneveld, F., Nowakowska, N.E., Bras, J., et al. (2017). Neuroblastoma is composed of two super-enhancer-associated differentiation states. Nat Genet *49*, 1261-1266. 10.1038/ng.3899.
129. Gartlgruber, M., Sharma, A.K., Quintero, A., Dreidax, D., Jansky, S., Park, Y.G., Kreth, S., Meder, J., Doncevic, D., Saary, P., et al. (2021). Super enhancers define regulatory subtypes and cell identity in neuroblastoma. Nat Cancer *2*, 114-128. 10.1038/s43018-020-00145-w.
130. Ying, Z., He, T., Wang, X., Zheng, W., Lin, N., Tu, M., Xie, Y., Ping, L., Zhang, C., Liu, W., et al. (2019). Parallel Comparison of 4-1BB or CD28 Co-stimulated CD19-Targeted CAR-T Cells for B Cell Non-Hodgkin's Lymphoma. Mol Ther Oncolytics *15*, 60-68. 10.1016/j.omto.2019.08.002.
131. Dai, Q., Han, P., Qi, X., Li, F., Li, M., Fan, L., Zhang, H., Zhang, X., and Yang, X. (2020). 4-1BB Signaling Boosts the Anti-Tumor Activity of CD28-Incorporated 2(nd) Generation Chimeric Antigen Receptor-Modified T Cells. Front Immunol *11*, 539654. 10.3389/fimmu.2020.539654.
132. Guedan, S., Posey, A.D., Jr., Shaw, C., Wing, A., Da, T., Patel, P.R., McGettigan, S.E., Casado-Medrano, V., Kawalekar, O.U., Uribe-Herranz, M., et al. (2018). Enhancing CAR T cell persistence through ICOS and 4-1BB costimulation. JCI Insight *3*. 10.1172/jci.insight.96976.
133. Hirabayashi, K., Du, H., Xu, Y., Shou, P., Zhou, X., Fuca, G., Landoni, E., Sun, C., Chen, Y., Savoldo, B., and Dotti, G. (2021). Dual Targeting CAR-T Cells with Optimal Costimulation and Metabolic Fitness enhance Antitumor Activity and Prevent Escape in Solid Tumors. Nat Cancer *2*, 904-918. 10.1038/s43018-021-00244-2.
134. Bonneville, M., O'Brien, R.L., and Born, W.K. (2010). Gammadelta T cell effector functions: a blend of innate programming and acquired plasticity. Nat Rev Immunol *10*, 467-478. 10.1038/nri2781.
135. Rei, M., Pennington, D.J., and Silva-Santos, B. (2015). The emerging Protumor role of gammadelta T lymphocytes: implications for cancer immunotherapy. Cancer Res *75*, 798-802. 10.1158/0008-5472.CAN-14-3228.
136. Di Lorenzo, B., Simoes, A.E., Caiado, F., Tieppo, P., Correia, D.V., Carvalho, T., da Silva, M.G., Dechanet-Merville, J., Schumacher, T.N., Prinz, I., et al. (2019). Broad Cytotoxic Targeting of Acute Myeloid Leukemia by Polyclonal Delta One T Cells. Cancer Immunol Res *7*, 552-558. 10.1158/2326-6066.CIR-18-0647.

137. Zhou, S., Liu, M., Ren, F., Meng, X., and Yu, J. (2021). The landscape of bispecific T cell engager in cancer treatment. Biomark Res *9*, 38. 10.1186/s40364-021-00294-9.
138. Goebeler, M.E., and Bargou, R.C. (2020). T cell-engaging therapies - BiTEs and beyond. Nat Rev Clin Oncol *17*, 418-434. 10.1038/s41571-020-0347-5.
139. Rozenbaum, M., Meir, A., Aharony, Y., Itzhaki, O., Schachter, J., Bank, I., Jacoby, E., and Besser, M.J. (2020). Gamma-Delta CAR-T Cells Show CAR-Directed and Independent Activity Against Leukemia. Front Immunol *11*, 1347. 10.3389/fimmu.2020.01347.
140. Gentles, A.J., Newman, A.M., Liu, C.L., Bratman, S.V., Feng, W., Kim, D., Nair, V.S., Xu, Y., Khuong, A., Hoang, C.D., et al. (2015). The prognostic landscape of genes and infiltrating immune cells across human cancers. Nat Med *21*, 938-945. 10.1038/nm.3909.
141. Jonus, H.C., Burnham, R.E., Ho, A., Pilgrim, A.A., Shim, J., Doering, C.B., Spencer, H.T., and Goldsmith, K.C. (2022). Dissecting the cellular components of ex vivo gammadelta T cell expansions to optimize selection of potent cell therapy donors for neuroblastoma immunotherapy trials. Oncoimmunology *11*, 2057012. 10.1080/2162402X.2022.2057012.
142. Liu, D., Zhao, J., Song, Y., Luo, X., and Yang, T. (2019). Clinical trial update on bispecific antibodies, antibody-drug conjugates, and antibody-containing regimens for acute lymphoblastic leukemia. J Hematol Oncol *12*, 15. 10.1186/s13045-019-0703-z.
143. Einsele, H., Borghaei, H., Orlowski, R.Z., Subklewe, M., Roboz, G.J., Zugmaier, G., Kufer, P., Iskander, K., and Kantarjian, H.M. (2020). The BiTE (bispecific T-cell engager) platform: Development and future potential of a targeted immuno-oncology therapy across tumor types. Cancer *126*, 3192-3201. 10.1002/cncr.32909.
144. Mody, R., Naranjo, A., Van Ryn, C., Yu, A.L., London, W.B., Shulkin, B.L., Parisi, M.T., Servaes, S.E., Diccianni, M.B., Sondel, P.M., et al. (2017). Irinotecan-temozolomide with temsirolimus or dinutuximab in children with refractory or relapsed neuroblastoma (COG ANBL1221): an open-label, randomised, phase 2 trial. Lancet Oncol *18*, 946-957. 10.1016/S1470-2045(17)30355-8.
145. Straathof, K., Flutter, B., Wallace, R., Jain, N., Loka, T., Depani, S., Wright, G., Thomas, S., Cheung, G.W., Gileadi, T., et al. (2020). Antitumor activity without on-target off-tumor toxicity of GD2-chimeric antigen receptor T cells in patients with neuroblastoma. Sci Transl Med *12*. 10.1126/scitranslmed.abd6169.
146. Majzner, R.G., Theruvath, J.L., Nellan, A., Heitzeneder, S., Cui, Y., Mount, C.W., Rietberg, S.P., Linde, M.H., Xu, P., Rota, C., et al. (2019). CAR T Cells Targeting B7-H3, a Pan-Cancer Antigen, Demonstrate Potent Preclinical Activity Against Pediatric Solid Tumors and Brain Tumors. Clin Cancer Res *25*, 2560-2574. 10.1158/1078-0432.CCR-18-0432.
147. Carpenter, E.L., and Mosse, Y.P. (2012). Targeting ALK in neuroblastoma--preclinical and clinical advancements. Nat Rev Clin Oncol *9*, 391-399. 10.1038/nrclinonc.2012.72.
148. Bosse, K.R., Raman, P., Zhu, Z., Lane, M., Martinez, D., Heitzeneder, S., Rathi, K.S., Kendsersky, N.M., Randall, M., Donovan, L., et al. (2017). Identification of GPC2 as an Oncoprotein and Candidate Immunotherapeutic Target in High-Risk Neuroblastoma. Cancer Cell *32*, 295-309 e212. 10.1016/j.ccell.2017.08.003.
149. Katoh, M. (2017). Canonical and non-canonical WNT signaling in cancer stem cells and their niches: Cellular heterogeneity, omics reprogramming, targeted therapy and tumor plasticity (Review). Int J Oncol *51*, 1357-1369. 10.3892/ijo.2017.4129.
150. Katoh, M. (2005). WNT/PCP signaling pathway and human cancer (review). Oncol Rep *14*, 1583-1588.

151. Chen, S., Wang, Y., Su, Y., Zhang, L., Zhang, M., Li, X., Wang, J., and Zhang, X. (2018). miR-205-5p/PTK7 axis is involved in the proliferation, migration and invasion of colorectal cancer cells. Mol Med Rep *17*, 6253-6260. 10.3892/mmr.2018.8650.
152. Golubkov, V.S., Prigozhina, N.L., Zhang, Y., Stoletov, K., Lewis, J.D., Schwartz, P.E., Hoffman, R.M., and Strongin, A.Y. (2014). Protein-tyrosine pseudokinase 7 (PTK7) directs cancer cell motility and metastasis. J Biol Chem *289*, 24238-24249. 10.1074/jbc.M114.574459.
153. Lhoumeau, A.C., Martinez, S., Boher, J.M., Monges, G., Castellano, R., Goubard, A., Doremus, M., Poizat, F., Lelong, B., de Chaisemartin, C., et al. (2015). Overexpression of the Promigratory and Prometastatic PTK7 Receptor Is Associated with an Adverse Clinical Outcome in Colorectal Cancer. PLoS One *10*, e0123768. 10.1371/journal.pone.0123768.
154. Shah, N.N., and Fry, T.J. (2019). Mechanisms of resistance to CAR T cell therapy. Nat Rev Clin Oncol *16*, 372-385. 10.1038/s41571-019-0184-6.
155. Fry, T.J., Shah, N.N., Orentas, R.J., Stetler-Stevenson, M., Yuan, C.M., Ramakrishna, S., Wolters, P., Martin, S., Delbrook, C., Yates, B., et al. (2018). CD22-targeted CAR T cells induce remission in B-ALL that is naive or resistant to CD19-targeted CAR immunotherapy. Nat Med *24*, 20-28. 10.1038/nm.4441.
156. Walker, A.J., Majzner, R.G., Zhang, L., Wanhainen, K., Long, A.H., Nguyen, S.M., Lopomo, P., Vigny, M., Fry, T.J., Orentas, R.J., and Mackall, C.L. (2017). Tumor Antigen and Receptor Densities Regulate Efficacy of a Chimeric Antigen Receptor Targeting Anaplastic Lymphoma Kinase. Mol Ther *25*, 2189-2201. 10.1016/j.ymthe.2017.06.008.
157. Watanabe, K., Terakura, S., Martens, A.C., van Meerten, T., Uchiyama, S., Imai, M., Sakemura, R., Goto, T., Hanajiri, R., Imahashi, N., et al. (2015). Target antigen density governs the efficacy of anti-CD20-CD28-CD3 zeta chimeric antigen receptor-modified effector CD8+ T cells. J Immunol *194*, 911-920. 10.4049/jimmunol.1402346.
158. Busch, D.H., Frassle, S.P., Sommermeyer, D., Buchholz, V.R., and Riddell, S.R. (2016). Role of memory T cell subsets for adoptive immunotherapy. Semin Immunol *28*, 28-34. 10.1016/j.smim.2016.02.001.
159. Fraietta, J.A., Lacey, S.F., Orlando, E.J., Pruteanu-Malinici, I., Gohil, M., Lundh, S., Boesteanu, A.C., Wang, Y., O'Connor, R.S., Hwang, W.T., et al. (2021). Author Correction: Determinants of response and resistance to CD19 chimeric antigen receptor (CAR) T cell therapy of chronic lymphocytic leukemia. Nat Med *27*, 561. 10.1038/s41591-021-01248-2.
160. van der Stegen, S.J., Hamieh, M., and Sadelain, M. (2015). The pharmacology of second-generation chimeric antigen receptors. Nat Rev Drug Discov *14*, 499-509. 10.1038/nrd4597.
161. Zhao, Z., Condomines, M., van der Stegen, S.J.C., Perna, F., Kloss, C.C., Gunset, G., Plotkin, J., and Sadelain, M. (2015). Structural Design of Engineered Costimulation Determines Tumor Rejection Kinetics and Persistence of CAR T Cells. Cancer Cell *28*, 415-428. 10.1016/j.ccell.2015.09.004.
162. Maude, S.L., Frey, N., Shaw, P.A., Aplenc, R., Barrett, D.M., Bunin, N.J., Chew, A., Gonzalez, V.E., Zheng, Z., Lacey, S.F., et al. (2014). Chimeric antigen receptor T cells for sustained remissions in leukemia. N Engl J Med *371*, 1507-1517. 10.1056/NEJMoa1407222.
163. Lee, D.W., Kochenderfer, J.N., Stetler-Stevenson, M., Cui, Y.K., Delbrook, C., Feldman, S.A., Fry, T.J., Orentas, R., Sabatino, M., Shah, N.N., et al. (2015). T cells expressing CD19

chimeric antigen receptors for acute lymphoblastic leukaemia in children and young adults: a phase 1 dose-escalation trial. Lancet *385*, 517-528. 10.1016/S0140-6736(14)61403-3.

164. Fesnak, A.D., June, C.H., and Levine, B.L. (2016). Engineered T cells: the promise and challenges of cancer immunotherapy. Nat Rev Cancer *16*, 566-581. 10.1038/nrc.2016.97.
165. Correia, D.V., Fogli, M., Hudspeth, K., da Silva, M.G., Mavilio, D., and Silva-Santos, B. (2011). Differentiation of human peripheral blood Vdelta1+ T cells expressing the natural cytotoxicity receptor NKp30 for recognition of lymphoid leukemia cells. Blood *118*, 992-1001. 10.1182/blood-2011-02-339135.
166. Jie, Y., Liu, G., Feng, L., Li, Y., E, M., Wu, L., Li, Y., Rong, G., Li, Y., Wei, H., and Gu, A. (2021). PTK7-Targeting CAR T-Cells for the Treatment of Lung Cancer and Other Malignancies. Front Immunol *12*, 665970. 10.3389/fimmu.2021.665970.